FOUNDATION INSTRUMENTATION AND GEOPHYSICAL EXPLORATION

October 14, 1983
Clarksville, Indiana

OHIO RIVER VALLEY SOILS SEMINAR XIV

TA
710
.A1
O440
1983

ORVSS-14

Foundation Instrumentation and Geophysical Exploration

October 14, 1983

8:00 Registration

Morning Session - Presiding: C. Robert Ullrich
University of Louisville

8:45 Welcome

9:00 "Performance Monitoring of Pile Foundation Installations" by Patrick J. Hannigan

9:45 "A Case Study of a Tied-Back Soldier Pile and Lagging Retaining Wall" by Gerald P. Madej

10:30 Coffee Break

11:00 "Field Measurements of Tie-Back Bar Performances in an Excavation Bracing" by Andrew Bodocsi and Mark Lockwood

11:45 "Rapid Construction of a Combined Coal Refuse Embankment" by Barry K. Thacker and James A. Schad

12:30 Luncheon

Afternoon Session - Presiding: Mark J. Schuhmann
Law Engineering Testing Co.

1:45 "Use of Spectral Analysis Techniques for Structural and Foundation Vibration Analyses" by Vincent P. Drnevich and John R. Hall, Jr.

2:30 "Use of Spectral Analysis of Surface Waves Method for Determination of Moduli and Thicknesses of Pavement Systems" by Soheil Nazarian, Kenneth H. Stokoe, II, and W. R. Hudson

3:15 Coffee Break

3:45 "Ground Penetration Radar: A New Tool in Geotechnical Engineering" by James Fowler

4:30 "Borehole Geophysics as Applied to a Foundation Investigation in Limestone: A Case History" by Robert White

5:15 Afternoon Session ends

6:30 Cocktails

7:30 Dinner and Evening Session

Presiding: Nicholas G. Schmitt
Law Engineering Testing Co.

Speaker: George F. Sowers

Topic: "Measure of Measurements"

PROCEEDINGS OF THE FOURTEENTH OHIO RIVER VALLEY SOILS SEMINAR

FOUNDATION INSTRUMENTATION AND GEOPHYSICAL EXPLORATION

October 14, 1983
Marriott Inn
Clarksville, Indiana

Sponsored by

KENTUCKY GEOTECHNICAL GROUP, ASCE

UNIVERSITY OF LOUISVILLE
DEPARTMENT OF CIVIL ENGINEERING

UNIVERSITY OF KENTUCKY
DEPARTMENT OF CIVIL ENGINEERING
OFFICE OF CONTINUING EDUCATION

and

CINCINNATI GEOTECHNICAL GROUP, ASCE

UNIVERSITY OF CINCINNATI
DEPARTMENT OF CIVIL AND ENVIRONMENTAL ENGINEERING

KENTUCKY TRANSPORTATION CENTER
LIBRARY

ORVSS XIV ORGANIZING COMMITTEE

Nicholas G. Schmitt, Chairman
Law Engineering Testing Company
Louisville, Kentucky

Mark J. Schuhmann
Law Engineering Testing Company
Louisville, Kentucky

C. Robert Ullrich
Department of Civil Engineering
University of Louisville
Louisville, Kentucky

Barry K. Thacker
Geologic Associates, Inc.
Knoxville, Tennessee

EXHIBITORS

BRAINARD-KILMAN DRILL CO.
P.O.Box 487
Tucker, GA 30084

CHRISTENSEN DIAMOND PRODUCTS
P.O.Box W 2215
Indianapolis, IN 46241

CENTRAL MINE EQUIPMENT CO.
6200 North Broadway
St. Louis, MO 63147

DIEDRICH DRILLING
2008 Ohio Street
La Porte, IN 46350

DOUBLEWAL CORPORATION
7 West Main Street
Plainville, CT 06062

HOGENTOGLER & COMPANY, INC.
P.O.Box 385
Gaithersburg, MD 20760

JANELL, INC.
AMOCO FABRICS
6130 Cornell Road
Cincinnati, OH 45242

LONGYEAR COMPANY
P.O.Box 1368
Minneapolis, MN 55440

MACCAFERRI GABIONS, INC.
P.O.Box 43A
Williamsport, MD 21795

MOBIL DRILLING COMPANY, INC.
3807 Madison Avenue
Indianapolis, IN 46227

REINFORCED EARTH CO.
4100 Executive Park Drive, Suite 9
Cincinnati, OH 45241

TENSAR, INC.
1101 West Lake Street
Oakdale, IL 62268

VIBRA-TECH ENGINEERS, INC.
706 Rockville Pike
Rockville, MD 20852

TABLE OF CONTENTS

PERFORMANCE MONITORING OF PILE FOUNDATION INSTALLATIONS by Patrick J. Hannigan

A CASE STUDY OF A TIED-BACK SOLDIER PILE AND LAGGING RETAINING WALL by Gerald P. Madej

FIELD MEASUREMENTS OF TIE-BACK BAR PERFORMANCES IN AN EXCAVATION BRACING by Andrew Bodocsi and Mark Lockwood

RAPID CONSTRUCTION OF A COMBINED COAL REFUSE EMBANKMENT by Barry K. Thacker and James A. Schad

USE OF SPECTRAL ANALYSIS TECHNIQUES FOR STRUCTURAL AND FOUNDATION VIBRATION ANALYSES by Vincent P. Drnevich and John R. Hall, Jr.

USE OF SPECTRAL ANALYSIS OF SURFACE WAVES METHOD FOR DETERMINATION OF MODULI AND THICKNESSES OF PAVEMENT SYSTEMS by Soheil Nazarian, Kenneth H. Stokoe, II, and W. R. Hudson

GROUND PENETRATION RADAR: A NEW TOOL IN GEOTECHNICAL ENGINEERING by James Fowler

BOREHOLE GEOPHYSICS AS APPLIED TO A FOUNDATION INVESTIGATION IN LIMESTONE: A CASE HISTORY by Robert White

THE SPT - A SUMMARY OF SOME RECENT STUDIES by Charles O. Riggs

PERFORMANCE MONITORING OF PILE FOUNDATION INSTALLATIONS

Patrick J. Hannigan

Abstract

The bearing capacity of a pile foundation is often evaluated simply by using the penetration resistance or blows per foot the pile encountered during driving in a wave equation bearing graph. While hammer performance and soil behavior have significant influences on pile penetration resistance values, their influence is often overlooked because they are not as readily observed and recorded as penetration resistance. This can lead to significant capacity prediction errors when hammer performance or soil behavior are different than that assumed.

This paper describes the pile driving analyzer instrumentation system of monitoring pile foundation installations. Two case histories are presented where the pile driving analyzer and CAPWAP computer program were used to monitor hammer performance and evaluate soil behavior. Wave equation bearing graphs developed from the pile driving analyzer and CAPWAP data are compared to bearing graphs based on general hammer performance values and soil behavior assumptions from soil boring data. The bearing graph comparison clearly indicates how unexpected hammer performance or soil behavior can greatly reduce the factor of safety against bearing capacity failure used in deep foundation design.

Introduction

Foundation engineers have often evaluated pile foundation installations based upon the penetration resistance the piles encountered during driving. Dynamic pile driving formulas, such as the Engineering News Record Formula, have been used for many years to evaluate pile capacities in this way. Several researchers (1), (2) have demonstrated the inaccuracy of the Engineering News Record and other dynamic formulas, yet they continue to be used because of their simplicity.

A more accurate method of evaluating pile capacity based upon pile penetration resistance can be obtained from the wave equation. The term "wave equation" is generally applied to computer programs that simulate the pile driving process. In these programs, the pile and driving system are represented by a series of masses connected by weightless springs. Soil resistances along the pile are modeled by springs and dashpots attached to each pile mass. The two most widely used wave equation programs are the WEAP and TTI programs which were developed under the sponsorship of the US Department of Transportation. A detailed description of the wave equation approach may be found in the users manuals of both programs (3), (4).

One of the main results of a wave equation analysis is a bearing graph which relates the ultimate pile capacity to the pile penetration resistance in blows per inch or foot. While the wave equation approach is generally regarded as the most accurate way to evaluate pile capacity based upon penetration resistance, its accuracy is largely dependent upon how well the assumed input parameters model the actual soil and hammer characteristics. For a given pile hammer and cushion, the wave

equation input assumptions include the hammer efficiency and the hammer cushion stiffness and coefficient of restitution. The wave equation input assumption for the soil model include the soil resistance distribution, the soil damping constants along the pile and at the pile tip, as well as the soil quake or elastic displacement along the pile shaft and at the pile tip.

The purpose of this paper is to demonstrate that typical wave equation input assumptions can result in significant capacity prediction errors when soil behavior or hammer peformance is different than that assumed. The pile driving analyzer and CAPWAP computer program can be used to determine hammer performance and soil behavior, thereby greatly increasing the accuracy of wave equation capacity predictions. Brief descriptions of this equipment as well as two case histories are presented to illustrate this technique.

The Pile Driving Analyzer

The pile driving analyzer instrumentation system consists of two accelerometers, two strain transducers, the pile driving analyzer, a four channel tape recorder, and an oscilloscope. The accelerometers and strain transducers are typically attached to the pile, two pile diameters below the pile top with bolts. The wires from each gauge are collected at a connection box which hangs from the helmet by a chain or wire. A single cable carries the gauge signals from the connection box to the pile driving analyzer located on the ground.

The pile driving anaylyer is a small field computer which processes the strain and acceleration signals from the gauges. For each hammer blow, the strain signals are filtered, averaged, and converted into a force versus time wave whereas the accelerometer signals are filtered, averaged, and intergrated to obtain velocity versus time waves. The analyzer transmits the force, velocity, and acceleration versus time waves to a four channel tape recorder where the signals are permanently recorded on magnetic tape for later analysis. At the same time, the waves are displayed on an oscilloscope so that the quality of the data can be evaluated during driving.

For each blow, the analyzer prints up to five selected output quantities on a paper tape as well as shows the results of two of the selected quantities on LCD displays. The available output quantities include the impact force and velocity at the pile top, the maximum energy transferred to the pile top, as well as the maximum force, velocity, acceleration, and displacement at the pile top. In addition, several other quantities useful in evaluating pile capacity, tension and compression stresses, pile integrity, and hammer performance can be obtained. A more detailed description of the pile analyzer's capabilities and usage is summarized by Goble, Rausche and Likins (5).

One of the latest additions to the analyzer is the capability to compute the maximum momentum of the hammer ram at impact using the principals of impulse and linear conservation of momentum. This technique, developed by Likins (6), can be used to determine the wave equation hammer efficiency of air-steam or drop hammers.

CAPWAP Analysis

CAPWAP (Case Pile Wave Analysis Program) is a wave equation type computer program developed by Rausche (7) that uses the pile top force and acceleration data measured by the pile driving analyzer to determine the soil resistance forces acting on the pile and at the pile tip. The computer program input data includes a segmented pile model, the recorded acceleration wave, and an assumed soil model consisting of soil resistances, quakes, and damping values for each pile segment and the pile tip. With this input data, the program generates a predicted force wave which is compared with the force wave recorded in the field by the pile driving analyzer. By adjusting the soil model during repetitive computer runs, the computer programer strives to achieve a match between the force wave predicted by the program with the force wave measured in the field by the analyzer. If the predicted and measured force waves agree well, the accuracy of the soil model solution is checked by using the measured force wave as input to obtain a predicted pile top velocity. If the predicted and measured pile top velocity waves also agree, it can be concluded that an accurate soil model has been obtained.

The CAPWAP soil model used to obtain the force and velocity wave matches provides the engineer with the ultimate pile capacity, the soil resistance distribution along the pile, the soil damping constants along the pile and at the pile tip, as well as the soil quake values along the pile and at the pile tip.

Wave Equation Input Parameters

As discussed earlier, several input assumptions are required in a wave equation analysis including the soil resistance distribution, the soil damping constants, the soil quakes, the hammer efficiency and the hammer cushion stiffness and coefficient of restitution. Representative soil input parameters can be easily obtained from the CAPWAP analysis leaving only the hammer and cushion properties to be determined.

The hammer efficiency, cushion stiffness and cushion coefficient of resititution are generally determined through repetitive wave equation runs. These input parameters are varied until the wave equation predicted pile top force and energy match the pile top force and energy measured by the pile driving analyzer.

The wave equation hammer efficiency for air-steam or drop hammers can be directly determined with the pile driving analyzer, thereby reducing the number of wave equation interations. As discussion earlier, the analyzer can compute the ram momentum at impact which is equal to the product of ram mass times ram velocity. Since ram mass and momentum are known, the ram velocity at impact can be computed. Wave equations compute the ram velocity at impact of air-steam or drop hammers from:

$$V_{ram} = \sqrt{2 \cdot g \cdot H \cdot e} \qquad \text{(Equation 1)}$$

where:

V_{ram} = ram velocity at impact

g = acceleration due to gravity

H = hammer stroke

e = wave equation efficiency

Once the ram impact velocity has been determined using the analyzer data, the wave equation hammer efficiency can be computed from Equation 1.

Case History No. 1

On this dock construction project, HP-12 X 53 H-piles with a design capacity of 80 tons were installed using a Link-Belt 520 hammer. The hammer cushion consisted of five, 0.55 inch thick by 10-7/8 inch O.D. micarta plates and four, 0.25 inch thick by 10-7/8 inch O.D. aluminum plates in an alternating pattern. The general soil profile consisted of 22 ft of water over 20 ft of soft silty clay and 30 ft of stiff to very stiff silty clay. The piles were expected to refuse in a hard to very hard sandy clay glacial till located 50 ft below the mudline. The soil profile is illustrated in Figure 1 along with a representative pile driving record.

Prior to construction, a WEAP wave equation analysis was performed using generally recommended input parameters for the hammer performance and anticipated soil conditions (3). A wave equation hammer efficiency of 95% was used for the diesel hammer. The soil resistance distribution was estimated using a pile-adhesion approach. This input data indicated that the ultimate pile capacity of 160 tons could be achieved at a penetration resistance of 11 blows per inch.

During construction, selected production piles were monitored with the pile driving analyzer. Pile analyzer measurements indicated approximately 13 ft-kips of energy was typically being delivered to the pile top. This corresponds to a energy transfer ratio, pile top energy divided by the rated hammer energy, of 43%. Energy transfer

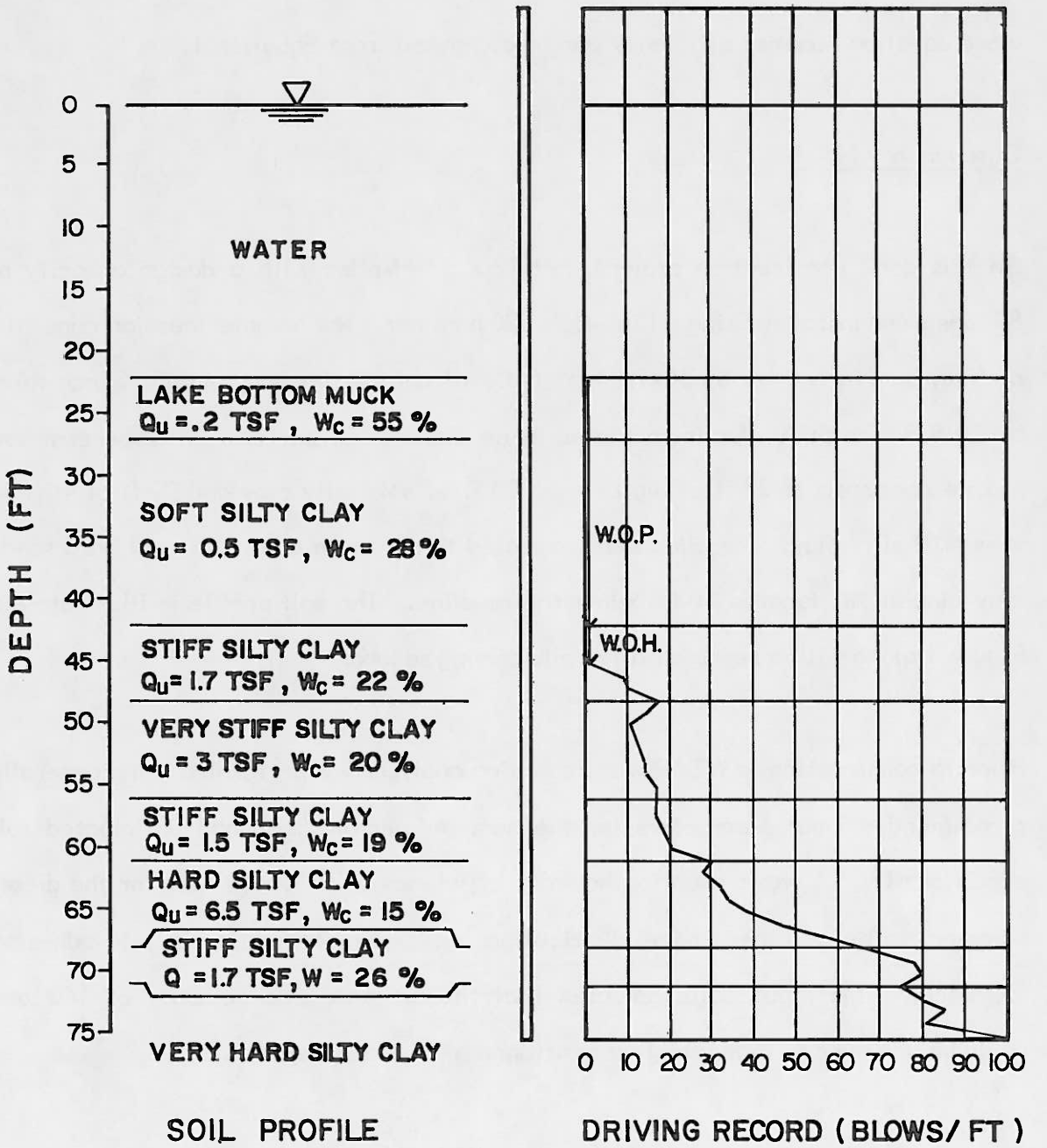


FIGURE 1. CASE HISTORY NUMBER 1
SOIL PROFILE AND DRIVING RECORD

ratios of 40 to 60% are representative of typical hammer performance. The pile top force at impact was typically on the order of 300 kips and the pile top velocity at impact was generally 9.7 feet per second.

The analyzer data and CAPWAP analyses were used to refine the preconstruction wave equation. The CAPWAP analysis indicated ultimate pile capacities on the order of 115 tons at the end of drive. The refined wave equation also indicated that ultimate pile capacities only on the order of 110 to 120 tons could be obtained at refusal driving conditions. The dramatic change in obtainable pile capacity between the original and the refined wave equations was due to a large pile tip quake of 0.4 inches which is four times greater than the generally assumed value of 0.1 inches. The original wave equation bearing graph based on assumed parameters and the refined wave equation bearing graph are presented in Figure 2. The assumed and refined input data are presented in Table 1.

Authier and Fellenius (8) demonstrated that when a large quake exists, a given hammer will not be able to drive a given pile to the same capacity that it could ordinarily if small quakes were encountered. Therefore, larger hammers which deliver greater energy are often required to overcome large tip quakes and to attain the desired pile capacity.

Additional pile driving analyzer testing and CAPWAP analyses were performed on production piles two to three weeks after initial driving. This testing indicated that an additional 30 tons of capacity could be anticipated due to soil set-up or freeze.

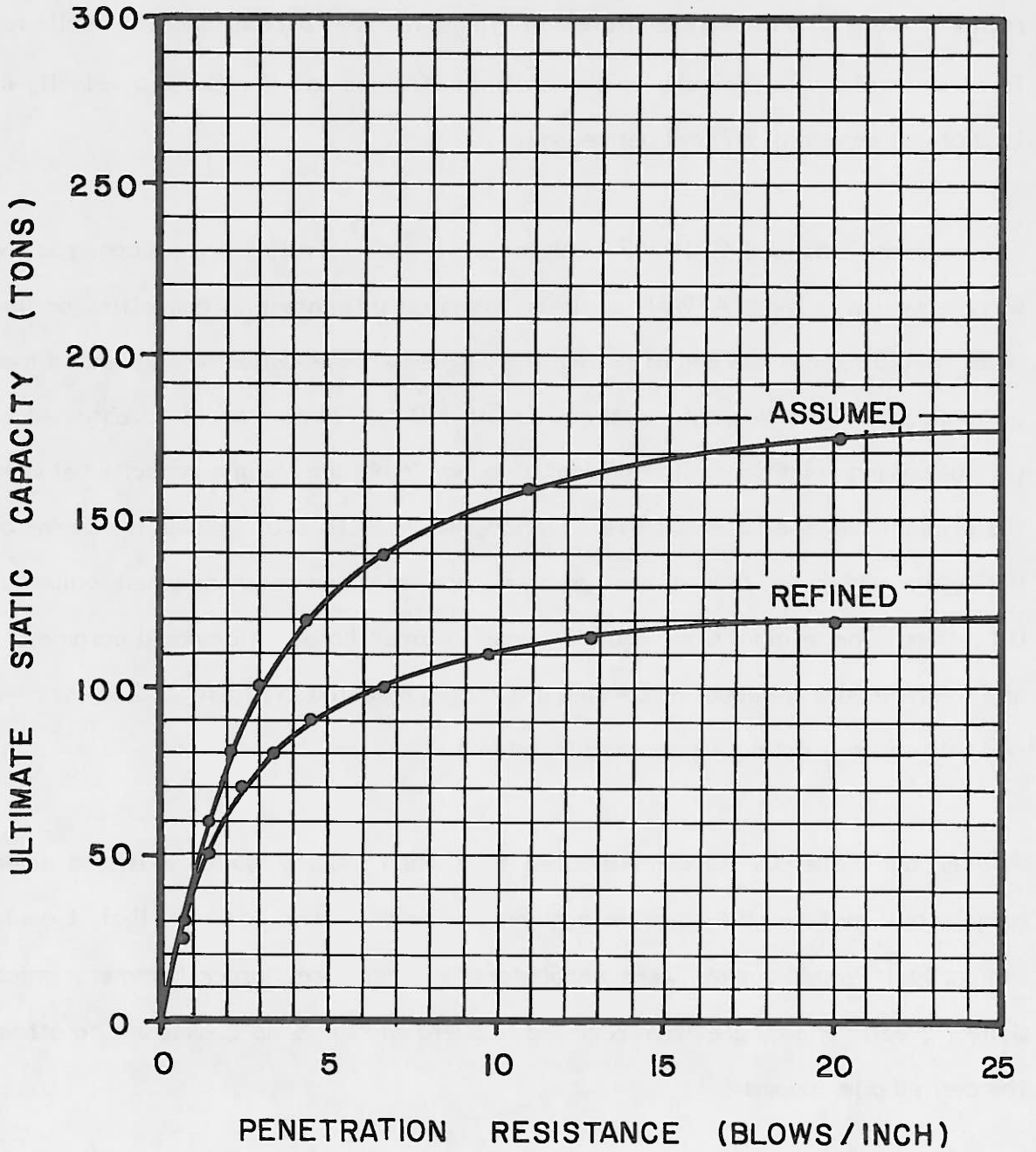


FIGURE 2. CASE HISTORY NUMBER 1
WAVE EQUATION BEARING GRAPHS

TABLE 1

WAVE EQUATION DATA SUMMARY

	Case History #1		Case History #2	
	Assumed	Refined	Assumed	Refined
Hammer Efficiency (%)	95%	95%	70%	59%
Cushion Stiffness (k/in)	15,500	15,500	13,800	13,800
Coefficient of Restitution	.80	.90	.65	.68
Skin Friction Resistance (%)	78	64	30	8
End Bearing Resistance (%)	22	36	70	92
Side Damping (sec/ft)	.20	.15	.20	.16
Tip Damping (sec/ft)	.10	.08	.05	.04
Side Quake (in.)	.10	.12	.10	.15
Tip Quake (in.)	.10	.40	.10	.20
Driving Criteria (blows/in.)	11	12	12	12
Predicted Capacity at Driving Criteria	160	115	235	200
Factor of Safety	2	1.4	1.9	1.6

It should noted that significant soil freeze was generally not anticipated in this area, and therefore had not been included in determining the original allowable pile capacity.

In summary, the unexpected soil behavior reduced the anticipated end of drive capacities from approximately 160 to 120 tons. Unanticipated soil freeze counterbalanced the unexpected soil behavior resulting in a foundation factor of safety generally on the order of 1.9 to 2.1. If soil freeze had not developed, significant foundation cost increases would likely have occurred since a larger hammer and crane, or additional foundation piles would have been required to meet the design requirements.

Case History No. 2

Case history number 2 is a plant expansion project where 125 ton design capacity pipe piles were installed with a Vulcan 010 hammer. The pipe piles had an outside diameter of 9-5/8 inches and a wall thickness of 0.53 inches. A 9.5 inch O.D. by 1 inch thick boot plate was attached to the bottom of each pile. The hammer cushion consisted of 7 inches of Force 10. The general soil profile consisted of 5 ft of loose sand over 28 ft of very stiff to hard silty clay. The piles were expected to refuse in an extremely dense stony glacial till, comprised of silt, sand and cobbles at a depth of 35 to 40 ft. The soil profile is illustrated in Figure 3 along with a representative pile driving record.

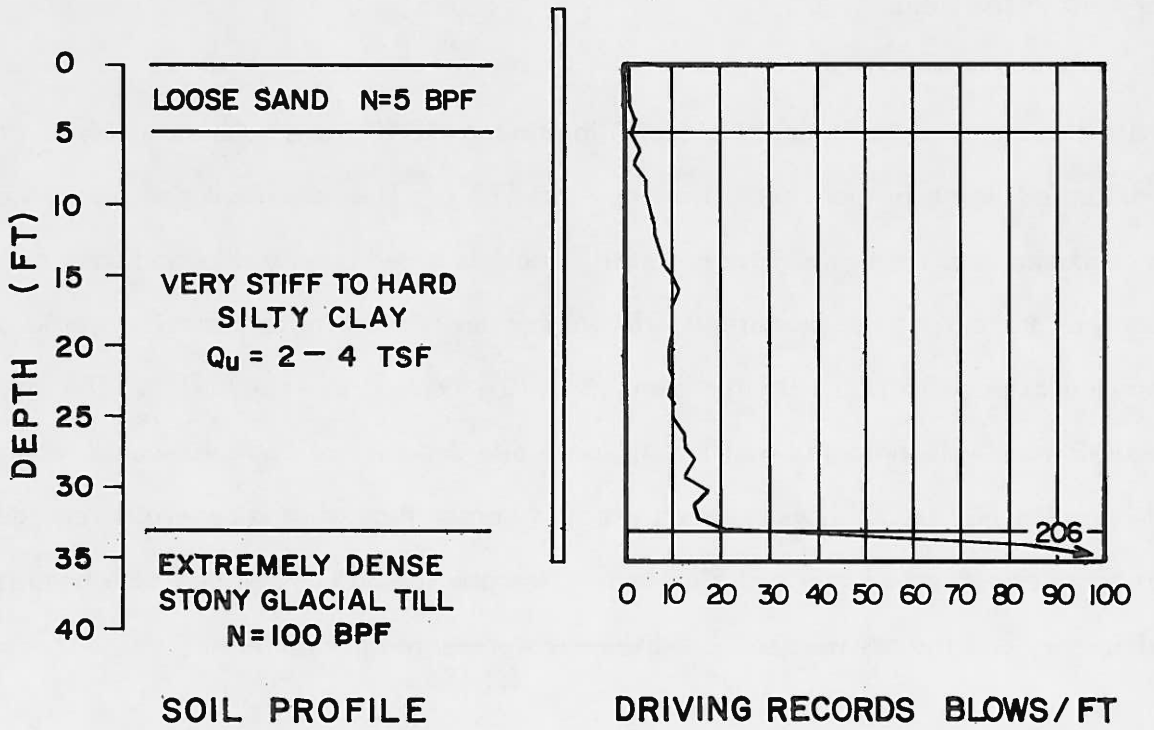


FIGURE 3. CASE HISTORY NUMBER 2
SOIL PROFILE AND DRIVING RECORD

Wave equation hammer efficiency factors for air-steam hammers range from 66% in the TTI wave equation manual to 80% in the WEAP wave equation hammer file. It is also noted in the WEAP manual that the 80% hammer efficiencies are hammer manufacturer's recommendations which reflect ideal conditions that are not usually present in the field.

With this range of hammer efficiencies in mind, a WEAP wave equation analysis was performed using a hammer efficiency of 70%. The assumed soil resistance distribution was determined from a static analysis based upon soil boring data. This analysis indicated approximately 30% of the desired ultimate capacity would be carried in skin friction with the remaining 70% carried in end bearing. The wave equation analysis indicated that the ultimate pile capacity of 250 tons would require driving the pile to 30 blows per inch which is harder than what is generally regarded as hammer refusal. Wave equation bearing graphs for 80%, 70%, and 66% hammer efficiency and the assumed soil conditions are presented in Figure 4.

A probe pile program was performed where several piles were monitored with the pile driving analyzer. The pile driving analyzer measurements indicated approximately 12.9 ft-kips of energy was typically being delivered to the pile top. This corresponds to an energy transfer ratio of 39% which is slightly below normal performance levels. The pile top force and velocity at impact were generally on the order of 300 kips and 10.9 feet per second, respectively. From the analyzer's ram momentum computations, it was determined that a wave equation efficiency factor of 59% would best represent the observed hammer performance.

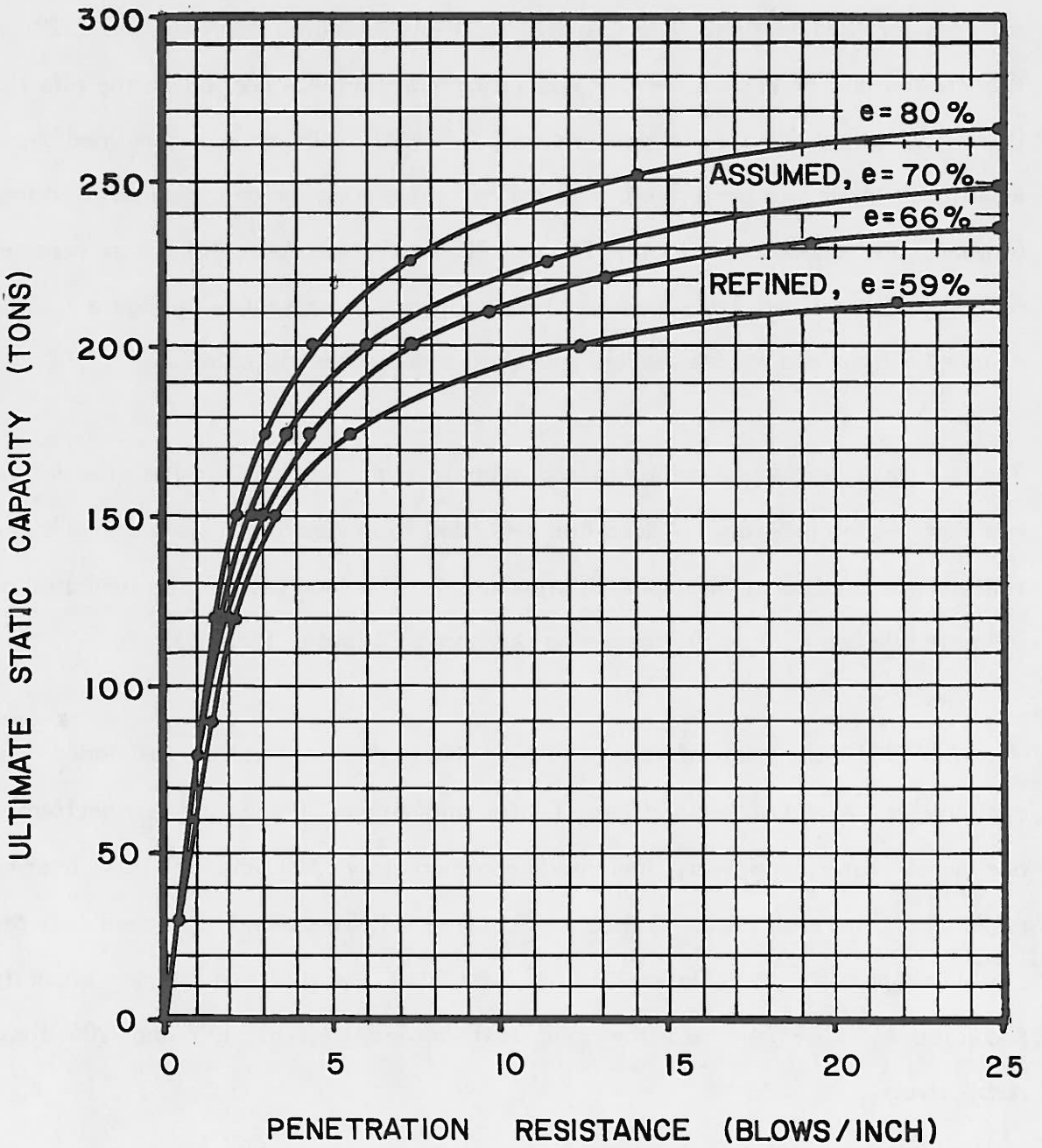


FIGURE 4. CASE HISTORY NUMBER 2
WAVE EQUATION BEARING GRAPHS

A CAPWAP analysis was also performed using the analyzer data obtained on a pile selected for load testing. The CAPWAP analysis indicated approximately 92% of the 212 ton end of drive CAPWAP capacity prediction was carried on the pile tip. Using the lower hammer efficiency and CAPWAP soil model, a refined wave equation analysis was performed. The refined wave equation analysis indicated that ultimate pile capacities of only 205 to 215 tons could be obtained at hammer refusal. The refined wave equation bearing graph is presented in Figure 4. The assumed and refined wave equation input data is presented in Table 1.

The pile load test was performed approximately one week after the pile driving analyzer testing program. A load cell was used to measure the applied load and a telltale was used to monitor pile tip movement. The load test results indicated an ultimate pile capacity of 345 tons using Davisson's Failure criteria (9).

The CAPWAP analysis indicated only 17 tons of skin friction resistance was available at the end of initial drive. Telltale movements in the load test performed one week later, however, indicated approximately 140 tons of skin friction resistance. Therefore, approximately 123 tons of soil freeze had developed over the one week period. It is interesting to note that the pile end bearing capacity predicted by CAPWAP and the load test agreed well at 195 and 205 tons, respectively.

In summary, the hammer performance at this site was not as good as anticipated in the preconstruction wave equation analysis. However, the pile foundations could be installed with the hammer since significant soil freeze compensated for the lower than anticipated end of drive capacity.

Conclusions

Pile capacities are often evaluated using the pile penetration resistance in a wave equation bearing graph. In these instances, it is important that the wave equation input data used to develop the bearing graph be as representative of the hammer and soil conditions as possible.

The two case histories presented herein have demonstrated that wave equation capacity predictions using conventional input assumptions can be significantly in error when the input assumptions do not accurately model hammer performance or soil behavior. The capacity prediction errors can be avoided or at least minimized using readily available instrumentation equipment and analysis techniques. The pile driving analyzer and CAPWAP program can be used to select representative wave equation input parameters since they provide insight into the actual hammer performance and soil behavior.

REFERENCES

1. Agerschou, H.A., "Analysis of the Engineering News Pile Formula", Journal of the Soil Mechanics and Foundations Division, American Society of Civil Engineers, Vol. 88, No. SM5, October 1982, pp 1-11.

2. Poulos, H.G. and Davis, E.H., "Pile Foundation Analysis and Design", John Wiley & Sons, 1980, pp. 57-58.

3. Goble, G.G. and Rausche, F., "Wave Equation Analysis of Piles", Vol. 2 - User's Manual, U.S. Department of Transportation, March, 1981.

4. Hirsch, T.J., Carr, L., and Lowery, L.L., "Pile Driving Analysis - Wave Equation User's Manual", Vol. 2, U.S. Department of Transportation, April, 1976.

5. Goble, G.G., Rausche, F., and Likins, G.E., "The Analysis of Pile Driving A State-of-the-Art", Proc. of the International Seminar on the Application of Stress-Wave Theory on Piles, Stockholm, 1980, H. Bredenberg Editor, A.A., Balkema, Rotterdam, pp. 131-162.

6. Likins, G.E., "Evaluating the Performance of Pile Driving Hammers", Fifth Seminar on the Dynamics of Pile Driving, Philadelphia, May, 1983, 28 pp.

7. Rausche, F., "Soil Response from Dynamic Analysis and Measurements on Piles", Ph.D. Thesis, Case Western Reserve University, Cleveland, Ohio, 1970.

8. Authier, J. and Fellenius, B.H., "Quake Values Determined from Dynamic Measurements", Proc. of the International Seminar on the Application of Stress-Wave Theory on Piles, Stockholm, 1980, H. Bredenberg Editor, A.A. Balkema, Rotterdam, pp. 121-127.

9. Davisson, M.T., "High Capacity Piles", Proc. of the Lecture Series on Innovations in Foundation Construction, Department of Civil Engineering, Illinois Institute of Technology, May, 1973, pp. 81-112.

A CASE STUDY OF A TIED-BACK SOLDIER PILE AND LAGGING RETAINING WALL

by

Gerard P. Madej, P.E.

ABSTRACT

The design and performance aspects of a 40 foot high and 600 foot long tied-back soldier pile and wood lagging retaining wall will be presented. This wall was utilized to retain one side of the excavation for a nine story, one million square foot structure recently constructed in Michigan. The retained soil consisted of a mixed face of rubble fill and natural soil. A series of slope indicators and settlement points monitored horizontal and vertical movements of the wall and the retained earth. Load cells were used to measure tieback performance and to verify design assumptions.

The presentation will include wall design considerations, problems experienced during construction and maintenance of the wall, and a discussion of design assumptions and of the field instrumentation results. Sketches showing the field instrumentation results, design soil parameters and typical wall cross sections are included for reference purposes.

Legal considerations prevented publishing of the entire text of the presentation.

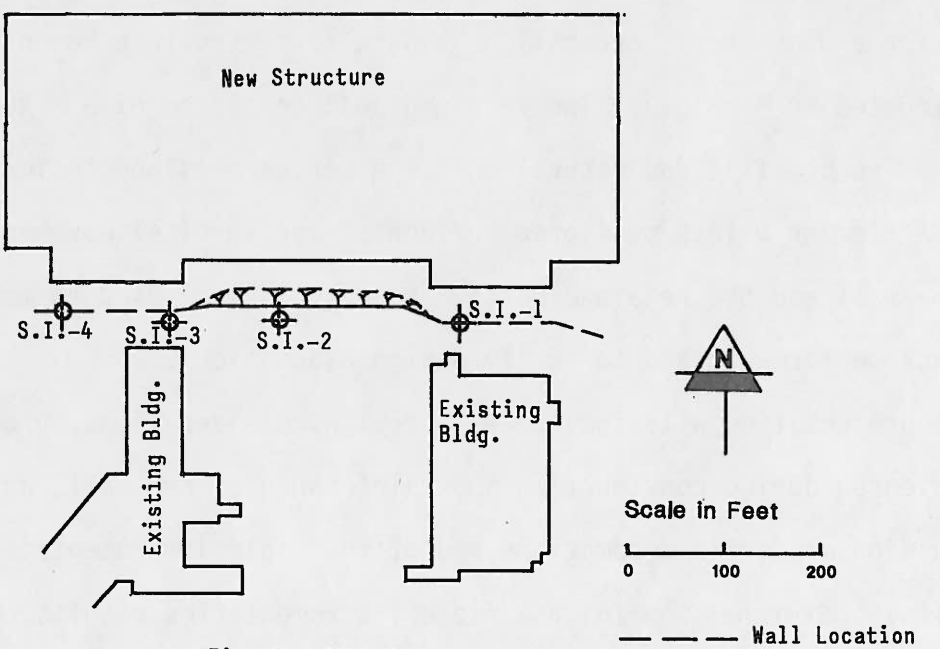


Fig. 1. SITE PLAN

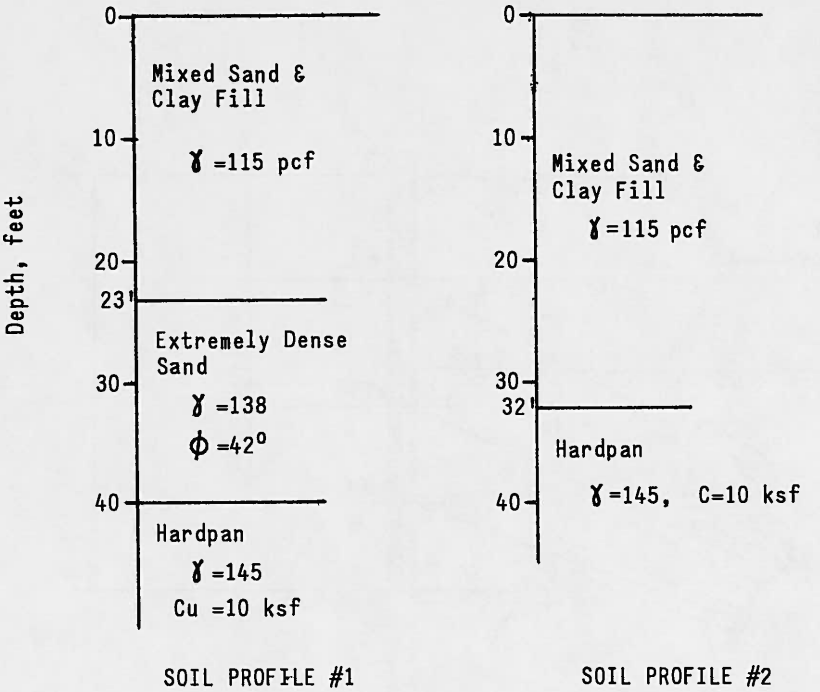


Fig. 2. DESIGN SOIL PROFILES

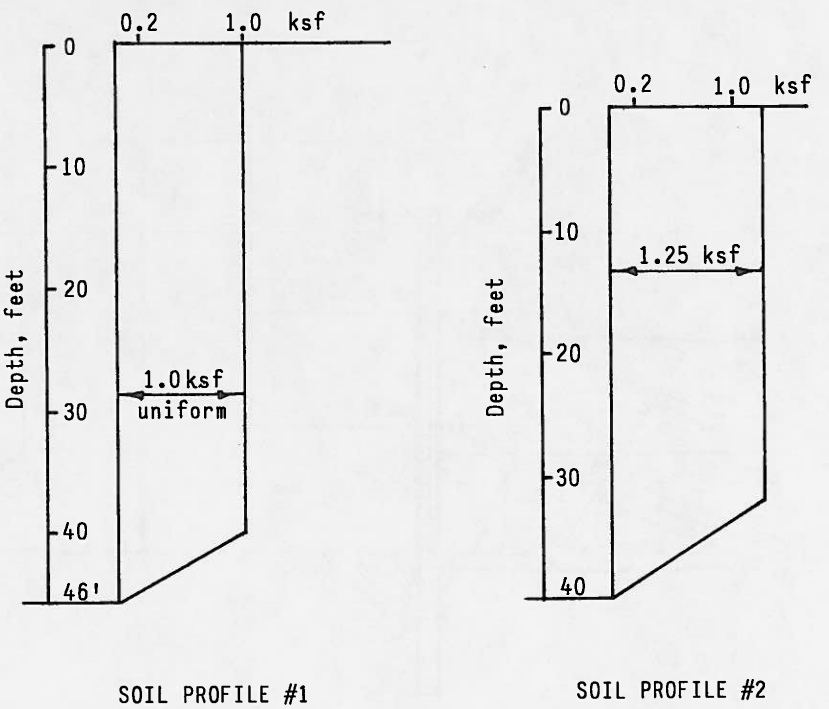


Fig. 3. DESIGN EARTH PRESSURE DIAGRAMS

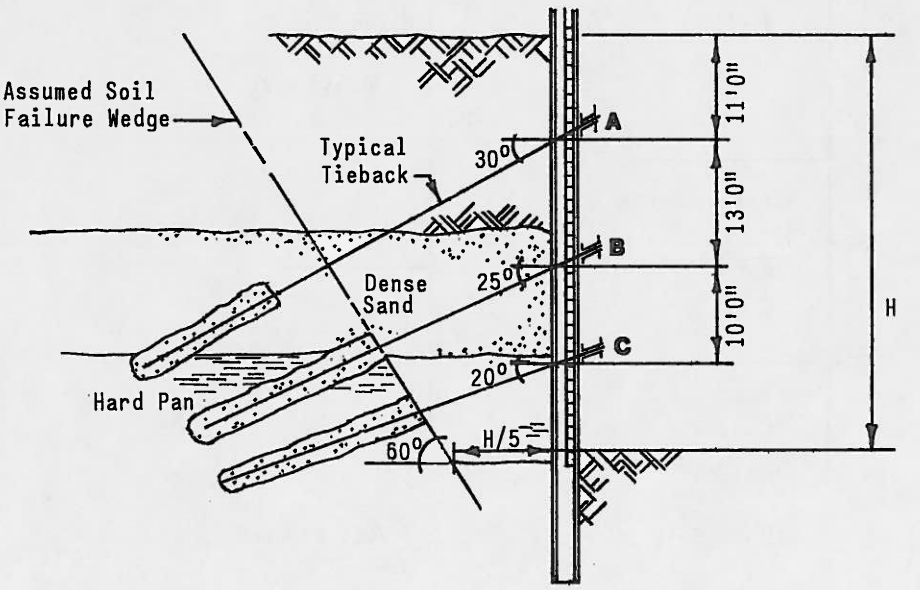


Fig. 4. TYPICAL WALL SECTION

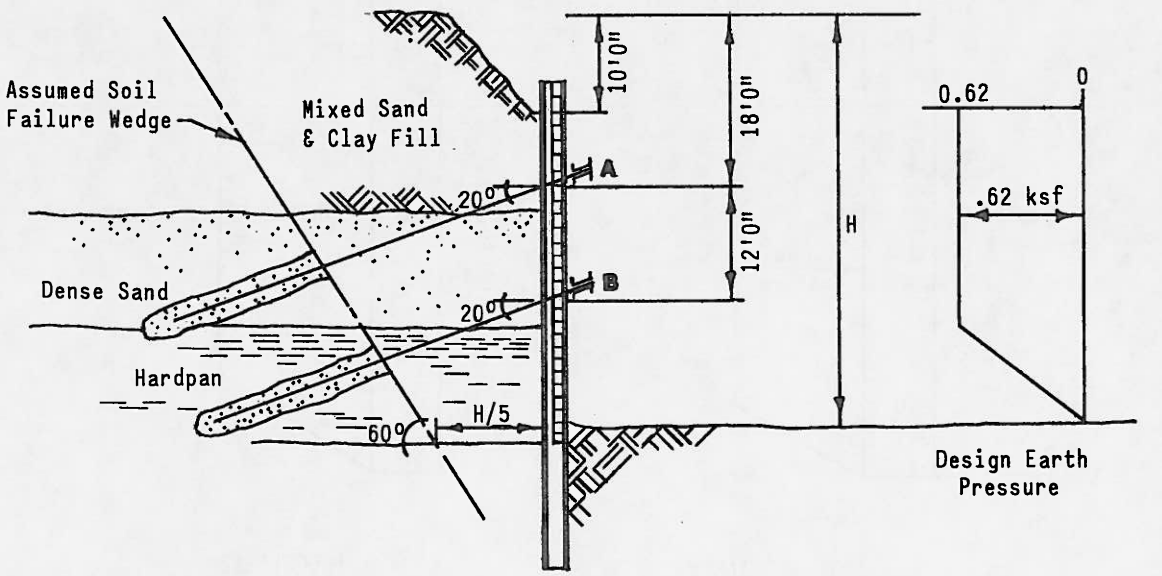


Fig. 5. CENTRAL AREA WALL SECTION AND DESIGN EARTH PRESSURES

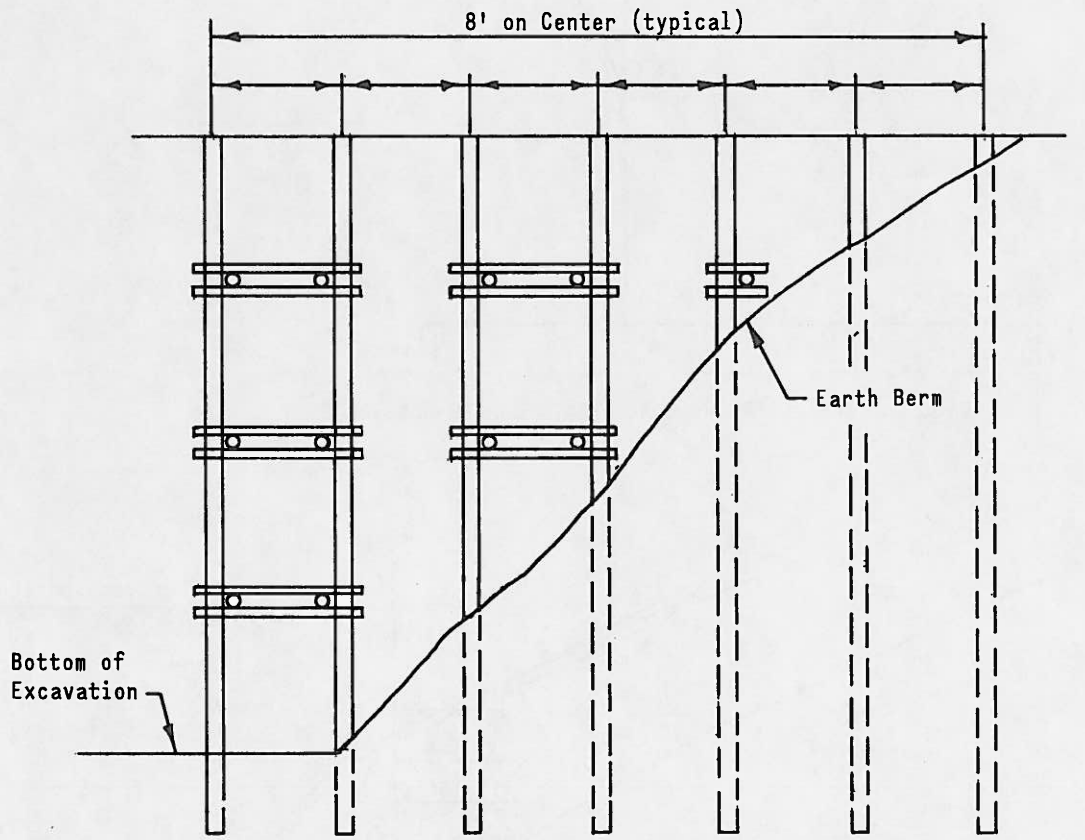


Fig. 6. EARTH BERM RESTRAINT AT EACH END OF THE WALL

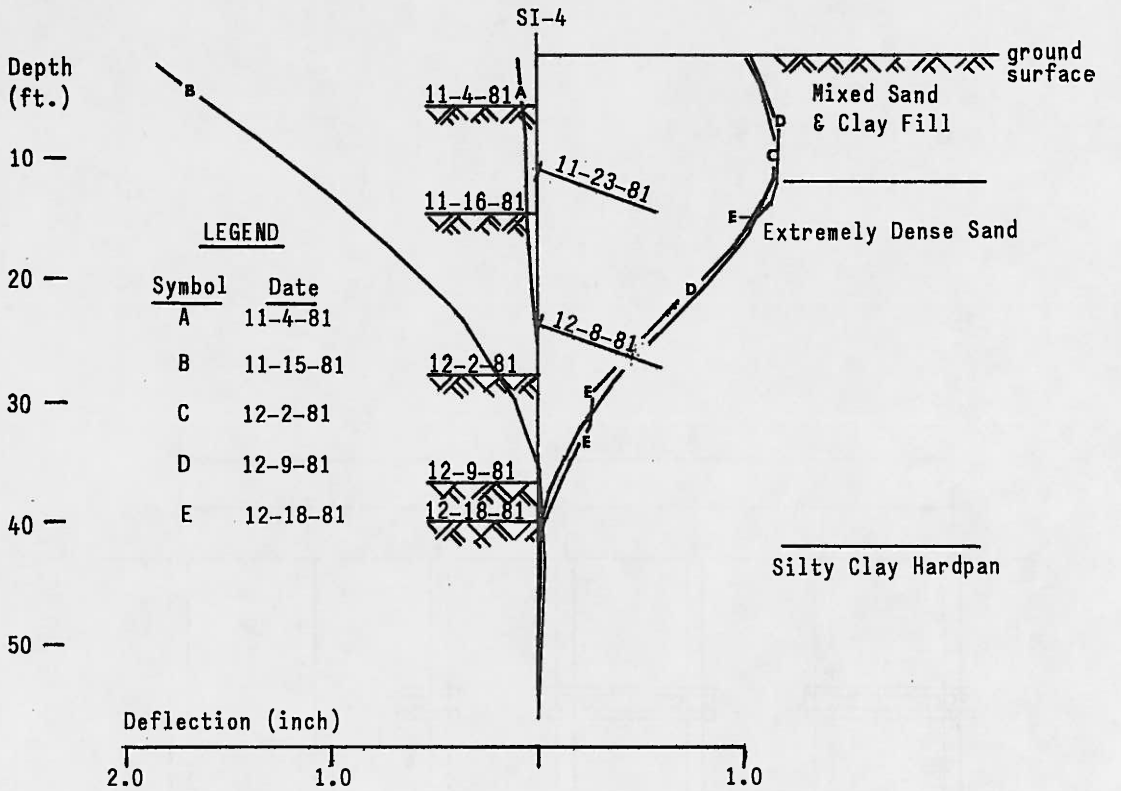


Fig. 7. HORIZONTAL WALL MOVEMENTS DURING CONSTRUCTION

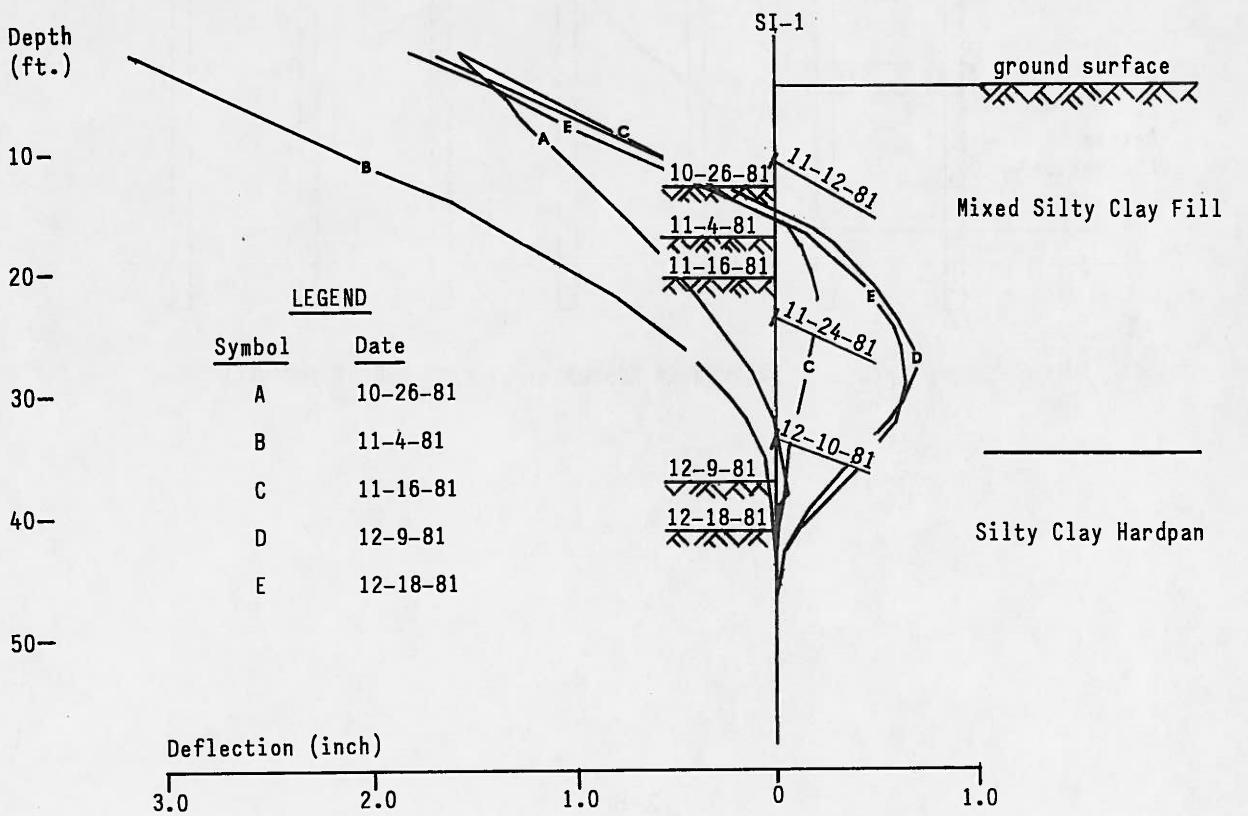


Fig. 8 HORIZONTAL WALL MOVEMENTS DURING CONSTRUCTION

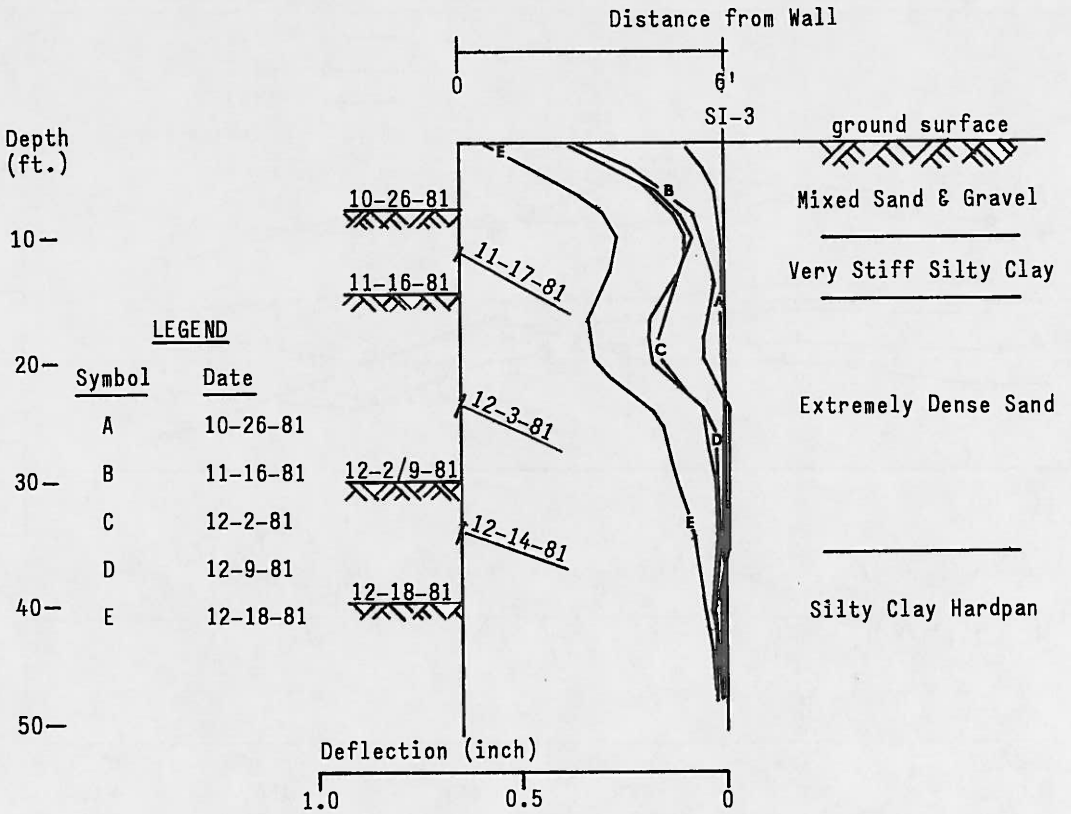


Fig. 9. HORIZONTAL SUBSOIL MOVEMENTS DURING WALL CONSTRUCTION

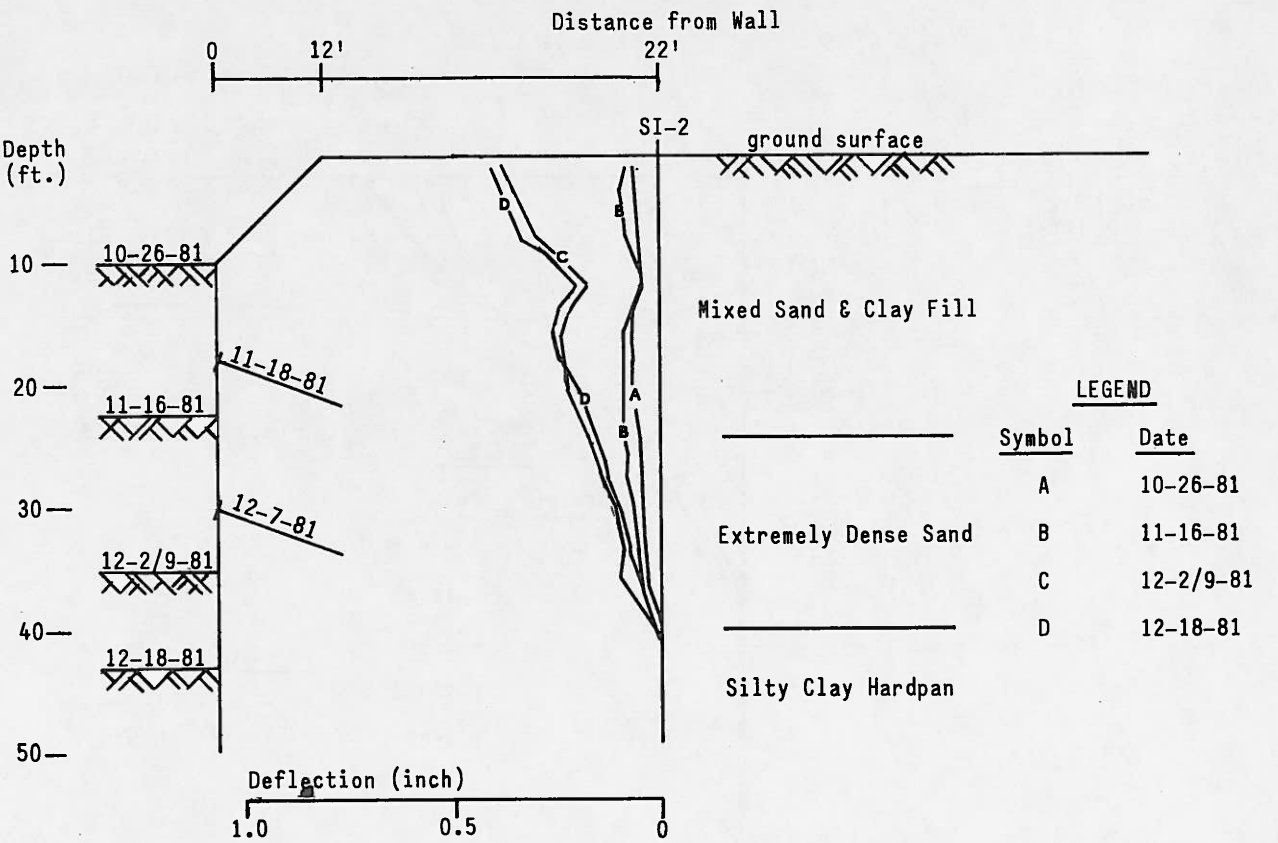


Fig. 10. HORIZONTAL SOIL MOVEMENTS DURING WALL CONSTRUCTION

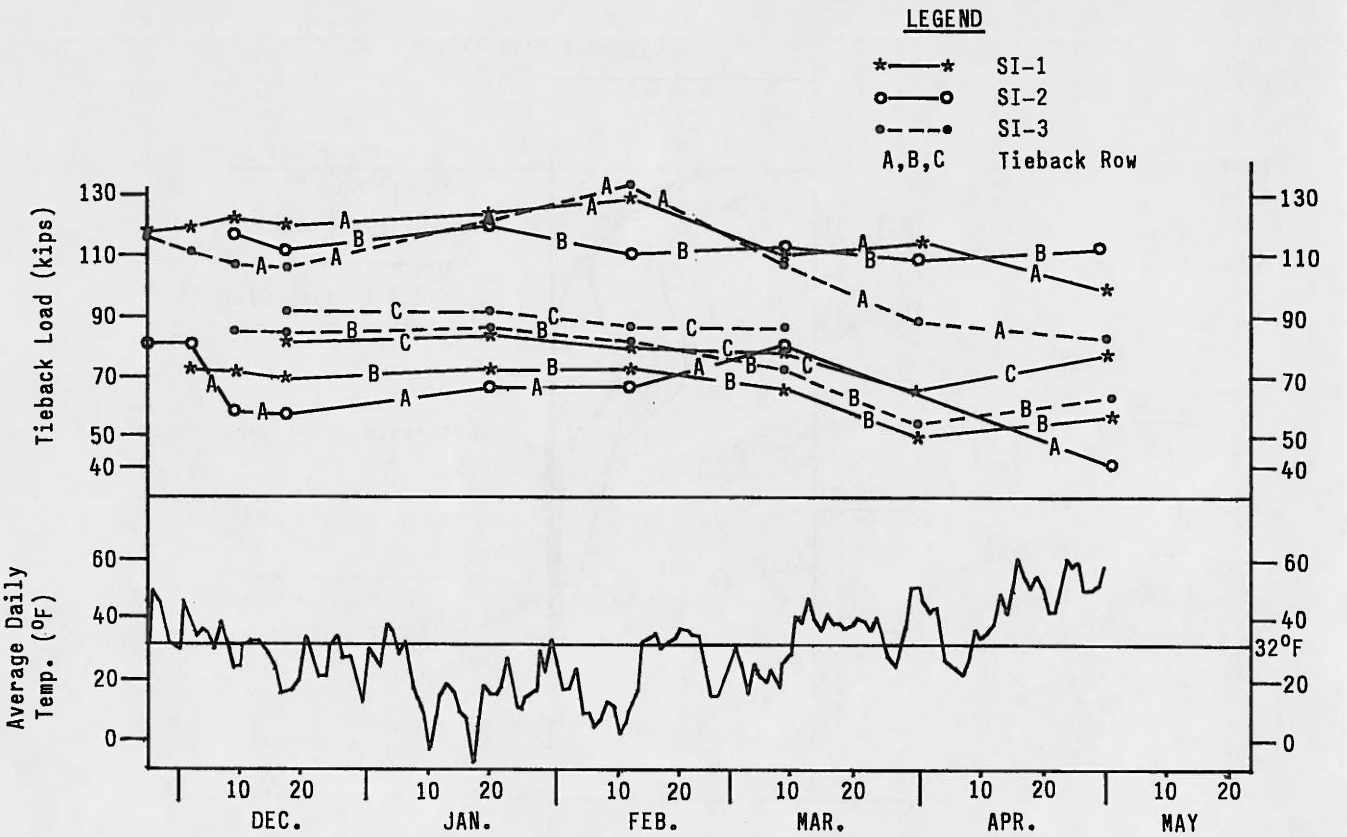


Fig. 11. TIEBACK LOAD AND TEMPERATURE VERSUS TIME

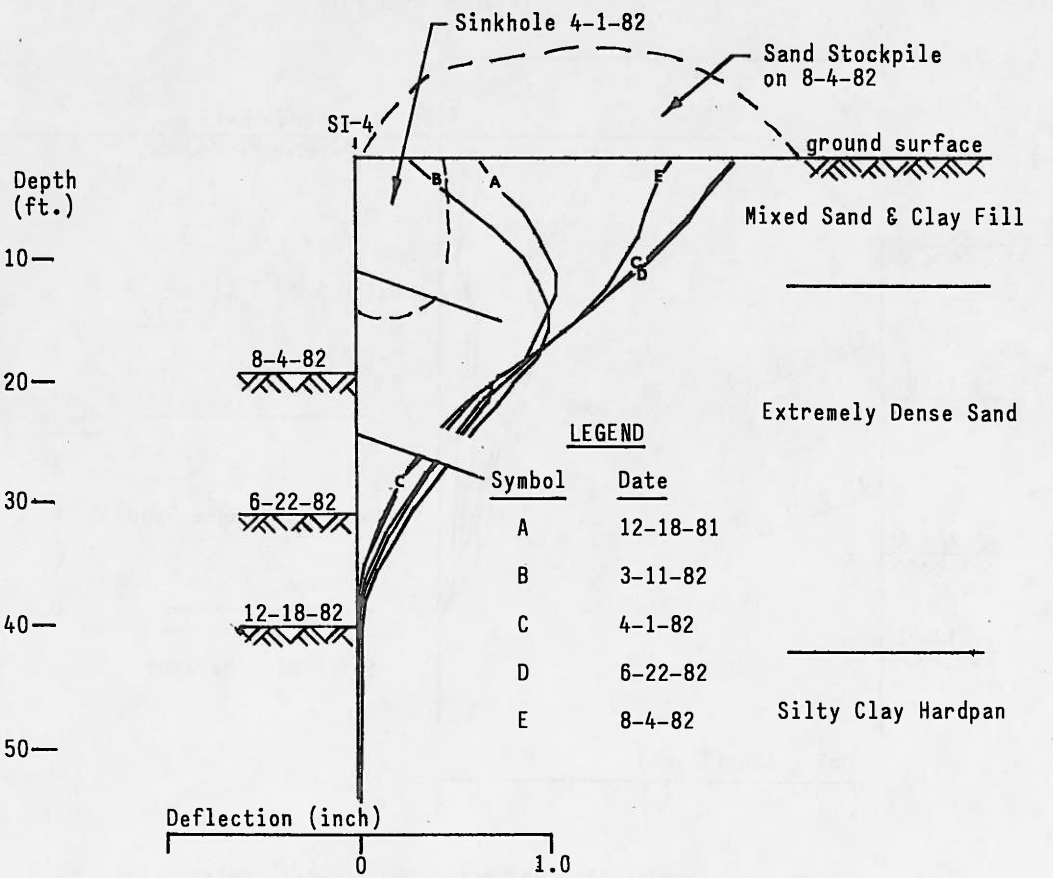


Fig. 12. HORIZONTAL WALL MOVEMENTS AFTER CONSTRUCTION

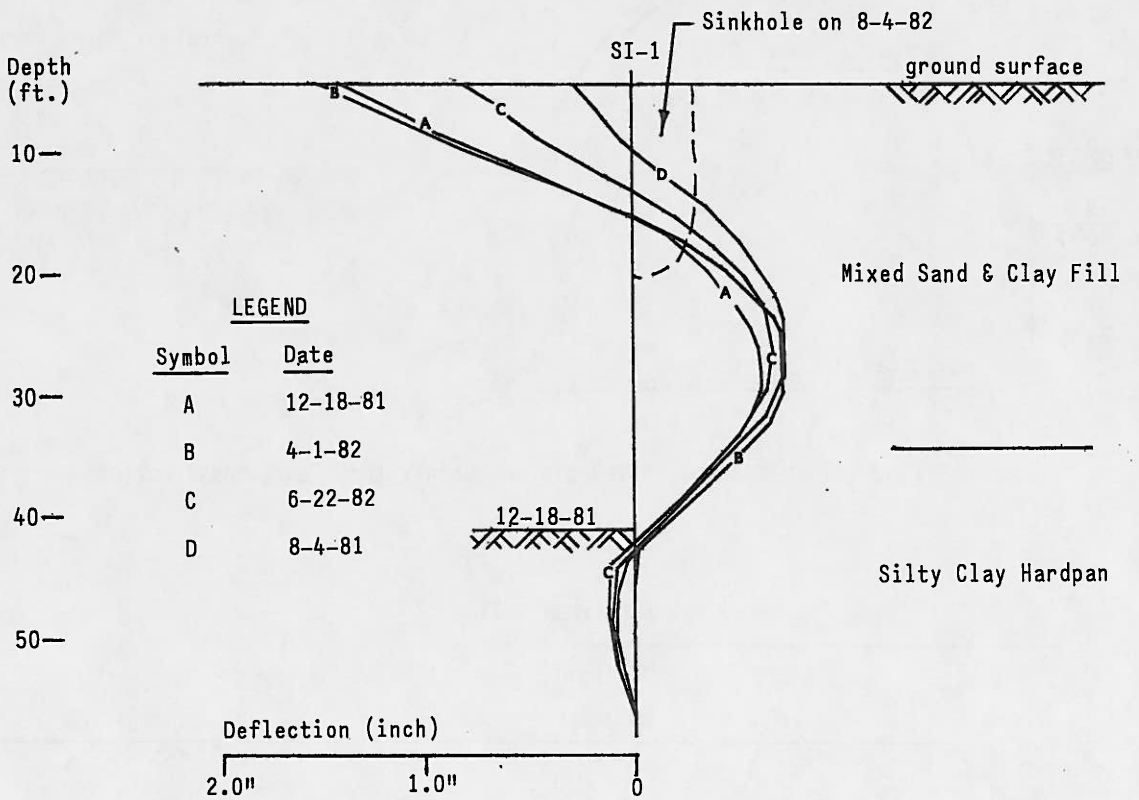


Fig. 13. HORIZONTAL WALL MOVEMENTS AFTER CONSTRUCTION

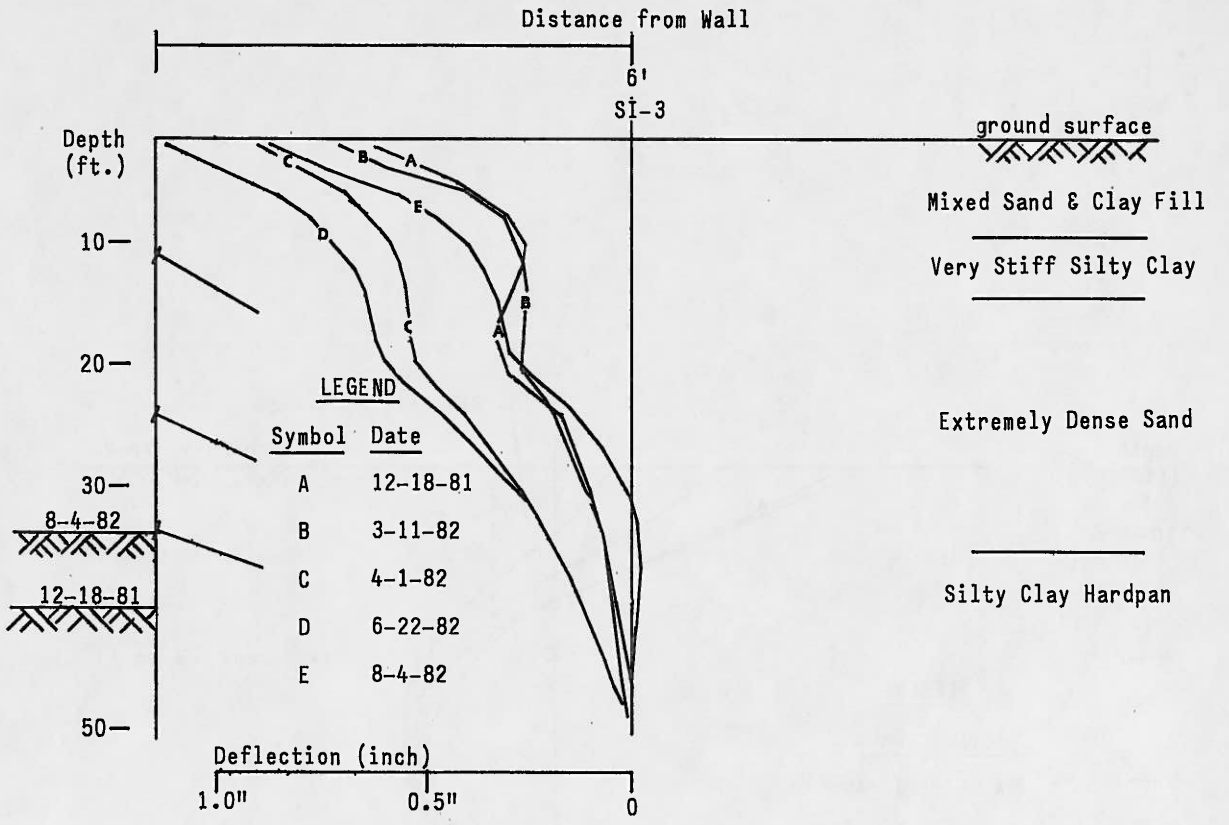


Fig. 14. HORIZONTAL MOVEMENTS OF SUBSOIL AFTER WALL CONSTRUCTION

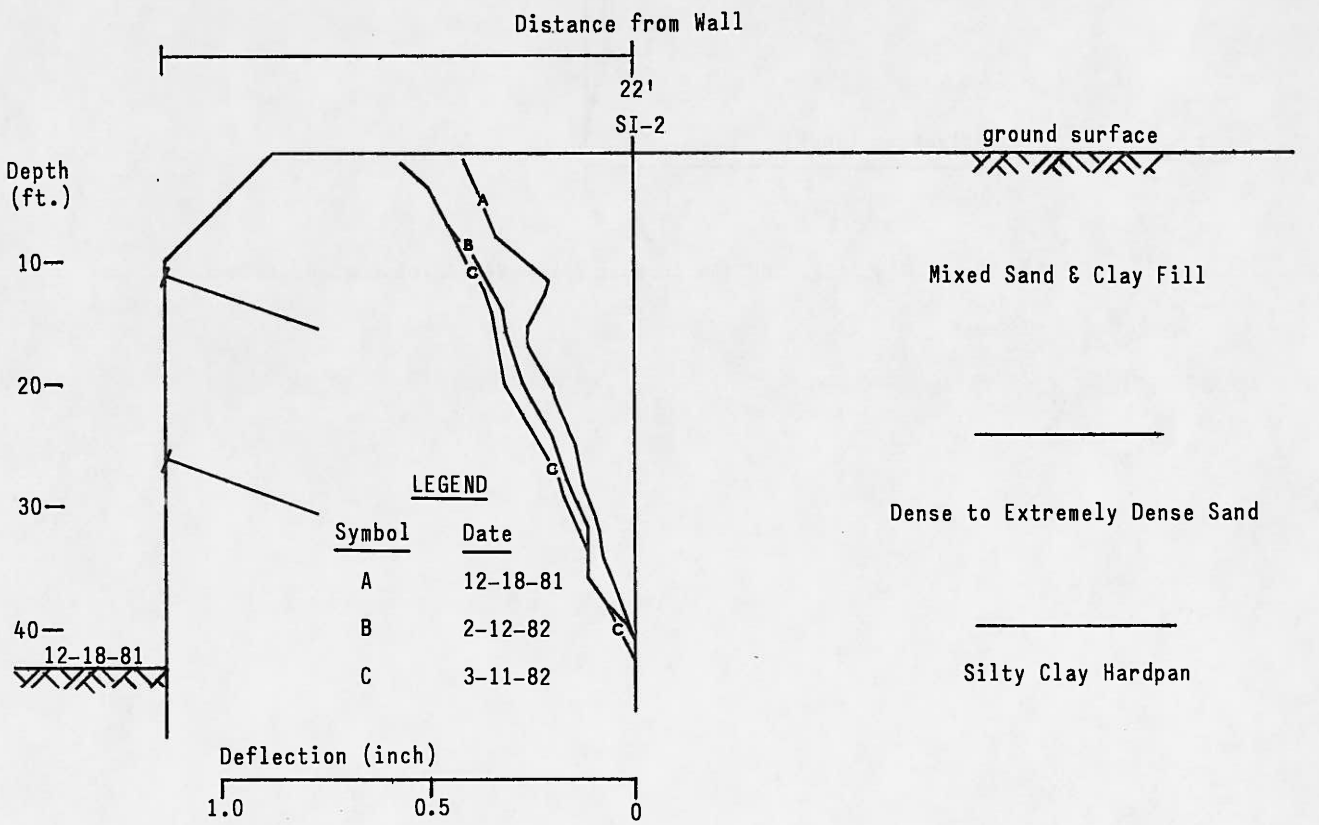


Fig. 15. HORIZONTAL MOVEMENTS OF SUBSOIL AFTER WALL CONSTRUCTION

FIELD MEASUREMENTS OF TIE-BACK BAR PERFORMANCES IN AN EXCAVATION BRACING

by

Andrew Bodocsi[1] and Mark Lockwood[2]

Abstract

The paper describes the methods and summarizes the results of performance measurements made on an excavation bracing project in downtown Cincinnati, Ohio. The excavation was made in sand and gravel, was approximately 37 ft. deep and was braced by a standard tie-back system using anchored Dywidag bars. The field measurements were concentrated on the south side of the excavation where the spread footings of an existing 17-story building were located only 1 ft. away from the edge of the excavation.

It is shown how the tie-back bar stresses were monitored by a hand-held extensometer that was moved from bar to bar to make the measurements. This method of monitoring bar forces was found to be simple, versatile and accurate enough to be used on a large number of tie-back bars on the project, and at minimum expense. The paper also describes how the use of

---

[1] Associate Professor of Civil Engineering, University of Cincinnati, Cincinnati, Ohio

[2] Geotechnical Engineer, The H. C. Nutting Company, Cincinnati, Ohio

the extensometer device helped to discover the effects of construction vibrations on the tie-back bar forces and how some of the tie-back bars temporarily lost a portion of their prestress forces. A hypothesis for this phenomenon is also presented.

Introduction

This case history documents the monitoring and performance of a tie-back bracing wall system which was subject to unexpected vibrations due to wrecking operations.

The wall was built in 1978 to temporarily support the sides of the deep excavation of the Fountain Square South Project in downtown Cincinnati, Ohio. A plan and side view of the south side of the site is shown in Figures 1a, 1b, 2a, and 2b. The excavation was approximately 37 ft deep below street level and covered one half of a city block. On its 400 ft wide south side, the excavation was bordered by buildings from 6 to 17 stories high, with basements and sub-basements ranging from 10 to 20 ft below street level. On the other three sides, the excavation was bounded by city streets. This paper is concerned with the south wall only.

Site Conditions

The subsoil profile was developed by The H. C. Nutting Company during their geotechnical investigation of the project. Concurrence with the profile was found during

construction. Figure 3 represents the typical profile based on data collected from borings and observations along the south wall of the project.

Lying below the street elevation of approximately 545 feet was a fill. It consisted of a 2 to 10 feet thick layer of sandy clay or sand and gravel with random materials which included cinders, brick, concrete and rubble fill. Underlying the fill was a dense to very dense coarse sand and gravel. This stratum reached downward to between elevations 512 to 522.

Lying below the dense sand and gravel were medium dense to dense, fine to medium sands with some coarse sand and a small fraction of fine gravel. These materials were encountered to elevation 505 to 512. Below these lay a medium dense to dense uniform fine or medium sand to an approximate elevation of 495. Thin to thick silt, sandy silt, and silty clay seams or lenses were prominent within this zone of the profile. This deposit was significant for two reasons: The bottom of the excavation was seated within this zone and provided the bearing surface for the building footings of the project; Also, the majority of the lower anchors on the south wall were installed in this layer.

Below the uniform sand was a layer of medium dense sand with gravel. Underlying this material was medium dense to dense

sandy silt or silty fine sand. Beneath that was a medium stiff to very stiff silty clay, clayey silt, and sand clay. These cohesive soils contained sand seams in the lower parts of the layer.

The cohesive soils were underlain by medium dense to very dense sand and gravel, often containing limestone floaters or fragments. Bedrock underlay the sand and gravel and was the Cincinnati Series (Ordovician Age) interbedded shale and limestone.

Local perched groundwater conditions were found above the silt and clay lenses within the subsoil profile. Two observation wells were installed and monitored for groundwater levels. The groundwater table was typically between elevations 470 to 475, that is, 25 feet or more below the bottom of the excavation.

The Bracing System

On the south side of the excavation, the bracing wall was constructed by using vertical 12 HP 53 piles spaced at 4 feet on center and driven 5 to 10 feet below the bottom of the planned excavation (Fig 4). With the progression of the excavation, horizontal reinforced concrete panel lagging was installed in 4 feet vertical increments. Also, at specified elevations, walers were provided for the attachment and anchorage of the tie-back bars. The tie-back bar

installations were made by an Air-trac drill with a percussion hammer. The hammer drove a 76 mm hollow string with a conical point countersink lead element which was to receive a threaded 1-1/4"dia. Dywidag bar. The point was advanced at a 10^{0} inclination to its design location at which time the bar was placed in the string and the conical point driven off. Grout was injected through an adaptor at the outer end of the string and pumped to the annular space at the end. The tie-back bars in the system were typically 30 feet long with 15 feet long anchor bulbs. To achieve only the 15 feet of anchor resistance, the 15 feet above the grout bulb was taped to inhibit bonding. The grout was pumped into the system under a 300 to 400 psi presssure. The drill string was extracted in 12 inch increments and pumped intermittently at design pressure. The process was repeated until the grout zone was completed. Each of the tie-back bars were prestressed to a proof load of 120 kips and then released to a design load of 100 kips. This prestress was based on the estimated at-rest earth pressure, the selected layout of the bars and an adequate safety factor.

In the middle segment of the south wall there was left intact the heavy reinforced concrete foundation wall of the wrecked Gibson Hotel building. The contractor drilled through this wall and tied it back to make it serve as an in-situ bracing wall.

Richard Goettle, Inc., General Contractors of Cincinnati, designed and constructed the tie-back wall.

Field Instrumentation and Monitoring Procedures

Nine test sections along the south wall were instrumented and monitored during the excavation and the early construction phases. The south wall was considered to be the most critical because of the high surcharge loads from adjacent structures, one of which on the east end was 17 stories high. Figures 1a and 1b provide a plan view of this wall and the location of the existing structures. Figures 2a and 2b present views of the south wall and show depths of adjacent footings, test section locations, and elevations of pertinent wall structures and instrumentation.

The City of Cincinnati provided a survey crew to monitor the horizontal and vertical wall movements. Two or three control points were established on all piles of the south wall for horizontal control. They also established vertical control on selected piles, as well as adjacent buildings. The horizontal control points furnished a complete wall movement profile. The vertical control provided a settlement check on the wall itself and the adjacent buildings. The east end of the south wall had control points at the top of the piles and 6 and 10 feet below. The west end had control points at the top of the piles and 17 feet below.

Three inclinometers were also installed along the south wall, but only one yielded usable results. The one on the east end became disconnected early in the construction phase and one of the two on the west end failed to give consistent results.

The tie-back bar loads were monitored by a hand-held, movable extensometer device which measured the loads with a 1% to 3% accuracy, or, in this case, within 1 to 3 kips. Figure 5 shows a version of this simple device, as it is positioned over a Dywidag bar in making a measurement.

To prepare the selected bars for measurements, they were given two reference punchmarks into which the prongs of the extensometer could be fitted. These marks were preferably put on top of deformations and were just deep enough to allow the positioning of the instrument. They were typically 5-1/2 inches apart and were made near the face of the bracing wall soon after the bars were grouted in place. At this time the initial "no-load" readings were taken. To facilitate the ensuing measurements, the two-channel walers were made with such spacing between the channels that the extensometer and the hands of the reader could fit between them. At the time of tensioning, a proof reading was taken on each test bar to check the accuracy of the extensometer measurement against the known jacking load. Another measurement was taken after the bar anchorages had been locked and seated. This was the initial "full-load" reading. It was found that the readings were somewhat influenced by the reader's technique,

especially the pressures one applied to the instrument. Usually 8 or 10 rapid consecutive readings were taken and an average of these was recorded as the true reading.

At this point, the questions of "Why should one use this method of bar force measurement? Why not just use load cells?" may be asked. To answer, the following advantages in using the extensometer method may be listed: a. It is cheap; b. It is simple; c. It cannot be disturbed or ruined by construction operations; d. One can have a great number of measurement points prepared for possible future use with little initial expense; and e. It can also be used as a supplementary system to the more sophisticated load cell installations. Specifically, if in working with a limited number of load cells on a project and getting some unexpected results on a given cell, one would wish he had another cell nearby to read. However, the expense of load cells usually dictate that they are distributed uniformly and sparingly over the whole project and there are usually no backup cells. On the other hand, it costs practically nothing to have potential extensometer stations set up around load cells and have them serve as backups.

There are, of course, also disadvantages to using the extensometer. The measurements are time consuming and require a lot of climbing. Also the walers may have to be modified slightly to allow access space for the readings.

Figures 1a, 1b, 2a and 2b show the test sections which were monitored. Altogether, 9 test sections and 27 tie-back bars were monitored on this project.

Performance of the Wall and Results of Measurements

The monitoring of tie-back bar forces started immediately after the bars had been tensioned. Readings were taken on the selected bars once a week during the construction of the south wall. After this period, readings were taken every 2 weeks since no sudden changes in bar loads were anticipated beyond the wall construction phase. This same schedule was maintained by the survey crews. Figure 6 shows the plots of the result of measurements on Test Section 27-28. These data are typical for these kind of installations. They show changes in bar forces due to prestress losses, due to the tensioning of adjacent tie-backs, due to load transfers, due to redistribution of loads as tie-backs at greater distances are tensioned, and due to the progress of the excavation below. In order to eliminate a seemingly complicated picture and to get a better view of the overall conditions, the writers averaged out the tie-back bar forces for all bars in both the east and west segments of the south wall, and plotted their variations with time (Fig 7 and 8). Also plotted were the overall average wall movements with time.

The analysis of these figures yielded some expected and also some unexpected results. On Figure 7, one can observe that on

the east segment of the wall prior to July 11, the overall tie-back forces were increasing as the excavation was being completed at the bottom. This was accompanied, as expected, by an overall small movement of the wall into the excavation. However, starting on July 11 and continuing into the early days of August, one observes a fairly dramatic change in tie-back behavior. During this period the average tie-back bar lost 13 kips of prestress, or 15% of its initial level as of July 11. Yet, as the bar forces were decreasing, the wall continued its movement into the excavation. This is important, because for these two phenomena to occur simultaneously, the bar anchorages had to be slipping. After August 8 the movements had stopped and a small recovery of bar forces had taken place. Beyond that, conditions had stabilized with respect to both bar forces and deflections.

On Figure 8 are shown the variations in the overall average bar forces and wall movements on the west segment of the south wall. Starting on July 13, it can be seen that the tie-back forces had gradually decreased and the rate of decrease had accelerated toward the first week of August. In three weeks, the average bar forces decreased by 17 kips, or by 20%. Up until August 3 the wall did not move, but then began to deflect into the excavation at a high rate. It was concluded again that the reason for either no movement of the wall, or any movement of the wall into the excavation while the bar forces were decreasing, had to be due to slipping anchorages. Between August 10 and 17 both bar forces and

movements were temporarily stable. Then, on August 17 the wall started to move again into the excavation, but at this time the tie-back forces reversed themselves and started to pick up and increased by some 12 kips per bar. This ultimately stopped the movements and stabilized the wall.

While the writers suspected that something unusual was happening to the wall between the middle of July and the middle of August, it took them some time to find an explanation for it. During the last two weeks in July and the early days of August a ramhoe and a wrecking ball were used in the excavation to wreck the old reinforced concrete foundation wall that ran in the N-S direction and which was directly connected to the foundation wall used as a bracing in the south wall (See Figure 1). Considerable vibrations were caused throughout the site by this operation. It can be observed that the period of wrecking operation coincided with the time when the above described tie-back force losses occurred in the south wall. In addition, the losses and the wall movements stopped after the wrecking operations stopped. Also, the test stations in the west segment were closer to the wrecked wall than those in the east segment, and they suffered greater tie-back force losses than those in the east segment. Therefore, these writers concluded that the tie-back anchor slippages must have been due to the vibrations in the soil-anchorage system, caused by the wrecking operation. Also, the writers hypothesize that the slippages were due to changes in the resisting shearing forces on the interfaces

between the grout bulbs and the soil as the system underwent vibrations. This change in the resisting stresses may be explained by changes in the effective normal stresses on the anchor interfaces, or by the vibration induced intermittent surges in the tie-back forces, or both. The endochronic theory for soils explains this phenomenon by the new concept called "shear travel" (See Valanis, et al., (3)).

When the losses occurred, the contractor was prepared to take corrective measures, such as retensioning selective tie-backs or even putting in extra tie-backs to compensate for the losses. However, before any action could be taken, the wrecker finished his job and left, and the ensuing measurements of tie-back forces indicated a cessation of losses and a sustained rise in bar forces. The wall was well again.

In analyzing the results of the measurements, the writers thought that the final tie-back force levels that resulted after the recovery of the wall must have a special meaning. Namely, the walls went through a sort of a shake-down, losing a considerable percent of their initial tie-back bar forces during the vibrations. But after the vibrations stopped the trend was reversed and the bar forces increased. This increase, however, did not take the bar forces back to their initial level, but only to a level that stopped the wall movements and which was needed to keep the wall in equilibrium. In order to compare these bar forces with

calculated values, the writers summed up the final overall average tie-back forces acting at two sections of the wall, one at each the east and west segments, and presented them in Figure 9. Also shown are the pressure distributions calculated from earth and surcharge loads behind the wall, using the modified Boussinesq formulas as given by Spangler & Handy (2). As can be seen, the correlation is very good and helps to establish confidence in these surcharge pressure formulas.

Conclusions and Current Research

The paper shows that on tie-back bracing systems the extensometer method of bar force measurement is a viable and even a recommended alternative to measurement by load-cells. By its nature the extensometer method allows the monitoring of many bar forces on a given project and thus provides a better overall view of the condition of a braced wall. Indeed, the writers attribute the discovery of the effects of vibrations on the anchorage capacity of tie-backs to their extensive use of the extensometer on the Fountain Square South Project. It is believed that many sources of vibrations, such as pile driving, wrecking operations, traffic and, most of all, earthquakes, could cause a degree of loss in anchorage capacity, and it is suspected that certain sustained vibrations may even cause failure of some installations. It is hypothesized that the reduction in

tie-back anchor capacity may be due to the slippage between the grouted anchor bulb and the surrounding soil.

The mechanism of anchor slippage and the magnitude of anchor force reductions due to vibrations need to be investigated. A research project on this subject is now in progress in the Department of Civil and Environmental Engineering of the University of Cincinnati.

Acknowledgements

The writers wish to express their gratitude for the encouragement and cooperation they received from Richard Goettle of Richard Goettle, Inc., General Contractors, the Turner Construction Company, the City of Cincinnati and The H. C. Nutting Company. Special thanks are expressed to Rick Merz for his help with the measurements.

References

1. Weatherby, D. E., Tiebacks, Federal Highway Administration, U. S. Department of Transportation, Report No. FHWA/RD-82-047, 1982.
2. Spangler, M. G., and Handy, R. L., Soil Engineering, Harper and Row, New York, 1982.
3. Valanis, K. C., and Reed, H. E., "New Endochronic Plasticity Model for Soils", Research Report NP-1388, Electric Power Research Institute, Palo Alto, California, 1980.

4. Goettle, R., Flaig, J. J., Miller, A. J., and Schaefer, S. E., "Deep Excavation and Buildings Supported by Tie-Back System", Proceedings of the 1972 Ohio River Valley Soils Seminar, Cincinnati, Ohio, 1972.
5. Schnabel, Jr., H., Tiebacks in Foundation Engineering and Construction, McGraw-Hill, New York, 1982.
6. Goldberg, D. T., Jaworski, W. E., and Gordon, M. D., Lateral Support Systems and Underpinning, Vol.1, Design and Construction, FHWA-RD-75-128, 1976.
7. Hanna, T. H., Sivapalan, E., and Senturk, A., "The Behaviour of Dead Anchors Subjected to Repeated and Alternating Loads", Ground Engineering, Vol.11, No.3., 1978.
8. Hanna, T. H., and Al-Mosawe, M. J., "Performance of Prestressed Anchors under Slow Repeated Loadings" Proceedings of the 10th International Conference on Soil Mechanics and Foundation Engineering, Stockholm, 1981.
9. Lockwood, M. E., In-situ Evaluation of an Anchored Retaining Wall, M. Sc. Thesis, University of Cincinnati, 1979.
10. Youd, T. L., "Densification and Shear of Sand During Vibration", Journal of the Soil Mechanics and Foundations Division", ASCE, Vol. 96, No.SM3, 1970.

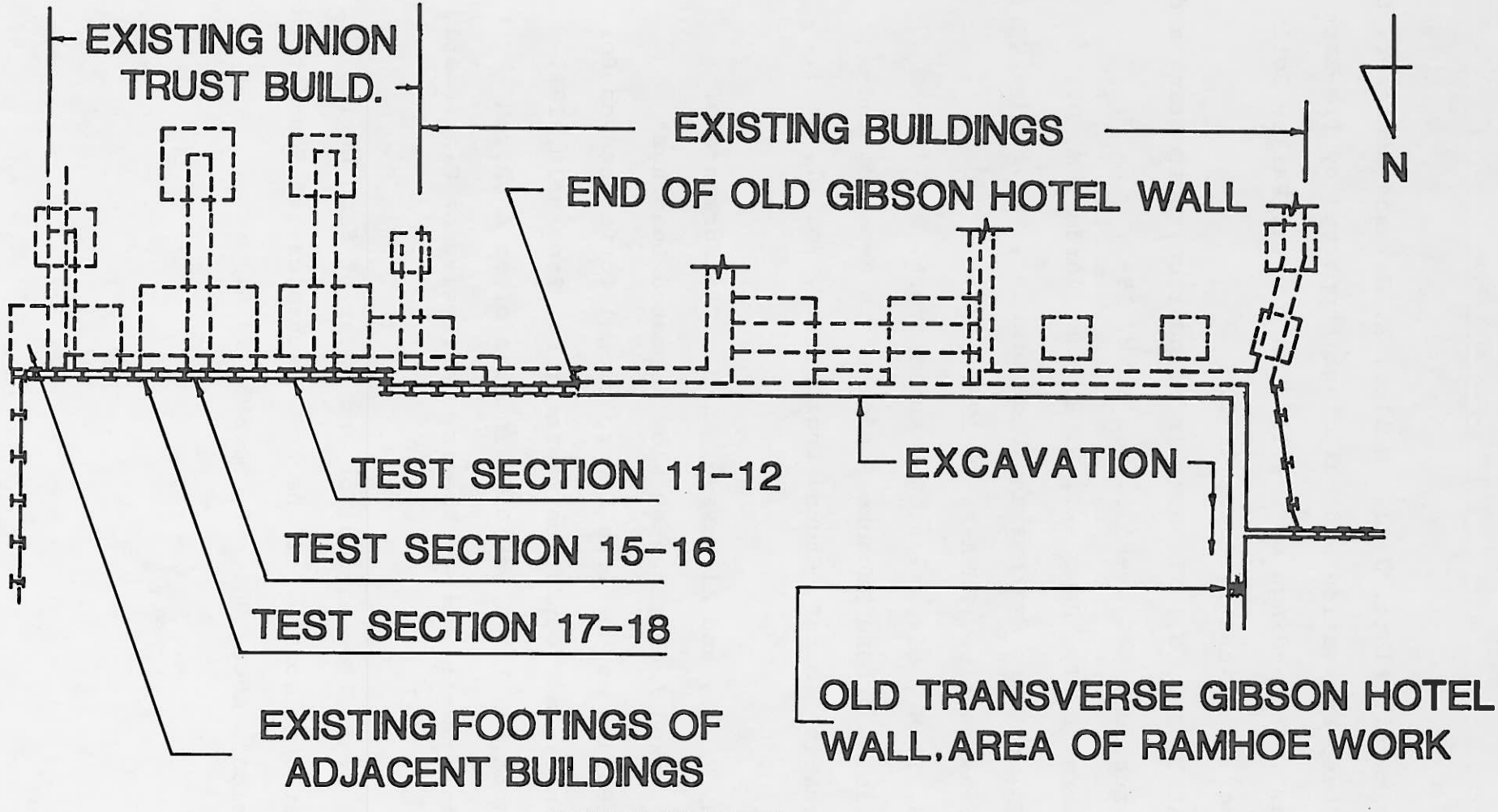


FIGURE 1a.
PLAN OF SOUTH TIE - BACK WALL - EAST SEGMENT

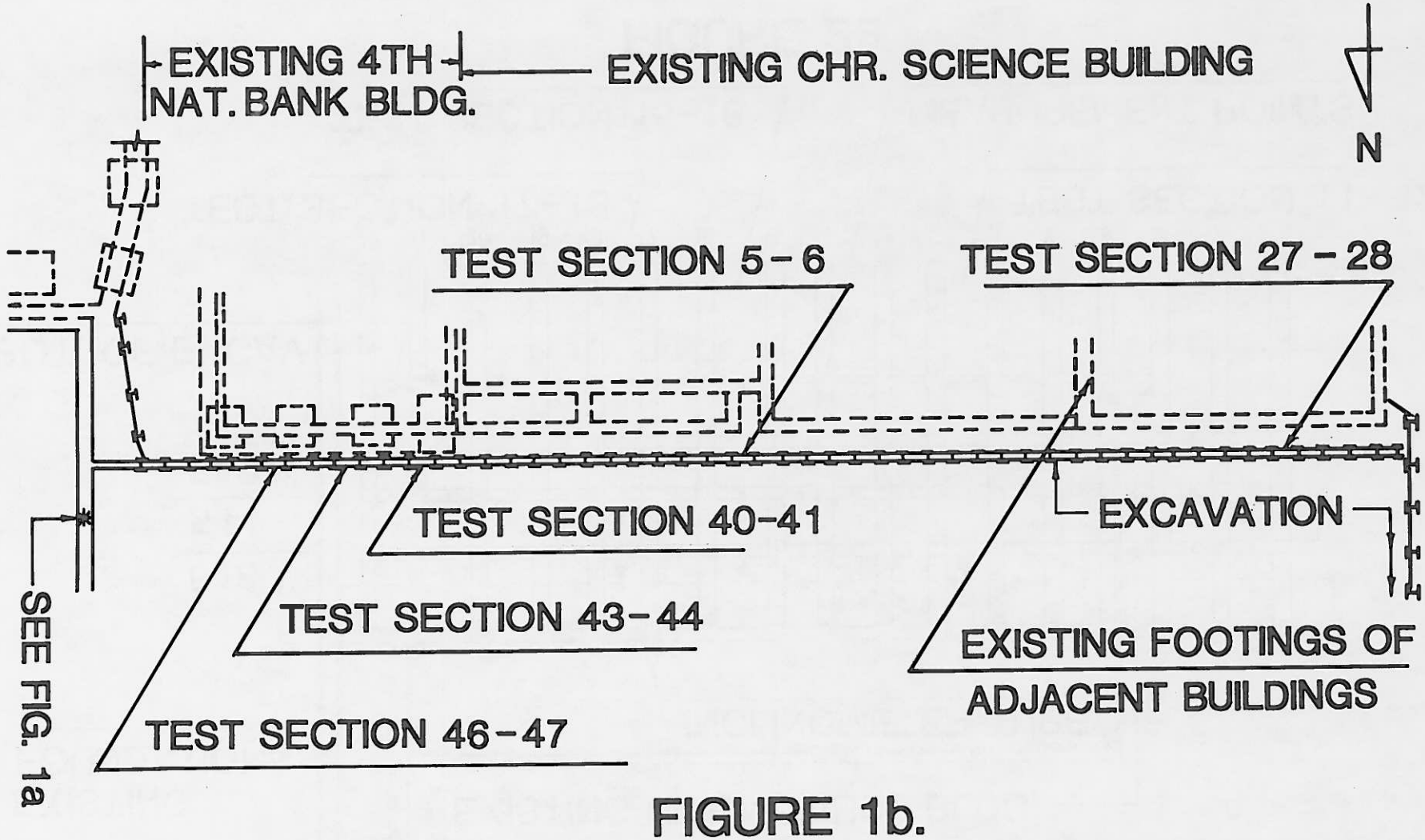


FIGURE 1b.

PLAN OF SOUTH TIE-BACK WALL - WEST SEGMENT

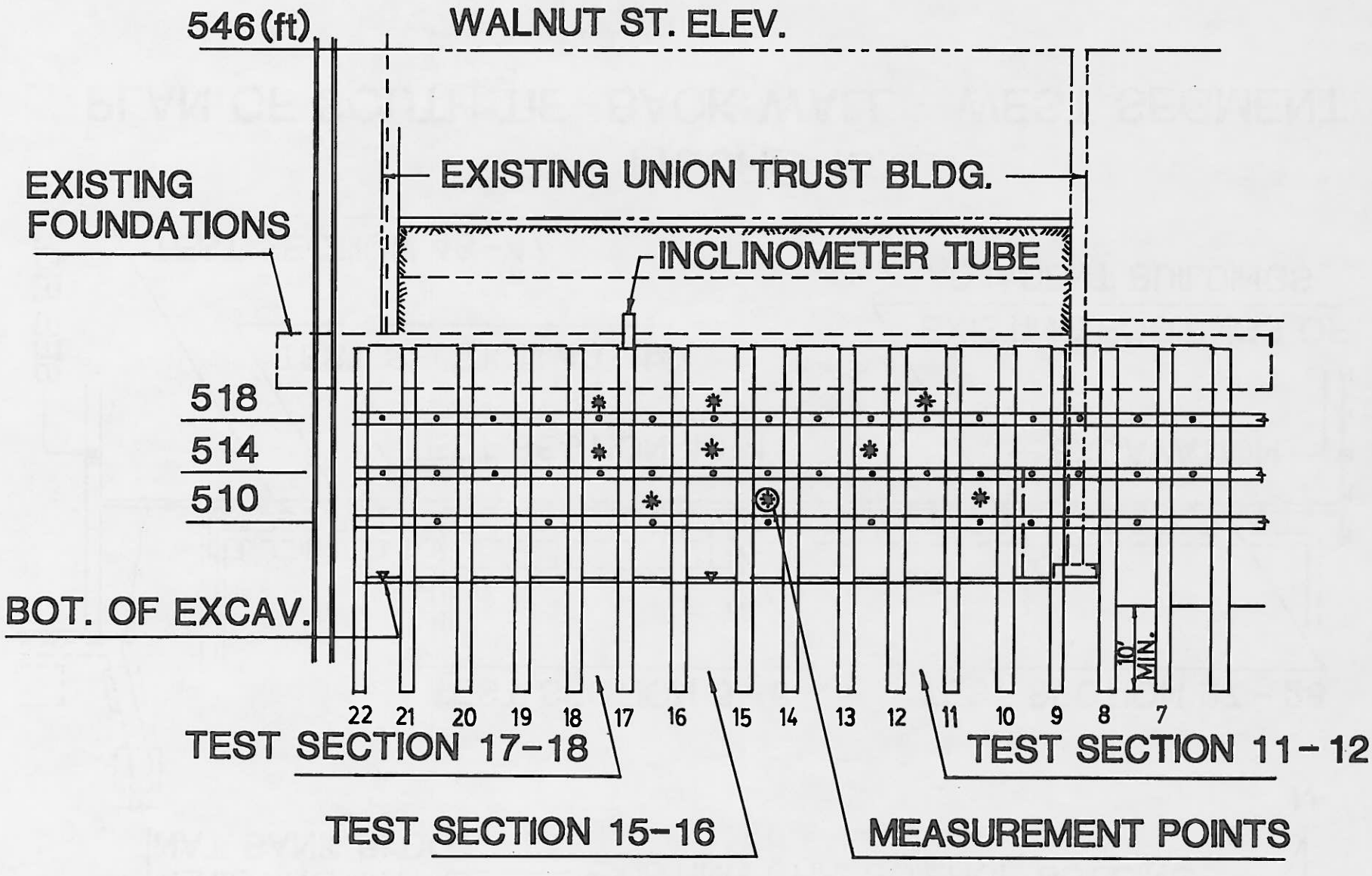


FIGURE 2a.
EAST SEGMENT OF SOUTH WALL

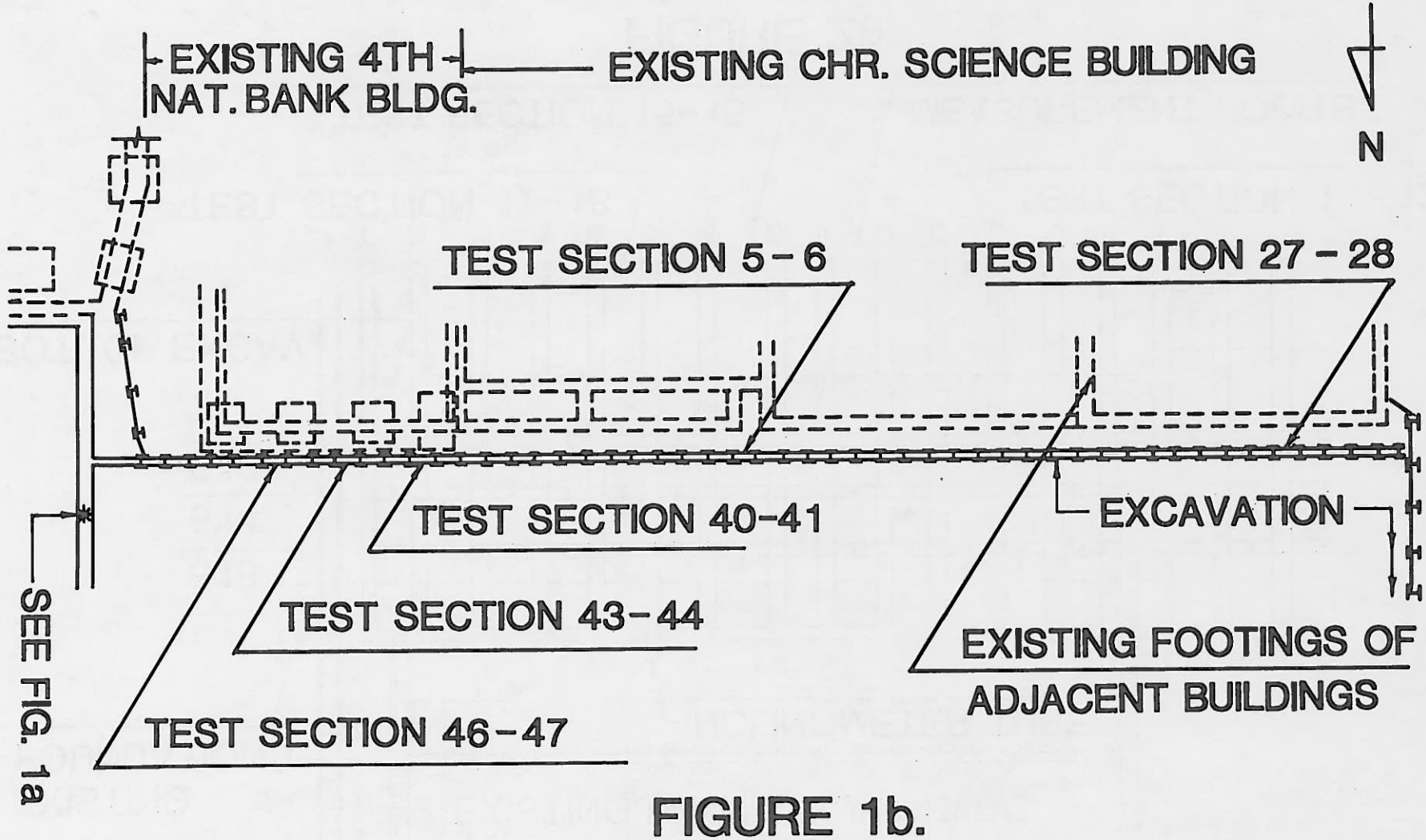


FIGURE 1b.

PLAN OF SOUTH TIE-BACK WALL - WEST SEGMENT

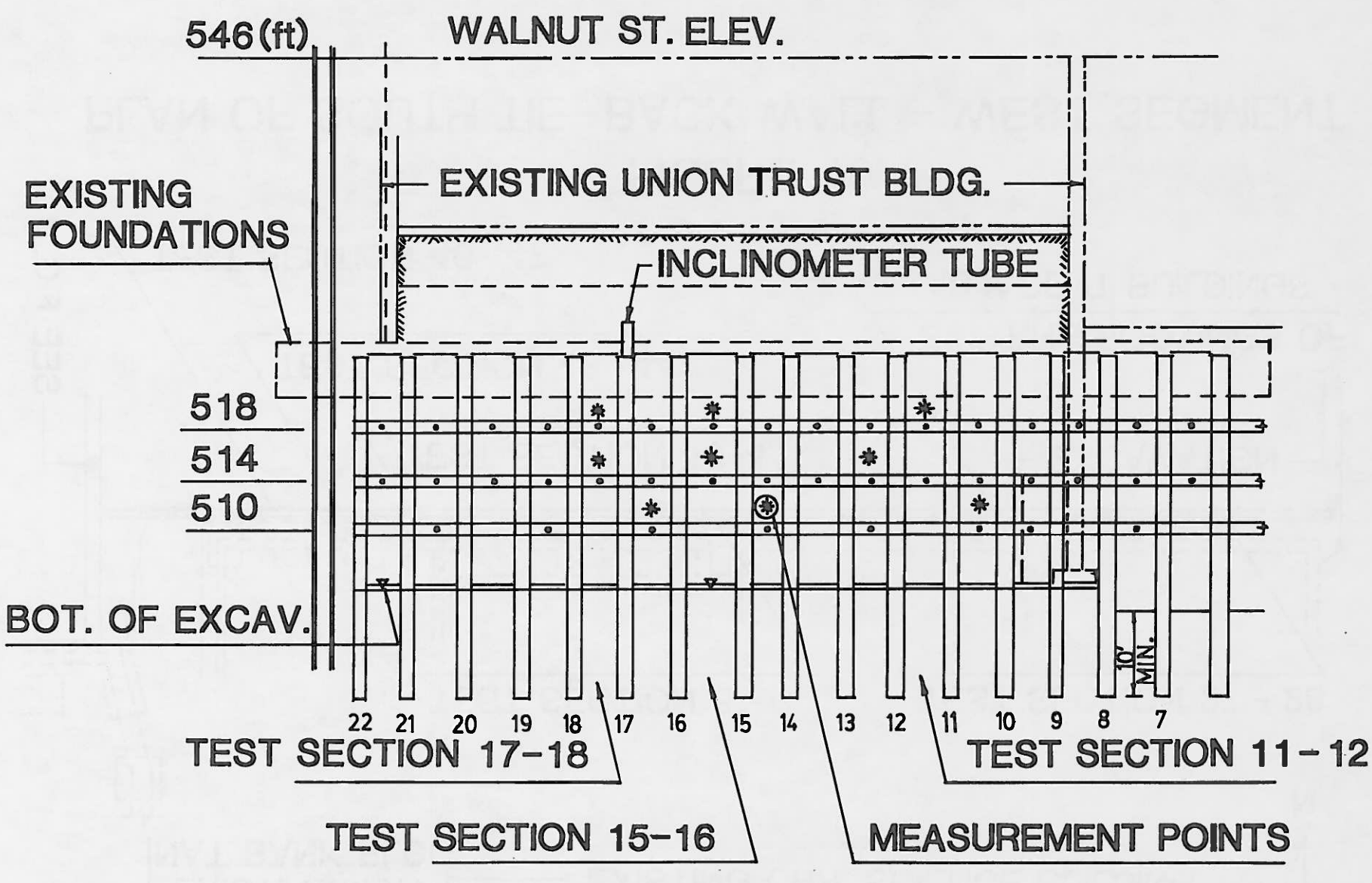


FIGURE 2a.
EAST SEGMENT OF SOUTH WALL

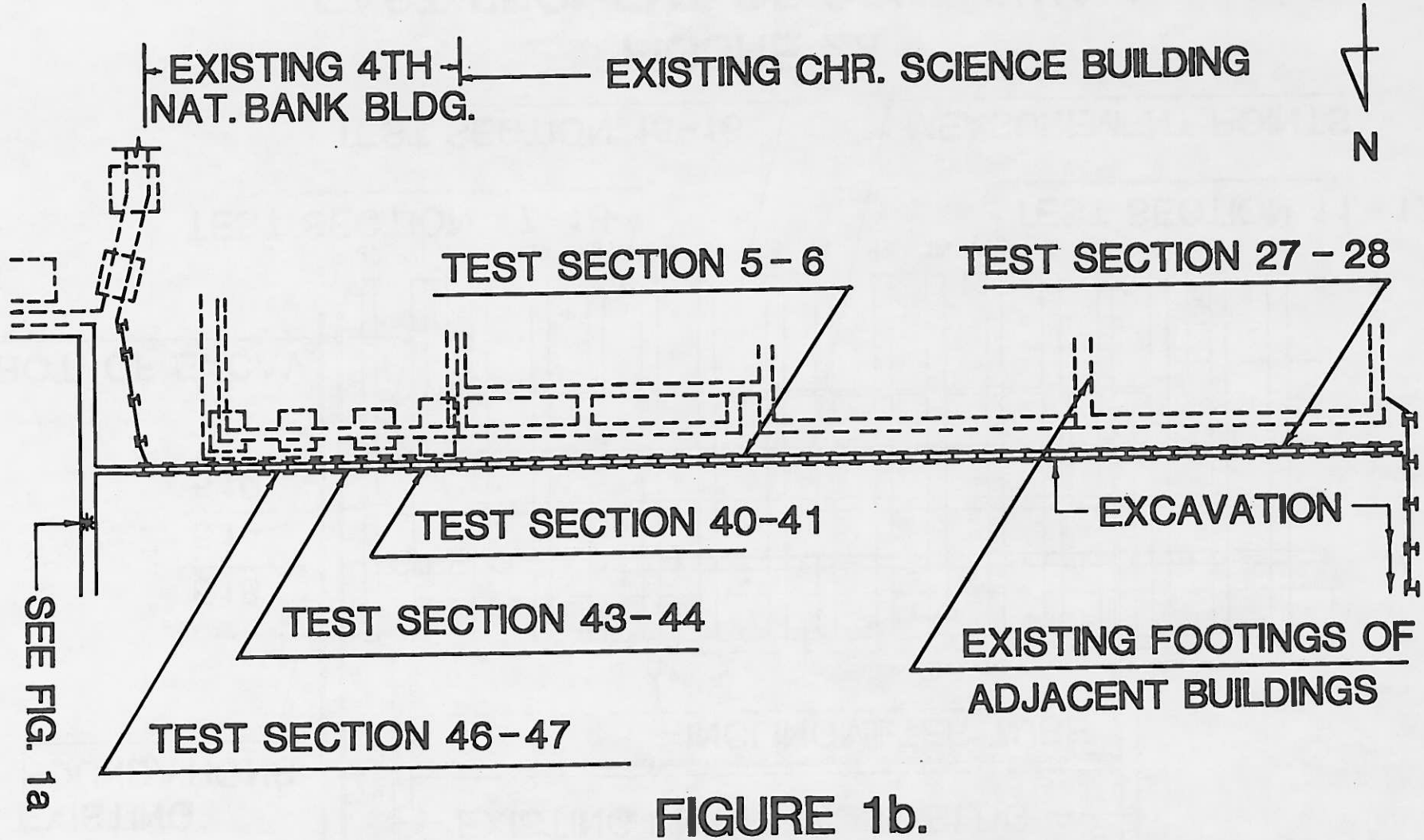


FIGURE 1b.

PLAN OF SOUTH TIE-BACK WALL - WEST SEGMENT

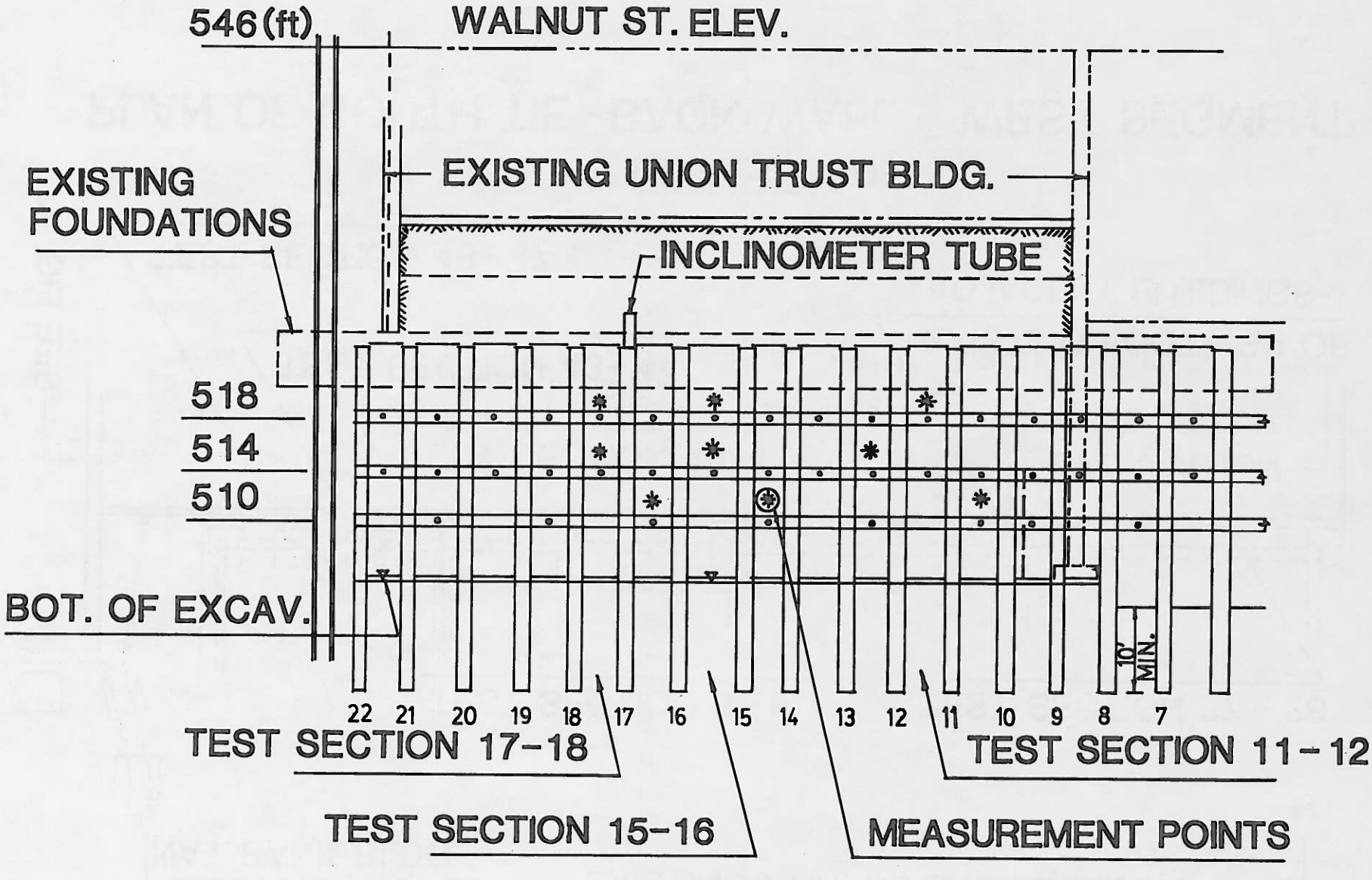


FIGURE 2a.
EAST SEGMENT OF SOUTH WALL

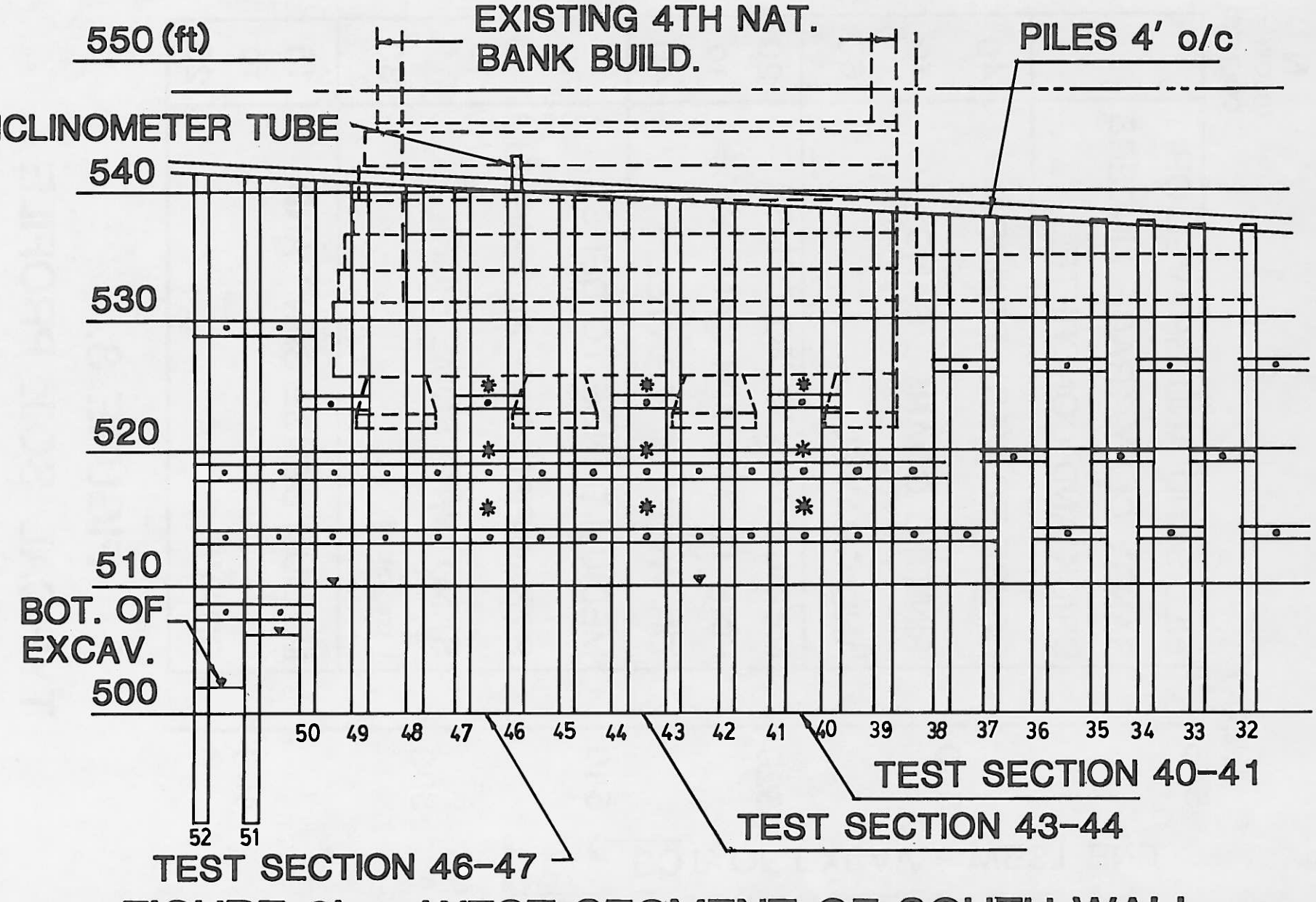


FIGURE 2b. WEST SEGMENT OF SOUTH WALL

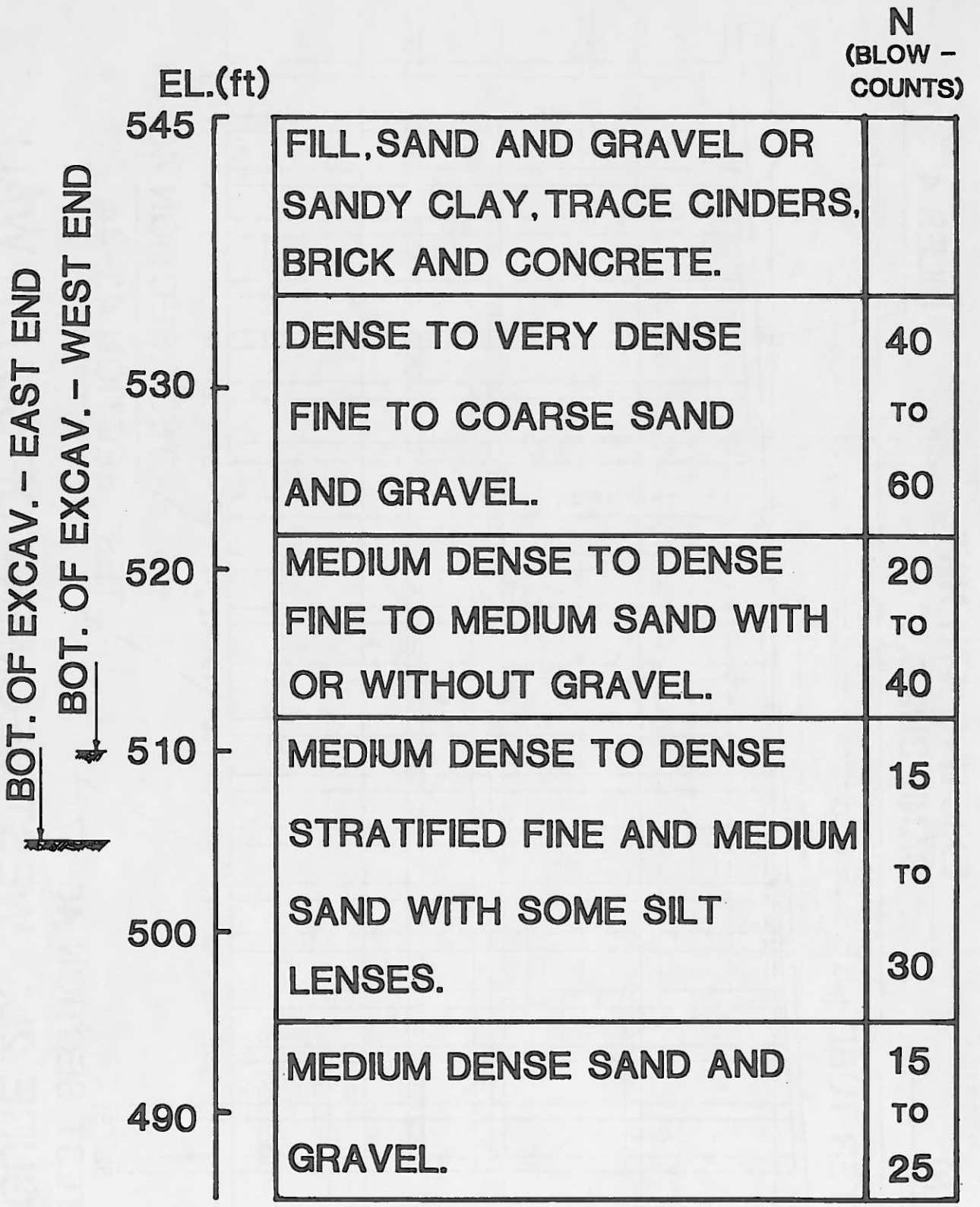


FIGURE 3.
TYPICAL SOIL PROFILE

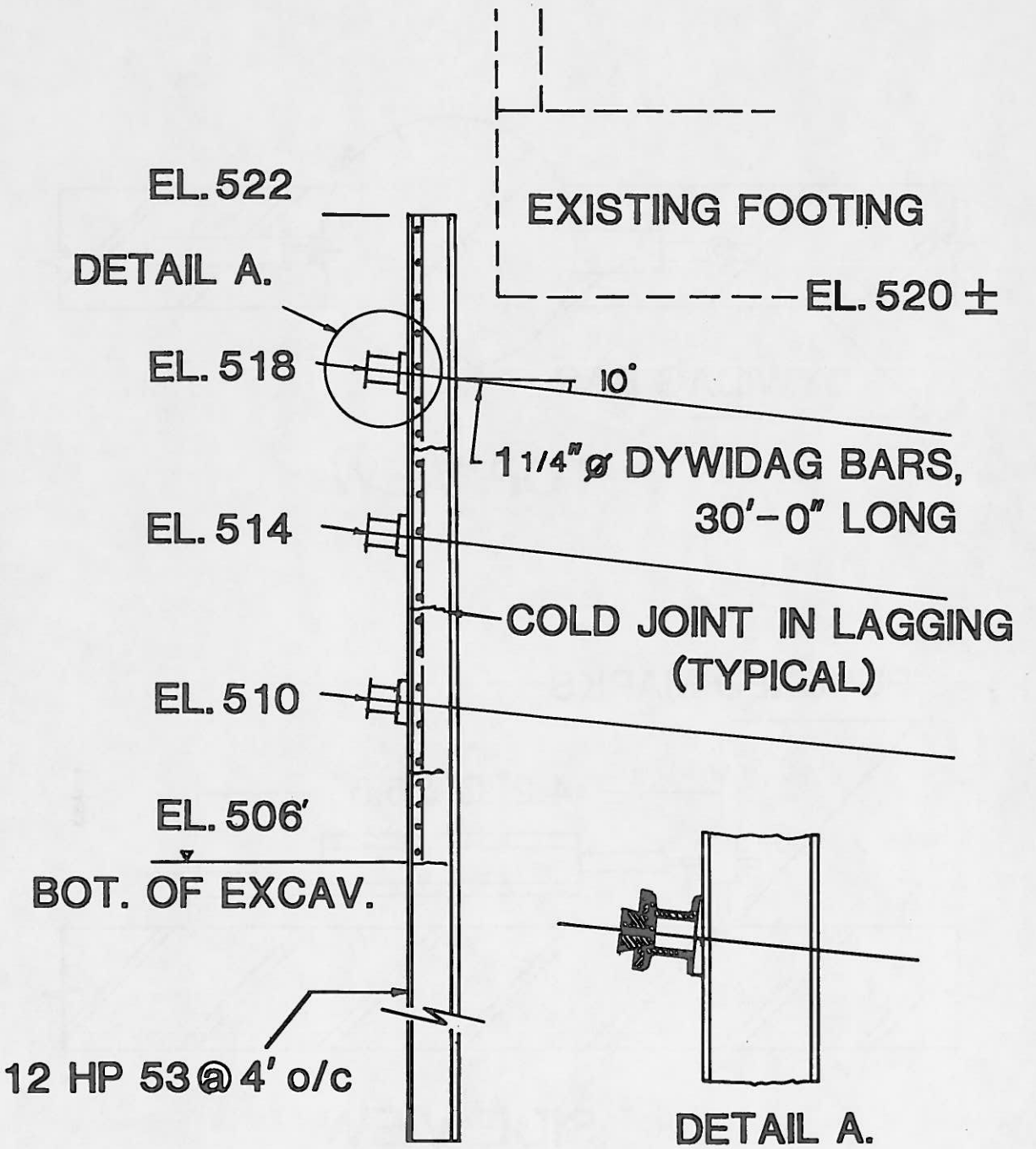
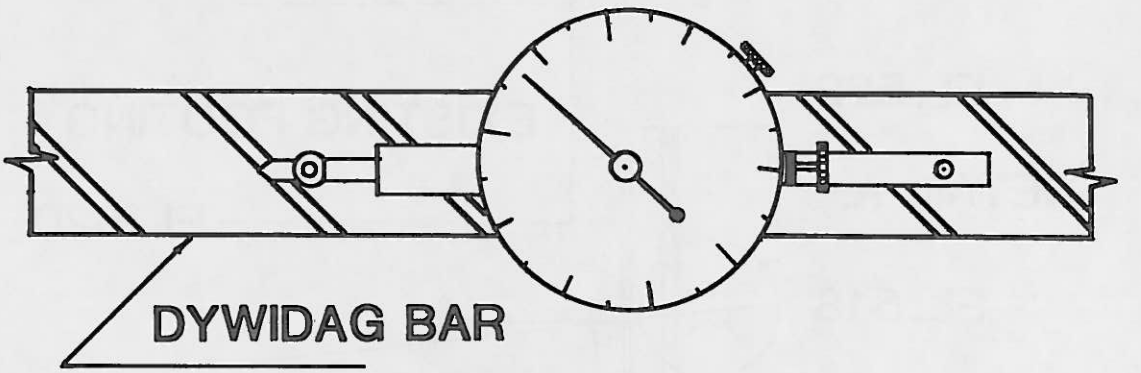
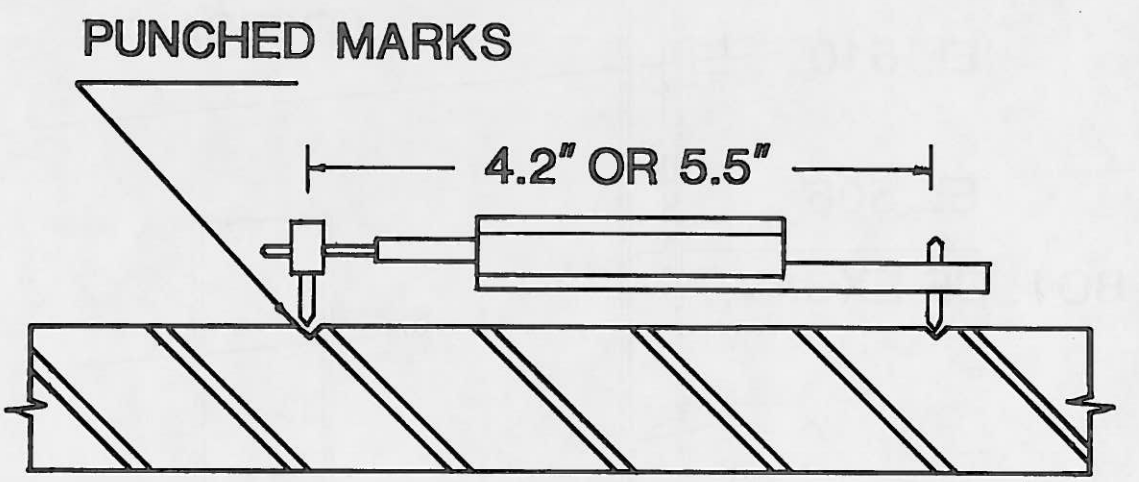


FIGURE 4.
TYPICAL CROSS SECTION
EAST END OF SOUTH WALL



TOP VIEW



SIDE VIEW

FIGURE 5.
VIEWS OF EXTENSOMETER

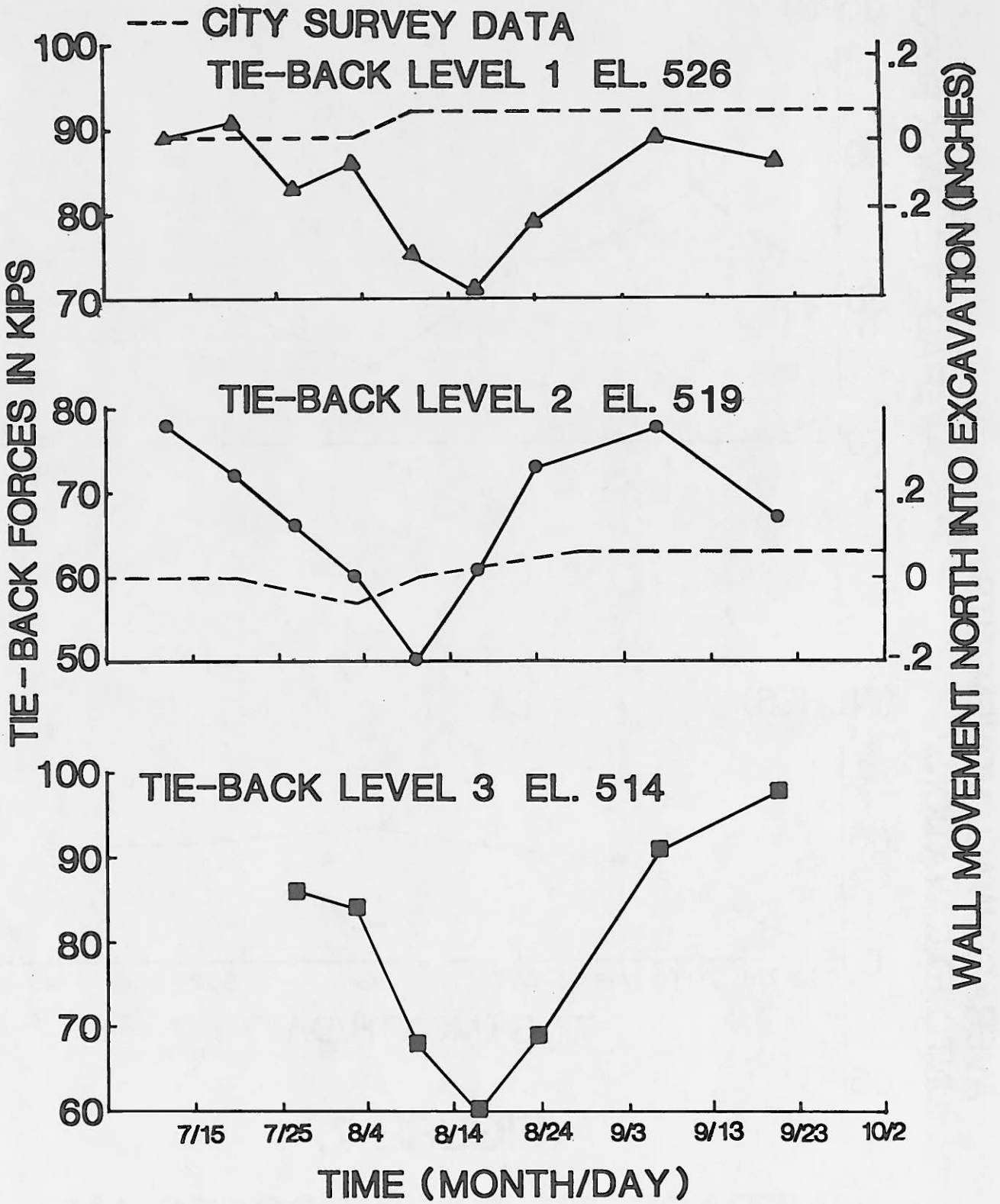


FIGURE 6. TIE-BACK FORCES vs. TIME (TEST SECTION 27-28)

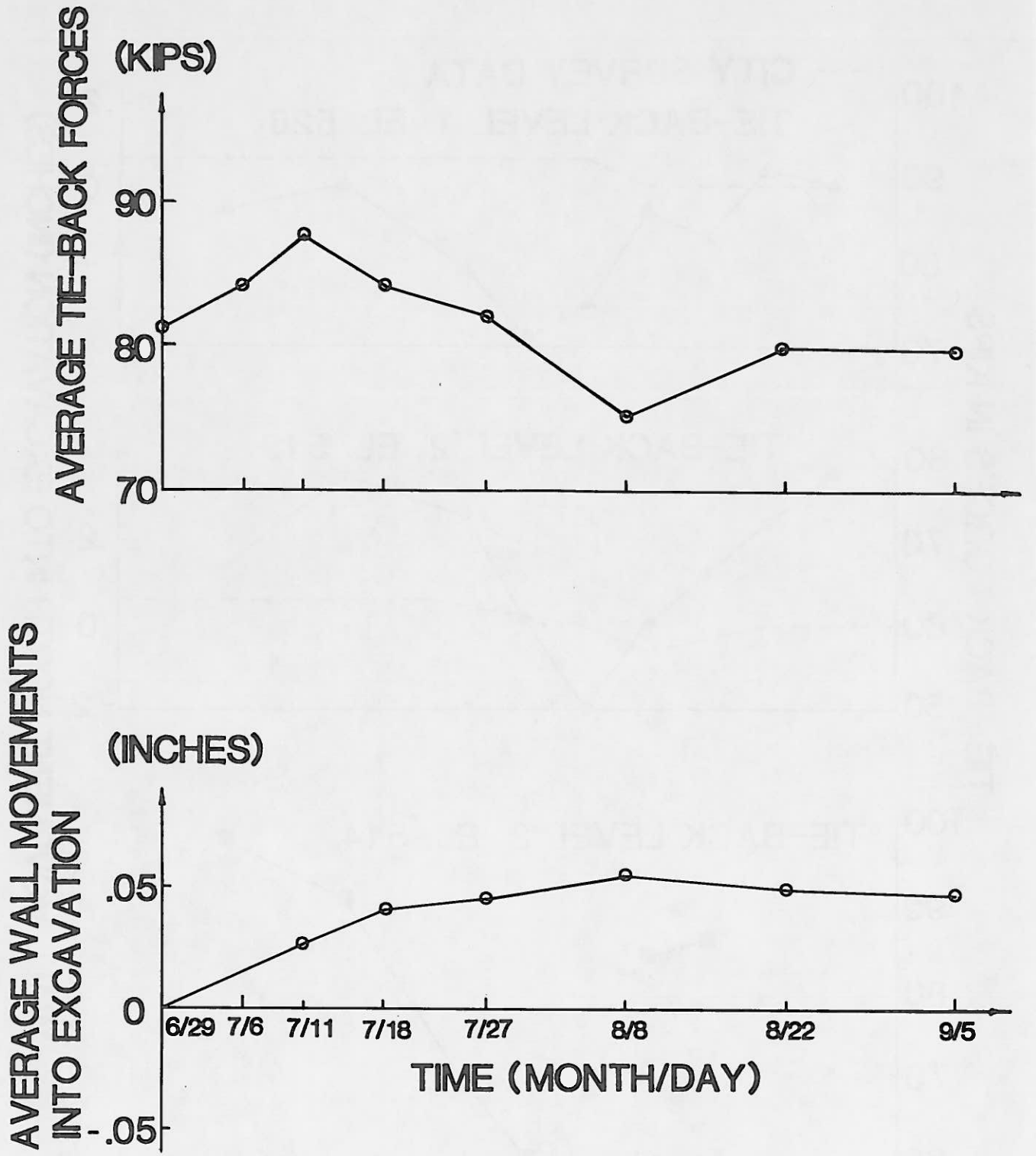


FIGURE 7.

AVERAGE TIE-BACK FORCES AND WALL MOVEMENTS (EAST SEGMENT)

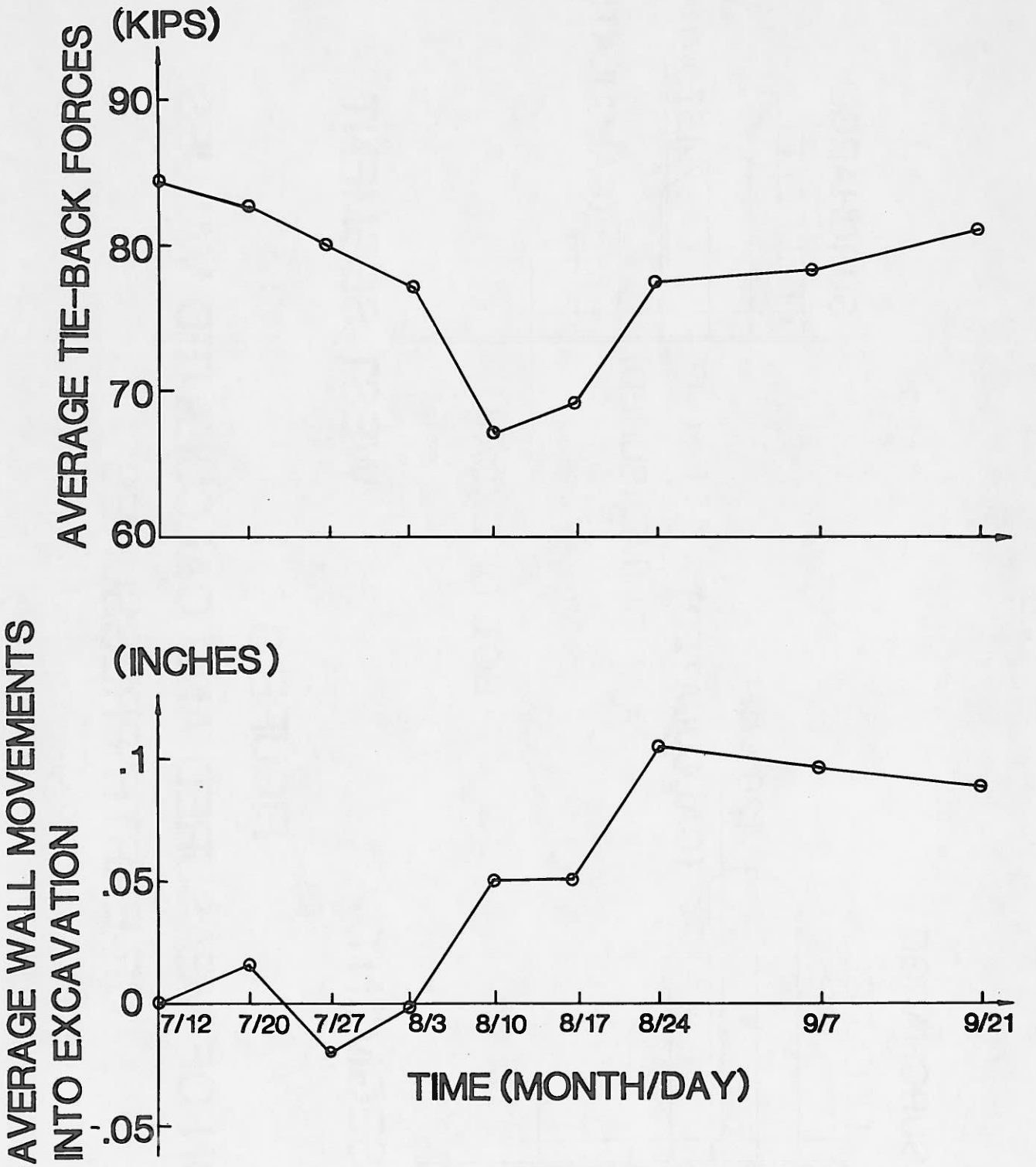


FIGURE 8.
AVERAGE TIE-BACK FORCES AND
WALL MOVEMENTS (WEST SEGMENT)

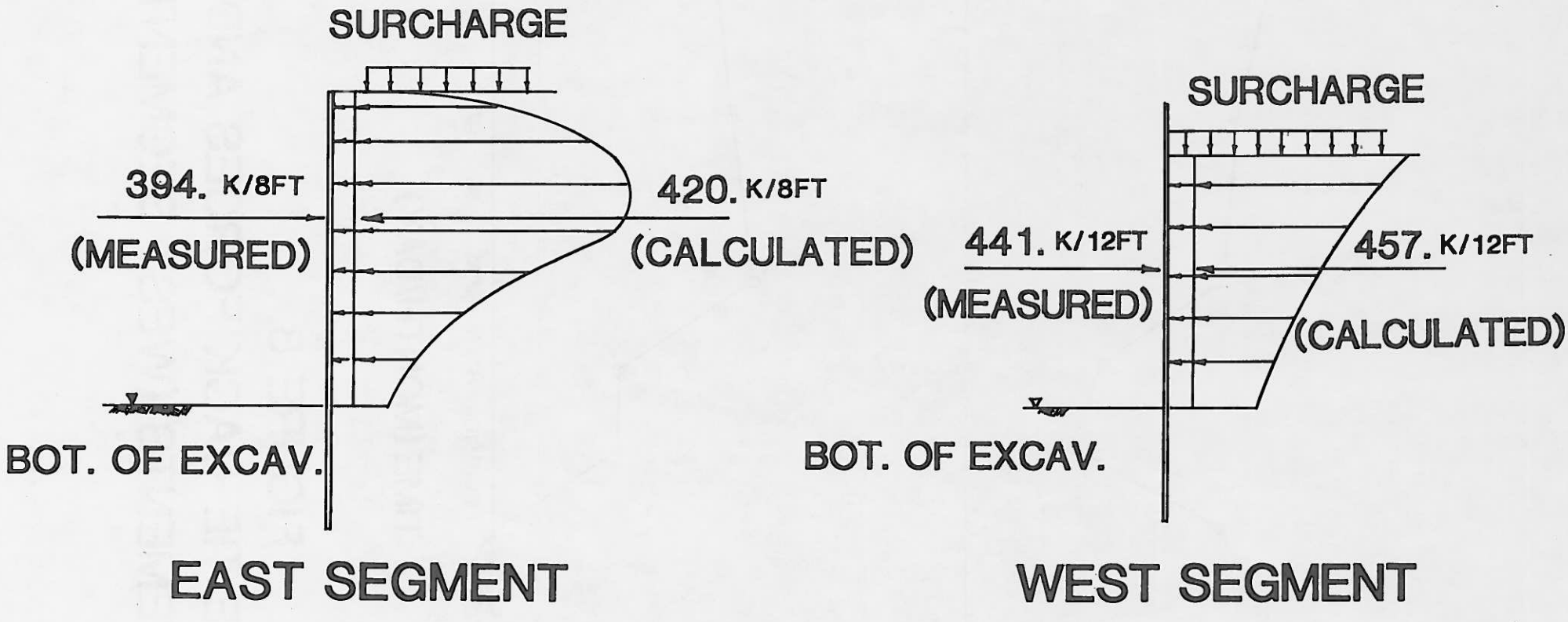


FIGURE 9.

COMPARISON OF MEASURED AND CALCULATED VALUES OF EARTH PRESSURES

RAPID CONSTRUCTION OF A COMBINED COAL REFUSE EMBANKMENT

by

Barry K. Thacker
Geologic Associates, Inc.
Knoxville, Tennessee 37932

and

James A. Schad
Westmoreland Coal Company
Big Stone Gap, Virginia 24219

Abstract. Presented herein is the case history of Stage 1 of the Bullitt Coal Refuse Disposal Facility. This embankment was constructed with combined coal refuse borrow (clayey, gravelly, sand size waste) to a height of 55 feet above a foundation of previously deposited combined coal refuse. Because of anticipated rapid construction, pneumatic piezometers were installed within the embankment and the underlying foundation to measure pore pressures during construction. The results of the monitoring program indicate that predictions of stability using a total stress method of analysis can be unsafe for a rapidly built embankment composed of cohesive waste.

INTRODUCTION

In the mining and power industries, cohesive soil and/or cohesive waste are being used to construct dams to retain a variety of wastes. As with any embankment composed of cohesive material, a critical phase with regard to stability is during and shortly after construction. Typically, designers of these waste disposal dams predict the stability for the end-of-construction condition by one of the following methods:

(1) total stress analyses using the strength parameters c and $\emptyset$; or
(2) effective stress analyses using the strength parameters $\bar{c}$ and $\bar{\emptyset}$ with estimates of construction pore pressures.

Both of the above design techniques have been borrowed from the designers of more conventional earth-fill dams (i.e., dams built for flood control and recreational purposes) (5,6,10).

Specifically, previous earth-fill dams have been designed using one of the above methods of stability analysis and then, during construction, pore pressures were measured to verify the design assumptions. Case histories of these embankments indicate that estimates of pore pressure used in effective stress analyses are often inaccurate because of the numerous assumptions that are required. These inaccuracies can be eliminated only by measuring construction pore pressures to verify the values used in design (2,3,7,8).

The same case histories also warn that total stress analyses can either over-estimate or under-estimate embankment stability for the end-of-construction condition. According to Bishop (2), "to work directly with undrained test results expressed in terms of total stress may be unsafe in low dams as it implies dependence on negative pore pressures which may subsequently dissipate; and uneconomical in high dams in wet climates as no account is taken of the dissipation of excess pore pressures during construction." Many designers of conventional earth-fill dams continue to use the total stress method of analysis because of its simplicity. The strength parameters c and $\emptyset$ can be determined in unconsolidated-undrained triaxial compression testing such that no estimates of construction pore pressures are required. The total stress strength parameters can then be input directly into computer aided stability analyses to estimate the computed minimum factor of safety. The designer often modifies the results of the total stress analysis, as necessary, based on previous experience of how the particular soils have behaved during construction.

Before applying these borrowed techniques, designers of waste disposal embankments should recognize the differences between waste disposal facilities and flood control/recreational structures. One major difference is in the respective rates of construction. During the disposal phase of a waste disposal facility, the rate of construction can be relatively slow when compared to construction of conventional earth-fill dams, thereby allowing excess pore pressures to dissipate. However, prior to disposal, construction of the initial waste retaining embankment can be rapid for the following reasons:

(1) many of these waste disposal structures are located in narrow hollows rather than in wide valleys;
(2) delays caused by the extensive regulatory review and approval process require that construction proceed rapidly to meet specified time schedules; and/or
(3) mining companies and utilities must have waste disposal capacity to continue operating and, as a result, they can often dedicate unlimited resources (labor and equipment) for a short period of time to complete these disposal structures so that their multi-million dollar operations can continue.

This paper presents the case history of the successfully constructed Stage 1 of the Bullitt Coal Refuse Disposal Facility. Because of the anticipated rapid construction, the stability at the end-of-construction was predicted using both a total stress analysis and an effective stress analysis with pore pressure estimates. To verify that the design assumptions were correct, pneumatic piezometers were installed to measure pore pressures during the critical two month construction period. Details of the design analyses and construction monitoring for the Bullitt Facility are presented in the following sections. Finally, methods of reducing excess construction pore pressures within waste disposal embankments are described.

BACKGROUND

The Bullitt Preparation Plant of Westmoreland Coal Company is located in southwestern Virginia near the town of Appalachia. Rejects from the plant consist of coarse coal refuse (primarily shale) and fine coal refuse (fine coal, silt, and clay). The plant was constructed in the early 1970's and was equipped with a filter which dewaters the fine refuse and allows the water to be recycled in the coal washing process (closed circuit system). The complex was designed to allow the dewatered fine refuse to be mixed with the coarse refuse, forming a combined refuse which was then trucked to a nearby valley for disposal. An aerial view of the original combined refuse fill is shown on Figure 1. Particle size distributions of the wastes obtained from the plant and from the disposal fill are included as Figure 2.

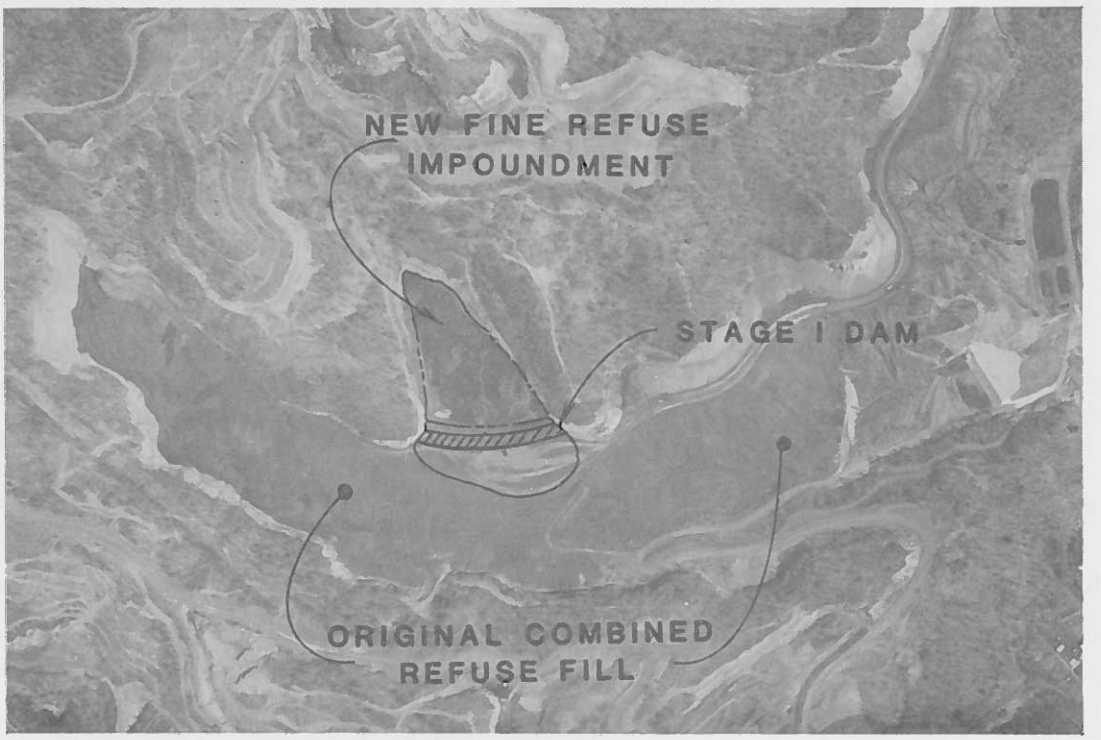


FIGURE 1. AERIAL VIEW OF THE BULLITT COAL REFUSE DISPOSAL FACILITY.

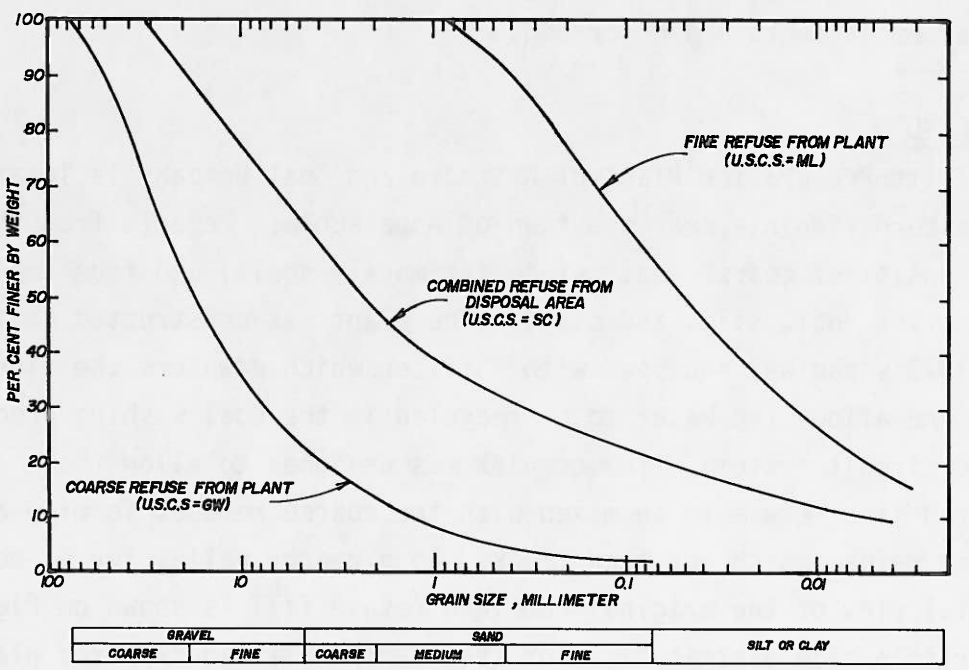


FIGURE 2. PARTICLE SIZE DISTRIBUTION

Even after dewatering, the fine refuse retained a high percentage of water which made compaction of the waste in the fill very difficult. To compensate for the low degree of compaction, the refuse fill was constructed on a relatively flat slope (approximately 10 horizontal to 1 vertical). By January 1982, the capacity of the refuse disposal hollow was becoming depleted. To provide for continued disposal of waste from the plant, the slopes of the existing refuse fill had to be steepened or a new refuse disposal hollow had to be found.

Westmoreland personnel decided that the most economical method of continued refuse disposal would be to separate the fine refuse from the coarse refuse. The coarse refuse could be used as borrow to construct an embankment and the fine refuse could be pumped to the disposal basin retained by the coarse refuse embankment. Before the new disposal mode could be initiated, however, an initial basin had to be created for the disposal of the fine refuse. Consequently, Westmoreland personnel decided to construct the Stage 1 embankment across one of the side hollows of the refuse fill as shown on Figure 1.

DESIGN

General

Stage 1 of the Bullitt Refuse Disposal Facility was designed to achieve a height of 55 feet above a foundation of existing combined coal refuse. As shown on Figures 1 and 3, Stage 1A of the embankment was designed to be built using primarily combined coal refuse fill obtained from the area of the future fine refuse impoundment. Subsurface exploration and testing of the combined refuse in the foundation indicated that, although saturated and soft when placed, the existing combined coal refuse had consolidated to a medium stiff consistency during the five years since it had been disposed. Underlying the existing combined refuse was a thin layer of residual silt and clay underlain by sandstone and shale as shown on Figure 3.

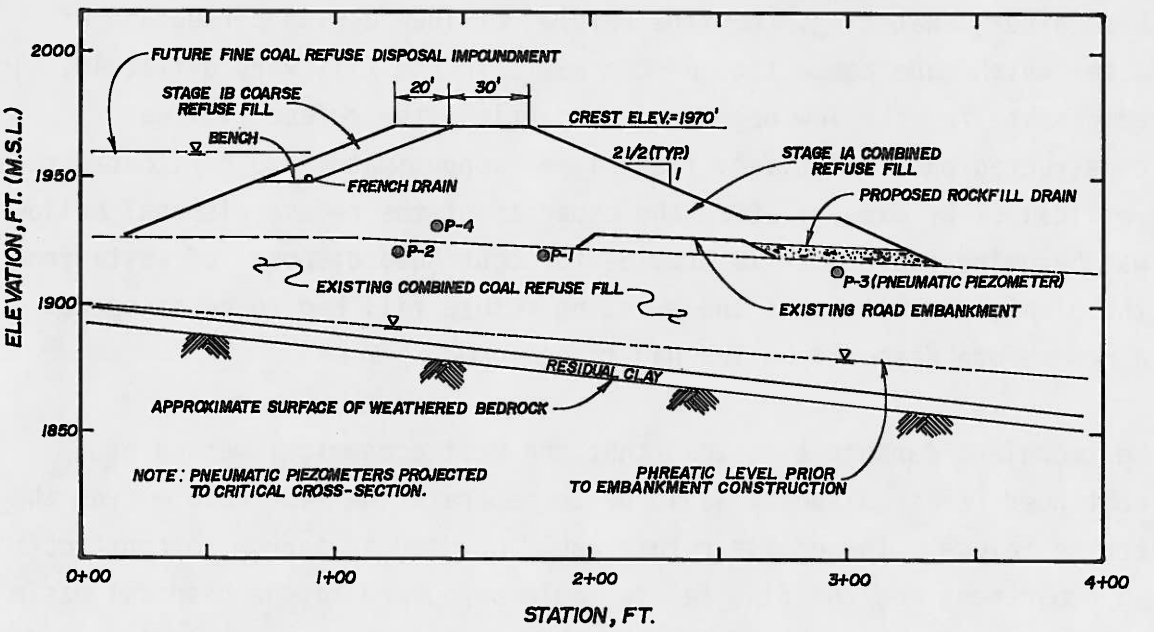


FIGURE 3. CROSS-SECTION OF BULLITT COMBINED COAL REFUSE EMBANKMENT (STAGE 1)

Drains were designed for installation beneath the downstream toe and within the upstream face of the Stage 1 embankment. At the downstream toe, the underdrain allows for dissipation of pore pressures during construction and also serves to intercept seepage during later stages of the facility. The upstream french drain enables dewatering of the fine refuse during future stages of upstream construction (i.e., fine refuse will serve as the foundation for future stages of the embankment). During Stage 1B (after the start of coarse refuse and fine refuse disposal), pervious coarse refuse placed on the upstream bench serves as an added filter for the french drain to reduce the likelihood of clogging. For comparison purposes, the coefficients of permeability of the fine refuse, coarse refuse, and combined refuse are 2×10^{-7} cm/sec, 5×10^{-5} cm/sec, and 3×10^{-7} cm/sec, respectively.

Because differential settlement of the existing combined refuse could cause cracking of the dam, a range of allowable moisture contents for the borrow was established from optimum moisture content to 3% over optimum. The resulting slightly plastic dam could then tolerate some

differential settlement without causing the embankment to crack. However, the relatively high placement moisture content could result in the embankment being constructed at near saturated conditions which would affect its stability during construction.

Stability Analyses

As previously described, many designers of waste disposal structures have adopted the methods developed by designers of conventional earth-fill embankments. For example, design guidelines published by the Mine Safety and Health Administration (10) state that "a total stress method of analysis is generally considered most appropriate for evaluating conditions during and immediately after construction of a coal refuse disposal facility". The referenced document recommends that the undrained triaxial compression test be used to determine strength parameters for total stress conditions. As will be described, designers of waste disposal structures should recognize that these recommendations and guidelines may result in inaccurate stability analyses for rapidly built structures composed of cohesive wastes.

A variety of triaxial compression tests were performed on samples of the undisturbed foundation combined refuse including unconsolidated-undrained (UU), consolidated-drained (CD), and consolidated-undrained with pore pressure measurements ($\overline{CU}$). In addition, unconfined compression tests were performed on selected undisturbed samples of the combined refuse. Figure 4 shows the failure envelopes for each of the tests. Triaxial tests were also performed on samples of the borrow that were remolded to the design embankment density. The strength parameters of the remolded (embankment) combined refuse were only slightly higher than the strength parameters measured for the undisturbed samples of combined refuse; therefore, both the foundation refuse and the embankment refuse were assigned the strength parameters included in Figure 4 for use in the stability analyses.

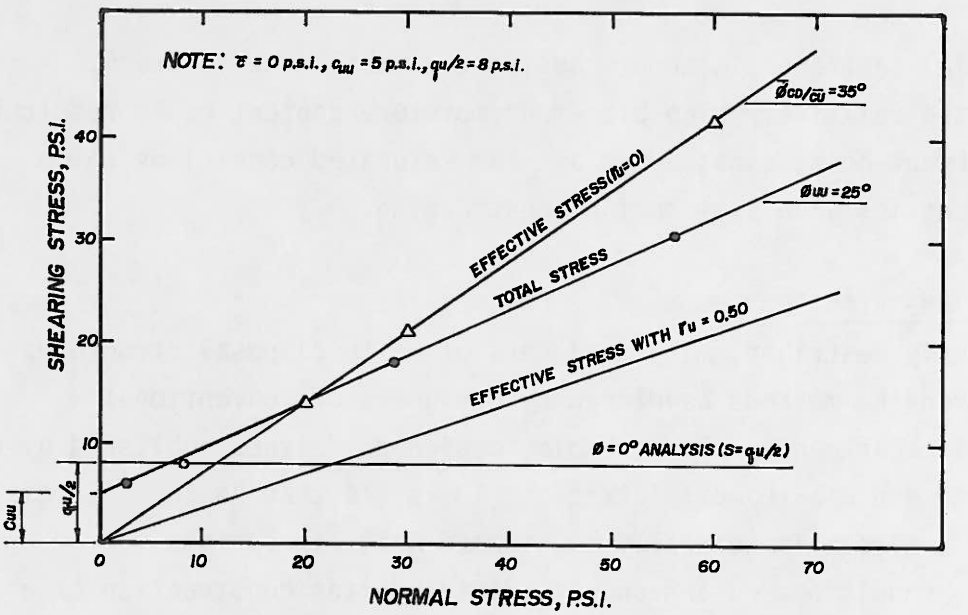


FIGURE 4. RELATIONSHIPS BETWEEN NORMAL STRESS AND SHEARING STRESS (BASED ON LABORATORY TESTING OF UNDISTURBED SAMPLES AND ESTIMATES OF CONSTRUCTION PORE PRESSURES).

During the consolidation phases of the applicable triaxial tests, volume versus time measurements were taken so that consolidation characteristics could be calculated. During the shearing phases of these tests, pore pressures which developed within the samples were measured. Coefficients of consolidation (c_v) and Skempton's pore pressure coefficients ($\bar{A}$ and $\bar{B}$) calculated from the laboratory data were then used to make estimates of construction pore pressures for use in the effective stress stability analyses.

Stability analyses for the Stage 1 dam are presented based on the following methods of analysis and embankment conditions:

(1) total stress analysis with unsaturated refuse using strength parameters c and ϕ from the UU test;
(2) total stress analysis with saturated refuse using strength parameter $s_u = q_u/2$;
(3) effective stress analysis with no pore pressure dissipation using strength parameters $\bar{c}$ and $\bar{\phi}$ with estimates of construction pore pressures based on $\bar{A}$ = 0.8 and $\bar{B}$ = 1; and

(4) effective stress analysis with partial pore pressure dissipation using strength parameters $\bar{c}$ and $\bar{\phi}$ with estimates of construction pore pressures based on c_v = 0.23 in^2/minute and a three month construction period.

In the effective stress analyses, the estimated excess pore pressures were expressed in terms of the pore pressure ratio, r_u, which equals the pore pressure at a given point divided by the total overburden pressure at that point. Figure 4 compares the effective stress failure envelope when r_u = 0.5 to the failure envelopes determined for the various triaxial compression tests. Results of the stability analyses are presented in Table 1.

TABLE 1. COMPARISON OF PREDICTED FACTORS OF SAFETY FOR THE STAGE 1 DAM

Method of Analysis	Minimum Static Factor of Safety	
	Downstream Slope	Upstream Slope
Total Stress		
Unsaturated condition (c,ϕ)	2.6	2.8
Saturated condition (q_u/2)	1.7	1.8
Effective Stress ($\bar{c}$, $\bar{\phi}$) With Pore Pressure Estimates		
No dissipation	1.2	1.3
Partial dissipation	1.5	1.6

Based on the results of the stability analyses and our previous experience with similar materials, the effective stress analysis using partial pore pressure dissipation was considered the best prediction of the factor of safety for the end-of-construction condition of the Stage 1 Bullitt Dam.

As shown on Figure 5, a slight variation in the pore pressure ratio (r_u) has a dramatic effect on the computed factor of safety of the Stage 1 dam. Because some partial dissipation of excess pore pressures was used in the design analysis, a construction pore pressure monitoring program

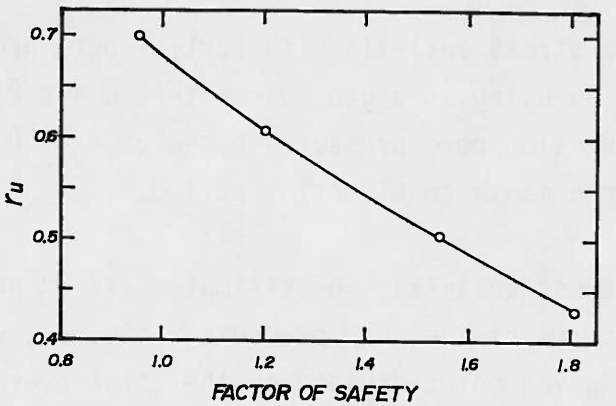


FIGURE 5. CALCULATED RELATIONSHIP BETWEEN THE FACTOR OF SAFETY OF THE STAGE I DAM AND r_u

was specified. As shown on Figure 3, the instrumentation included three pneumatic piezometers installed within the combined refuse fill of the foundation and one pneumatic piezometer installed within the combined refuse embankment.

CONSTRUCTION MONITORING

Construction of the Stage 1 embankment began in October 1982. The beginning of construction had been delayed for approximately two months to allow the state mining regulators to complete their review of the project. Consequently, the construction time had to be shortened to allow the embankment to be completed on schedule. Monitoring of the pneumatic piezometers became even more important in assessing the maximum safe rate of construction.

As shown on Figure 6, during the first month of construction, the embankment was completed to within 16 feet of its final design height. By this time, the construction pore pressures had risen to very high levels, especially piezometer P-4 which had been installed within the combined refuse embankment. The high pore pressures resulted even though the combined refuse borrow was compacted at near optimum moisture content throughout the construction. Subsequently, construction on the dam was stopped and construction efforts centered on completing the slurry (fine refuse) pipe line to the site. Within approximately two weeks, the pore pressures had dissipated to acceptable limits and the Stage 1A portion of the dam was completed to a crest elevation of 1970

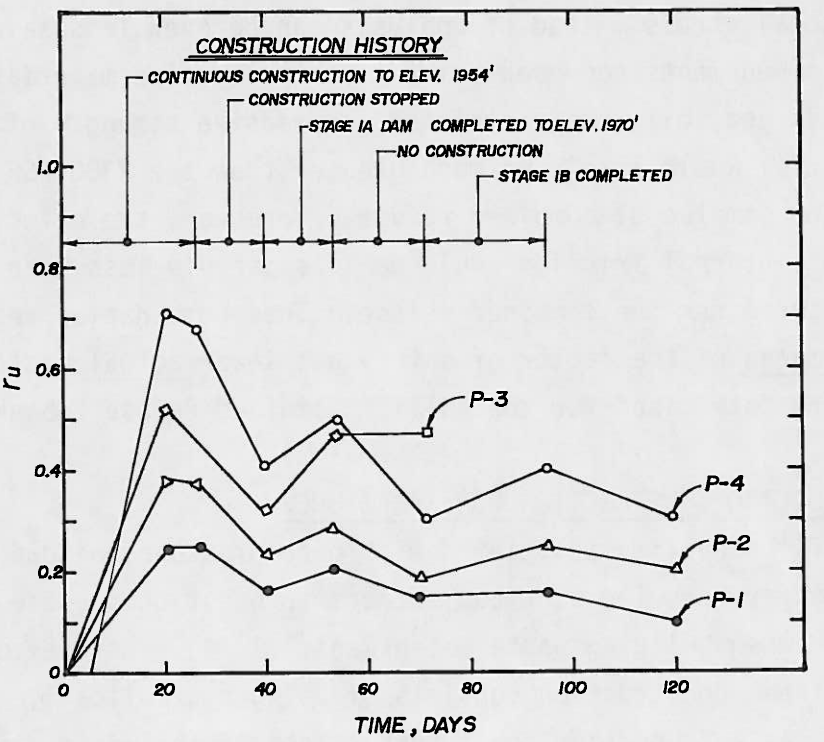


FIGURE 6. RELATIONSHIP BETWEEN TIME AND ru MEASURED DURING STAGE I CONSTRUCTION.

feet. As shown by comparing Figures 5 and 6, if the Stage 1A construction had continued to completion without allowing the pore pressures to dissipate, the embankment would have existed at a condition near failure.

COMPARISON OF PREDICTED VERSUS ACTUAL EMBANKMENT STABILITY

Effective stress analyses with design estimates and construction verification of excess pore pressure accurately predicted the minimum factor of safety for the rapidly built Stage 1 Bullitt Dam. Total stress analyses significantly over-estimated the minimum factor of safety of the dam during construction. If the stability of the embankment had been predicted based solely on a total stress method of analysis, the slopes could have been designed on an inclination of 2 (horizontal) to 1 (vertical) resulting in a predicted factor of safety of 1.5 against instability. If this hypothetical embankment had been constructed within a two-month period, then failure probably would have occurred.

The use of a total stress method of analysis can be even less safe for rapidly built embankments composed primarily of clay size material. For clay size wastes and soil, the unconfined compressive strength of the compacted material would likely be much greater than the 2300 PSF measured for the samples of combined refuse. Moreover, the effective stress angle of internal friction would be considerably less than the $\bar{\emptyset} = 35°$ as measured for the combined refuse. This combination results in higher estimates of the factor of safety but lower actual factors of safety than were determined for the Bullitt Combined Refuse Embankment.

METHODS FOR REDUCING CONSTRUCTION PORE PRESSURES

The problems of instability associated with pore pressure buildup within fine grained wastes have led previous authors to question the use of the upstream method when building waste embankments (1, 4). As previously described, upstream construction consists of using hydraulically deposited waste as a foundation for future stages of the waste disposal embankment. In the coal industry and other mining and milling processes, the upstream method is often the only means by which waste can be disposed economically. For example, in the steep terrain of the Appalachian coal fields, adequate borrow (either natural soil or coarse refuse from the processing plant) is not always available in sufficient quantities to build refuse disposal facilities in a manner where the entire dam is founded on natural ground (downstream method). For these coal preparation plants to continue operation, the upstream method of refuse disposal must be used.

The problems associated with the build-up of excess pore pressures during construction can be reduced by predicting excess pore pressures during design and then verifying the design values during construction. If unsafe pore pressures are a potential problem, the respective design should include measures for reducing the excess pore pressures to within safe limits. Two methods are presented for reducing construction pore pressures within waste embankments. These methods include staging construction of the embankment based on the results of pore pressure monitoring and/or installing synthetic wick drains.

The Bullitt Refuse Disposal Facility is an example of staging the construction such that excess pore pressures do not exceed safe limits. When measured pore pressures reach specified limits, construction is stopped. Only after the pore pressures have dissipated to within safe limits does the construction continue. At a coal refuse disposal site in eastern Kentucky, upstream construction continues until the pore pressures achieve certain levels. Afterwards, the coarse refuse is placed downstream of the dam to buttress the previous construction until the pore pressures in the fine refuse dissipate (9).

The other method of reducing construction pore pressures is to install synthetic wick drains within the fines during construction as shown on Figures 7 and 8. These wicks are installed on the surface of the fines at various stages during construction. As the fines accumulate, the wicks provide drainage paths to dissipate pore pressure when the coarse refuse embankment is eventually constructed (9). This technique is very similar in concept to the use of sand drains in conjunction with the preloading of soft clay deposits prior to building construction.

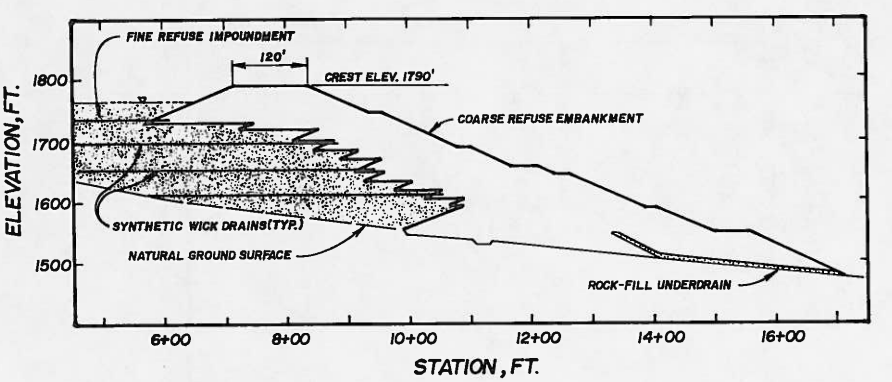


FIGURE 7. UPSTREAM CONSTRUCTION WITH SYNTHETIC WICK DRAINS.

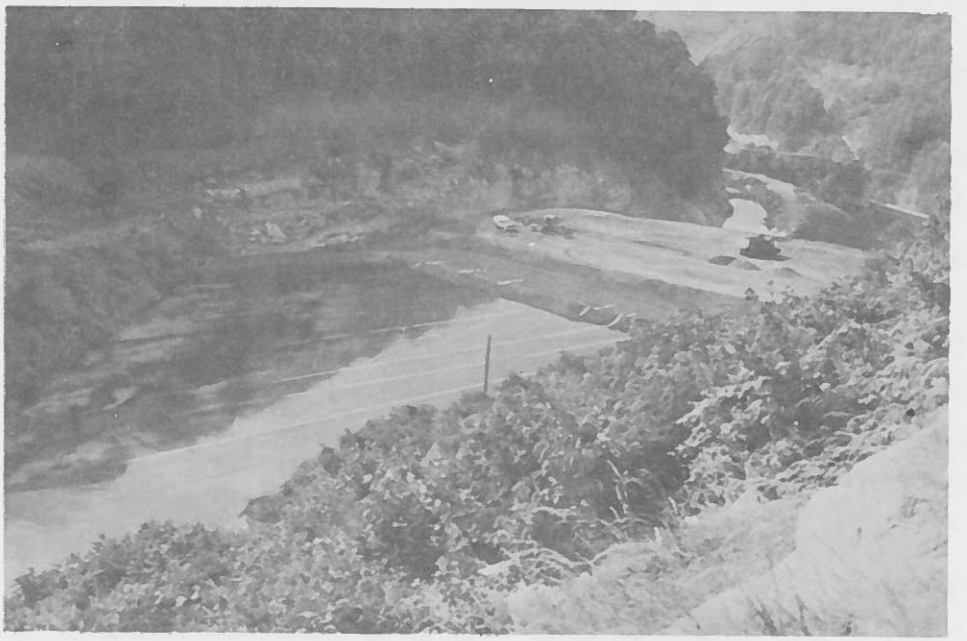


FIGURE 8. SYNTHETIC WICK DRAINS INSTALLED WITHIN FINE REFUSE IMPOUNDMENT.

The effectiveness of wicks in dissipating excess pore pressures within embankments built by the upstream method is illustrated by Figure 9. As shown thereon, pore pressures within a fine refuse deposit equipped with synthetic wicks (Alidrains) dissipate much more rapidly during upstream construction than do pore pressures within a similar fine refuse deposit without wicks.

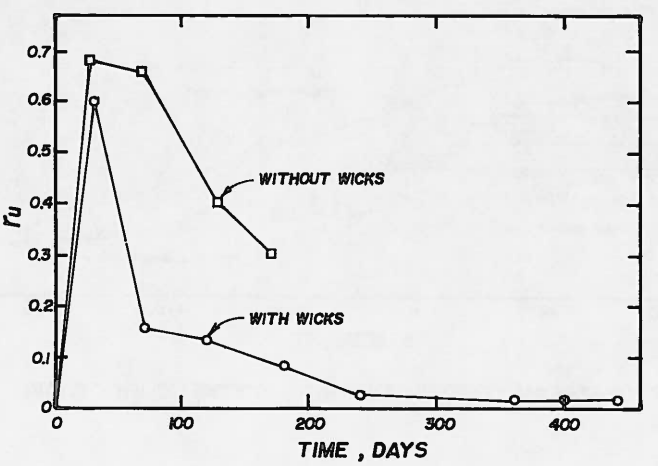


FIGURE 9. MEASURED RELATIONSHIP BETWEEN TIME AND ru WITHIN FINE REFUSE DEPOSITS WITH AND WITHOUT SYNTHETIC WICK DRAINS.

CONCLUSIONS

The use of total stress methods of analyses in predicting the stability of rapidly built cohesive waste embankments can be unsafe. Stability analyses using effective stress methods, verified by measuring pore pressures during construction, enabled the Bullitt Combined Refuse Embankment to be built rapidly, yet safely. Finally, current methods available for dissipating potentially unsafe pore pressures should be used when appropriate. Hopefully, this case history will make future designers of similar waste disposal facilities aware of the potential problems associated with rapid construction and challenge them to develop new methods to control pore pressures during construction.

REFERENCES

1. Al-Hussaini, M.M., D.J. Goodings, A.N. Schofield, and F.C. Townsend, "Centrifuge Modeling of Coal Waste Embankments," Proceedings, ASCE Journal of the Geotechnical Engineering Division, April 1982 and May 1983 (Closure).
2. Bishop, A.W. and L. Bjerrum, "The Relevance of the Triaxial Test to the Solution of Stability Problems," Proceedings, ASCE Research Conference on Shear Strength of Cohesive Soils, Boulder, Colorado, 1960, pp. 437-501.
3. Gibbs, H.J., J.W. Hilf, W.G. Holtz, and F.C. Walker, "Shear Strength of Cohesive Soils," Proceedings, ASCE Research Conference on Shear Strength of Cohesive Soils, Boulder, Colorado, 1960, pp. 33-162.
4. Highter, W.H. and R.F. Tobin, "Flow Slides and the Undrained Brittleness Index of Some Mine Tailings," Engineering Geology, Vol. 16: 71-82, 1980, pp. 71-82..
5. Lambe, T.W. and R.V. Whitman, Soil Mechanics, John Wiley and Sons, Inc., New York, N.Y., 1969, 553 pp.
6. Lowe, J., "Stability Analysis of Embankments," Proceedings, ASCE Conference on Stability and Performance of Slopes and Embankments, Berkeley, CA, 1969, pp. 1-35.
7. Moore, L.H., "Design and Construction of Highway Embankments in New York State," Proceedings, 8th Ohio River Valley Soils Seminar, Louisville, Kentucky, 1977, pp. 4-1 to 4-10.

8. Peterson, R., J.L. Jaspar, P.J. Rivard, and N.L. Iverson, "Limitations of Laboratory Shear Strength in Evaluating Stability of Highly Plastic Clays," Proceedings, ASCE Research Conference on Shear Strength of Cohesive Soils, Boulder, Colorado, 1960, pp. 765-791.
9. Thacker, B.K., P. Poynter, W.J. Rosen, and K.E. Darnell, "Design and Construction of the Abner Fork Slurry Impoundment: A Case History," Proceedings, 8th Annual Kentucky Coal Seminar, Pineville, Kentucky, 1982, 18 pp.
10. U.S. Department of the Interior, Mining Enforcement and Safety Administration, Engineering and Design Manual for Coal Refuse Disposal Facilities, 1974, (Prepared by E. D'Appolonia Consulting Engineers, Inc.), pp. 5.1 to 5.163.

NOTATION

$\bar{A}$ - pore pressure coefficient
$\bar{B}$ - pore pressure coefficient
c - cohesion intercept based on total stresses
$\bar{c}$ - cohesion intercept based on effective stresses
CD - consolidated-drained triaxial compression test
$\overline{CU}$ - consolidated-undrained triaxial compression test with pore pressure measurements
c_v - coefficient of consolidation
GW - well-graded gravel-sand mixture
ML - silt
q_u - unconfined compressive strength
r_u - pore pressure ratio
SC - clayey sand
s_u - undrained shear strength
USCS - Unified Soil Classification System
UU - unconsolidated-undrained triaxial compression test
ϕ - angle of internal friction based on total stresses
$\bar{\phi}$ - angle of internal friction based on effective stresses

USE OF SPECTRAL ANALYSIS TECHNIQUES FOR STRUCTURAL AND FOUNDATION VIBRATION ANALYSES

by

Dr. Vincent P. Drnevich, P.E.
Professor & Chairman
Department of Civil Engineering
University of Kentucky
Lexington, Kentucky 40506

Dr. John R. Hall, Jr.
Senior Consulting Engineer
Stone & Webster Engineering Corp.
245 Summer Street
Boston, Massachusetts 02107

ABSTRACT

For many structures and foundations, it is difficult or nearly impossible to predict the levels of vibration that may exist after construction. The reasons for this are many. In the first place, the dynamic forces that cause the vibration are rarely known with any degree of accuracy. Further, structures usually have many small details which influence their mass, stiffness, and damping. The vibration may be troublesome to persons or may have deleterious effects on equipment, connections, or the structure itself.

In cases where excessive vibrations exist, the procedure is to monitor the behavior with sensitive instruments that will allow for describing the magnitude and nature of the vibrations. Until recently, this was an arduous and demanding task because vibrations are usually very irregular in nature. A new electronic tool, the spectrum analyzer (frequency analyzer, or structural dynamics analyzer) gives the principal frequencies that make up a complicated vibration waveform. If measurements are made at two locations at the same time, the equipment can compare the waveforms and identify which frequencies the two have in common. There are many other features of these instruments which greatly simplify dynamic analyses of all types. Many of the features are discussed in the paper.

Two case studies are presented where the use of a spectrum analyzer greatly simplified dynamic analyses. In one of the cases, the analyzer was used to verify which of two solutions better solved a vibration problem.

MEASUREMENT OF VIBRATION

Vibrations of structures and foundations are measured with vibration transducers which may, depending on their type, measure acceleration,

velocity, or displacement. Quite frequently, these measurements are measured, recorded and plotted as functions of time. An example of a vibration record is given in Fig. 1. Note the irregularity of the vibration. This is due to a variation in both amplitude and frequency of the vibration.

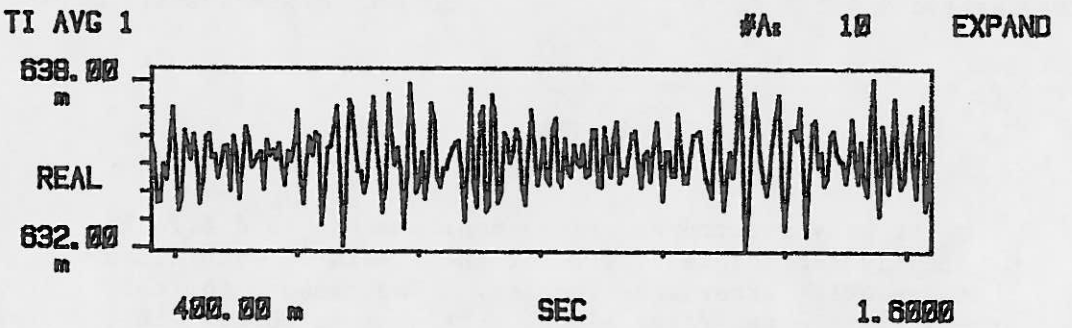


Fig. 1 An Example of a Vibration Record (Velocity versus Time)

THE NATURE OF SPECTRUM ANALYZERS

Spectrum analyzers are special electronic devices that accept electrical signals directly from vibration transducers or from recordings of transducer signals. They first convert the electrical signal to a digital value which is then placed in the memory portion of the analyzer. Most spectrum analyzers have specialized computers built into them which operate on the digitized signals with special programs which are also stored in the analyzer. They have provisions for displaying results on a screen or on a plotter which can be attached to the analyzer. Many analyzers have provisions for permanently storing data and programs on magnetic tapes or floppy disks.

The key to the power of the spectrum analyzer is the fact that data are stored digitally, i.e. as numbers. However, this means that a continuous signal of vibration must be represented by discrete values at some predetermined interval. For example, a 10 second vibration record may be represented by digital values at 0.001 second intervals of time. Variations

in data at intervals less than 0.001 second would be lost for this example.

Because the signals are digitized, a number of operations may be done on them. One signal may be added to another. This feature is used where there is much ambient noise associated with a signal. By adding subsequent measurements of the same signal, it is possible to reduce the effects of the ambient noise because it will be more random in nature and will tend to cancel previous measured values. This feature is called signal enhancement. Enhanced signals may be divided by the number of signals added to produce an average signal.

VIBRATIONS IN THE FREQUENCY DOMAIN

Other operations may be applied to the digitized transducer output as a function of time. One of the most powerful is to convert the signal from the time domain to the frequency domain. From mathematics, we know that a given behavior versus time can be represented as a Fourier series consisting of a number of terms that have an amplitude coefficient and a frequency value. A given transducer output versus time, once transformed to the frequency domain, can be represented by a plot of amplitude versus frequency as shown in Fig. 2. The transformed signal is referred to as the LINEAR SPECTRUM of the signal.

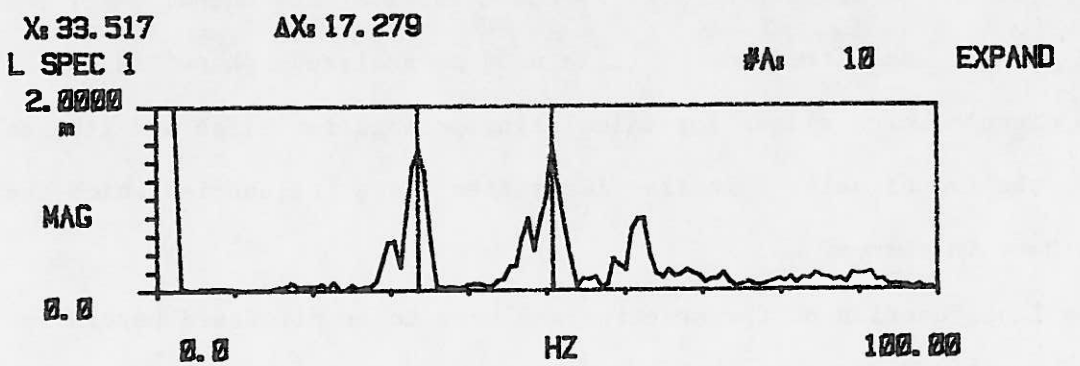


Fig. 2 Vibration Signal Transformed to the Frequency Domain.

The algorithm within the spectrum analyzer to do this is called the FAST FOURIER TRANSFORM (frequently referred to as FFT).

The peaks in the frequency domain signal identify the predominant frequencies in the signal and can be related to the frequencies of various components of the system being measured. Further, if the source of vibration has a known frequency, the effect of that frequency on other parts of the system (structure or foundation) can be isolated by looking at the amplitude values of the transformed signal from various points on the system.

SPECIAL FUNCTIONS IN THE FREQUENCY DOMAIN

Before going on to some examples of spectral analysis, several other functions need to be described. The first is AUTO POWER SPECTRUM or AUTO SPECTRUM. This function is just the magnitude squared of the LINEAR SPECTRUM. It allows for averaging of signals without the need for a synchronizing trigger of the signal recording.

Many spectrum analyzers allow for the simultaneous recording of more than one signal. Most have the capability to record two simultaneously, some can record four simultaneously. When more than one signal is recorded, signals can be compared and operations can be performed on both signals. The CROSS POWER SPECTRUM (or CROSS SPECTRUM) is the measure of the mutual power between two signals at each frequency. It is used to analyzed phase relationships between signals which allows for calculating propagation times and time delays between the two signals. It also identifies those frequencies which the two signals have in common.

The last function of the spectrum analyzer to be discussed herein is the TRANSFER FUNCTION. For all linear systems, there is a linear relation between cause and effect, e.g. force and displacement. The TRANSFER FUNCTION gives

this linear relation in the frequency domain. It is the LINEAR SPECTRUM of the output divided by the LINEAR SPECTRUM of the input. With this function, it is possible to define the dynamic stiffness and damping matrices of a structure.

In addition to the above described features, some spectrum analyzers are called structural dynamics analyzers. Many of these allow for graphically displaying the structure, performing a modal analysis of the structure, and animating the modal deformations of the structure for each mode. These features are quite helpful in assessing the reasonableness of a given analysis.

SOURCES OF VIBRATIONS

Structures and foundations may be analyzed by use of vibrations that are generated by machinery, traffic, wind, etc. In some cases, these vibrations are not of sufficient magnitude or are not available to provide data for the analysis. Then, vibrations must be artifically applied to the system. Two techniques are available for applying vibrations: impact loading and vibrator loadings. For impact loadings, an instrumented hammer is used to generate an impact at selected locations in the system. The dynamic force signal generated by the hammer at impact is connected to one channel of the spectrum analyzer while signals from vibration transducers at strategic locations on the structure or foundation are connected to the other channel(s). Typical force versus time curve generated by the impact and the displacement versus time response at a given location are shown in Fig. 3.

For some situations, it is preferable to attach a dynamic oscillator (shaker) to the structure or foundation. These devices produce dynamic forces which are proportional to the current applied to them. The frequency of the forces can range over a wide scale. Rather than apply dynamic forces at

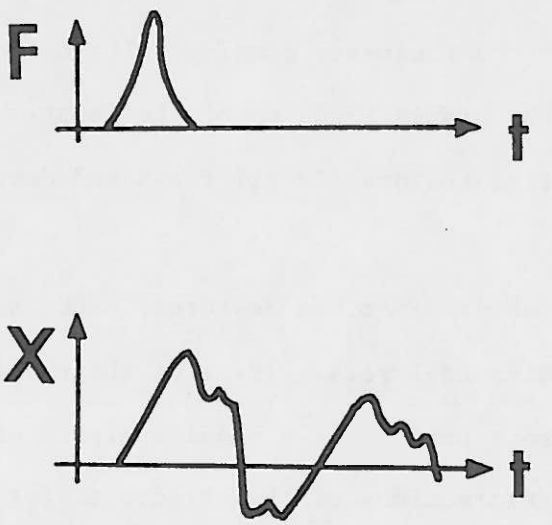


Fig. 3 Force and Resulting Displacement From Impact Loading

selected frequencies and perform an analysis for each frequency, it is common practice to apply a force that has a random amplitude and frequency (white noise). The resulting analysis will then give the response of the structure at all frequencies within the bandwidth of the frequencies applied.

ANALYSIS PROCESS

The analysis process usually begins by estimating the number of degrees of freedom the structure or foundation has. The degrees of freedom are related to the number of independent measurement parameters required to describe the motion. For example, a rigid footing foundation has six degrees of freedom; three for translation in each of the coordinate directions and three for rotation about each of the coordinate axes. A multi-story structure could have hundreds of degrees of freedom. For most analyses, only a small number of degrees of freedom have significance and most complicated structures can be modeled with fewer than ten to twenty degrees of freedom.

With vibration transducers attached to strategic points on the structure, data are obtained and stored. Then, relatively straight forward procedures are used within the analyzer for the analysis.

CASE HISTORY NO. 1 - VERTICAL PUMP

BACKGROUND - A vertical pump illustrated in Fig. 4 was experiencing motor bearing failure during testing of the pump after installation at a power plant. The pump was previously run at the manufacturer's test facility

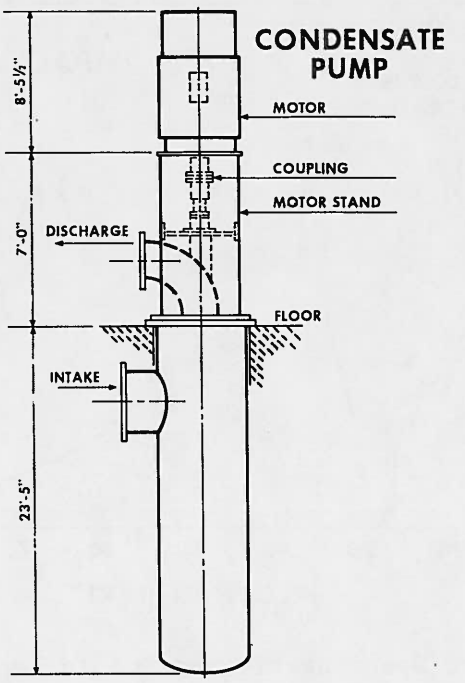


Fig. 4. Condensate Pump Mounted in Floor at Power Plant

without problem. Measurements on the pump at the power plant showed high vibration at the top of the motor when it was mounted on the motor stand but the same motor ran smoothly when supported on the floor. An investigation was undertaken to determine the cause of the high vibration using a dual channel spectrum analyzer.

IMPACT MEASUREMENTS - At the time of the investigation, the pump was not in operation and measurements were taken to determine the natural frequencies of the motor supported on the pump motor stand. This was performed by mounting two velocity transducers on the motor. One transducer was used as a reference with the other one being moved to various locations to measure relative motion and phase with respect to the reference.

Using the above technique and impacting the pump with a small hammer, it was possible to measure the first two predominant natural frequencies of the motor as shown in Fig. 5. The first mode frequency was at 465 rpm which is 39

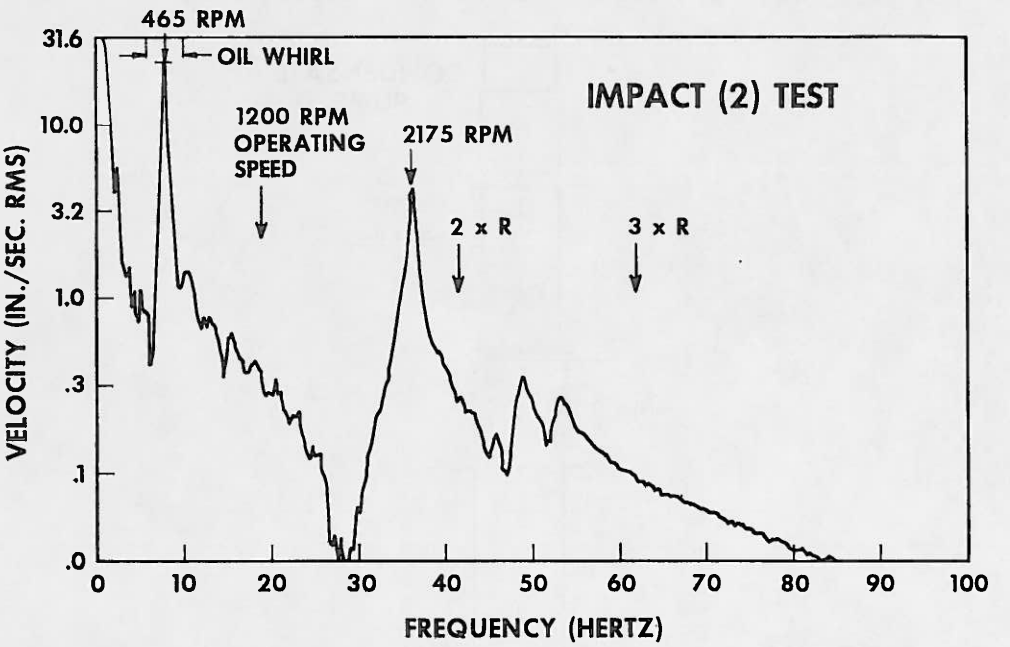


Fig. 5. Velocity Spectrum of Pump Due to Impact With Hammer

percent of the running speed of 1200 rpm. The second mode occurred at 2175 rpm which is well above the operating speed. It is observed that the resonant frequencies are well separated from the running speed and multiples thereof.

The mode shapes were determined from the measurements and are shown in Fig. 6 along with the motion of the top of the motor with the motor running at 1200 rpm. It is observed that the first and second modes are very similar to a cantilever beam. It can be concluded from the impact tests that the natural frequencies are controlled primarily by the stiffness of the motor stand and the stiffness of the floor or foundation supporting the motor stand. Thus, the difference in the vibration characteristics could be related to the difference between support stiffness at the manufacturer's facility (a steel grillage) and at the power plant (a concrete floor slab).

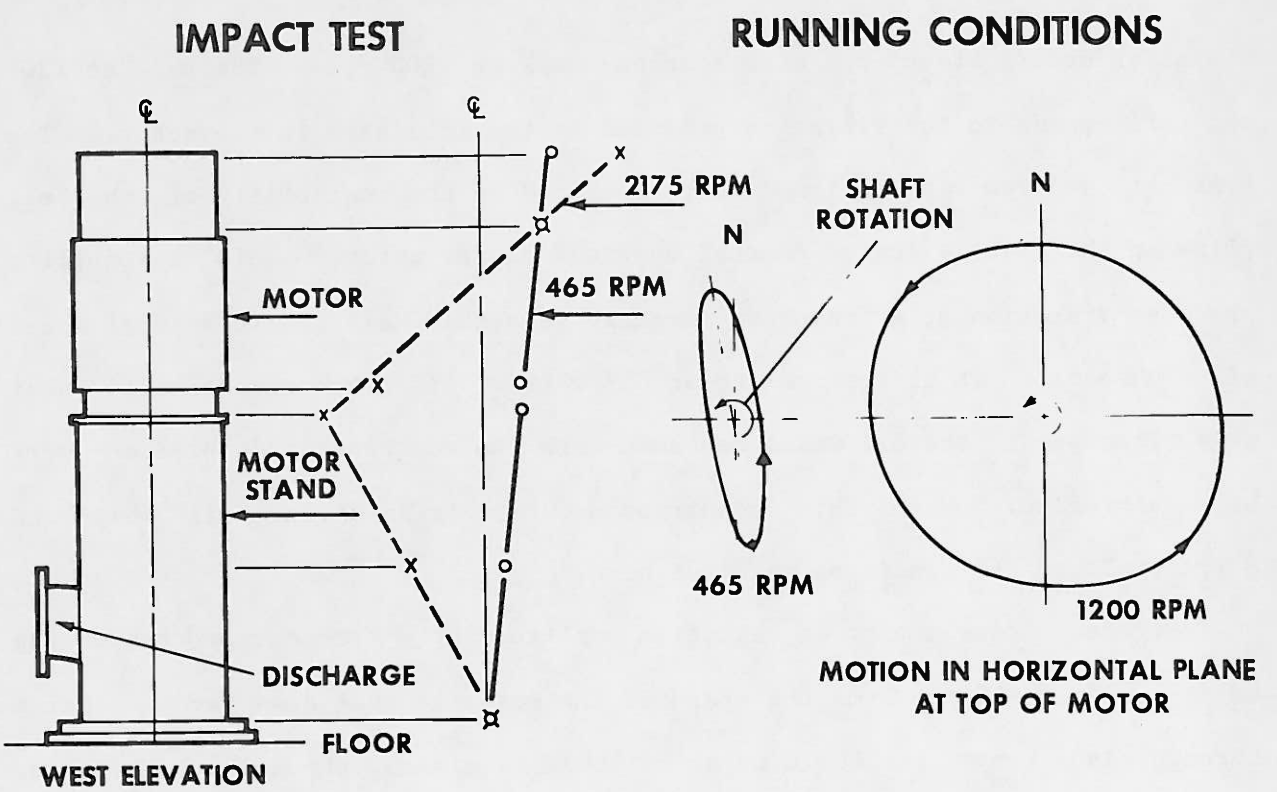


Fig. 6. Mode Shapes and Motion at Top of Pump

RUNNING VIBRATION - After running the motor for approximately five minutes, the vibration spectra was as shown in Fig. 7. It is observed that the highest

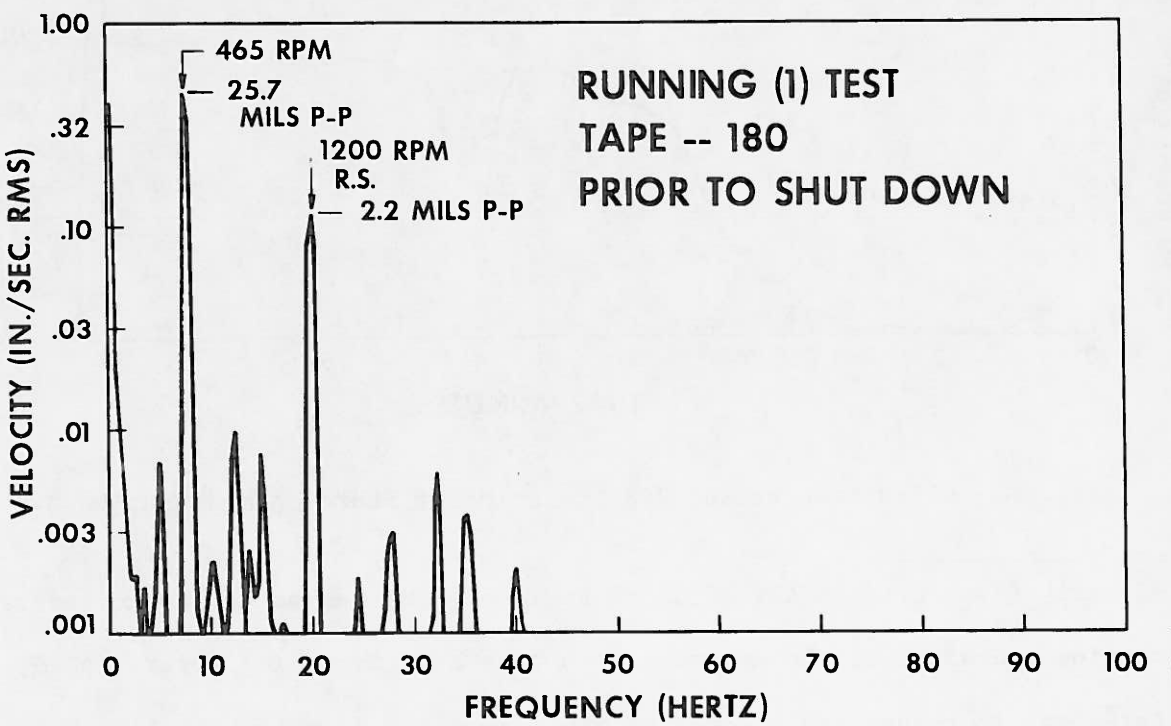


Fig. 7. Velocity Spectrum During Running at Operation Speed of 1200 RPM

vibration occurs at 465 rpm with a second peak at 1200 rpm. The peak at 1200 rpm corresponds to the vibration produced by the imbalance in the motor. The peak at 465 rpm was confirmed to be produced by the instability of the oil film in the lightly loaded journal bearings of the motor. This instability produces vibration at a frequency slightly less than half the rotational speed of the shaft. It is referred to as oil whirl. If a resonance exists near this frequency, the oil whirl can lock onto the resonance and produce very high vibration. When this condition occurs, it is called oil whip and corresponds to the condition measured here.

Figure 8 shows a plot of vibration amplitude at a frequency corresponding to a speed of 465 rpm from the start of the motor to shut down and coasting through 465 rpm. The build up of oil whip is clearly shown in the figure.

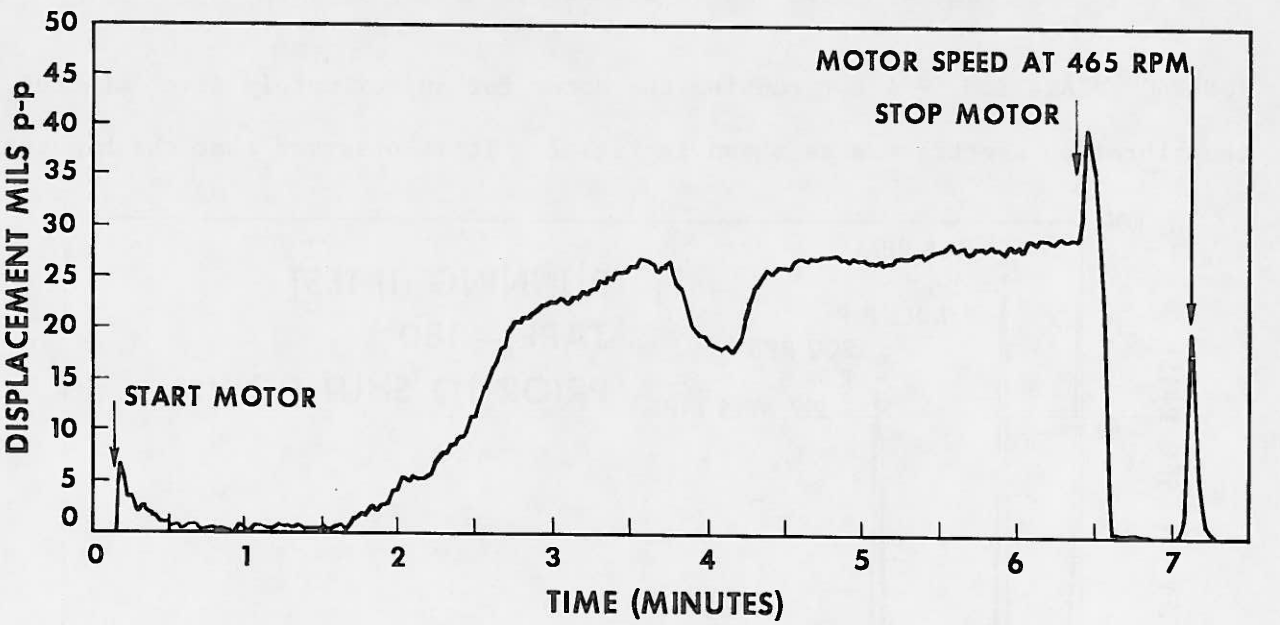


Fig. 8. Vibrations at 465 RPM Due to Motor Start Up and Shut Down.

Initially (just after START MOTOR in Fig. 8), the resonance is excited by the starting transient of the motor. With time and increasing motor speed, the vibration increases to a level of about 30 mils (30×10^{-3} inch or 0.7 mm),

peak to peak after which the motor was turned off and it coasted to a stop. At the point of shut off, the vibration temporarily increased and then dropped to zero. The drop off to zero at this frequency was due to the frequencies at which oil whirl occurs (slightly less than 50 percent of the operating speed) being below 465 rpm. The final peak in Fig. 8 is due to the motor coasting through 465 rpm as it came to a stop.

SOLUTIONS - The plant personnel had previously tried to eliminate the high vibration by clamping three channels to the motor support. A test was performed to evaluate the effectiveness of this solution by comparing the impact response before and after attachment of the braces. The results shown in Fig. 9 indicate that the change in system resonance at 465 rpm would not be

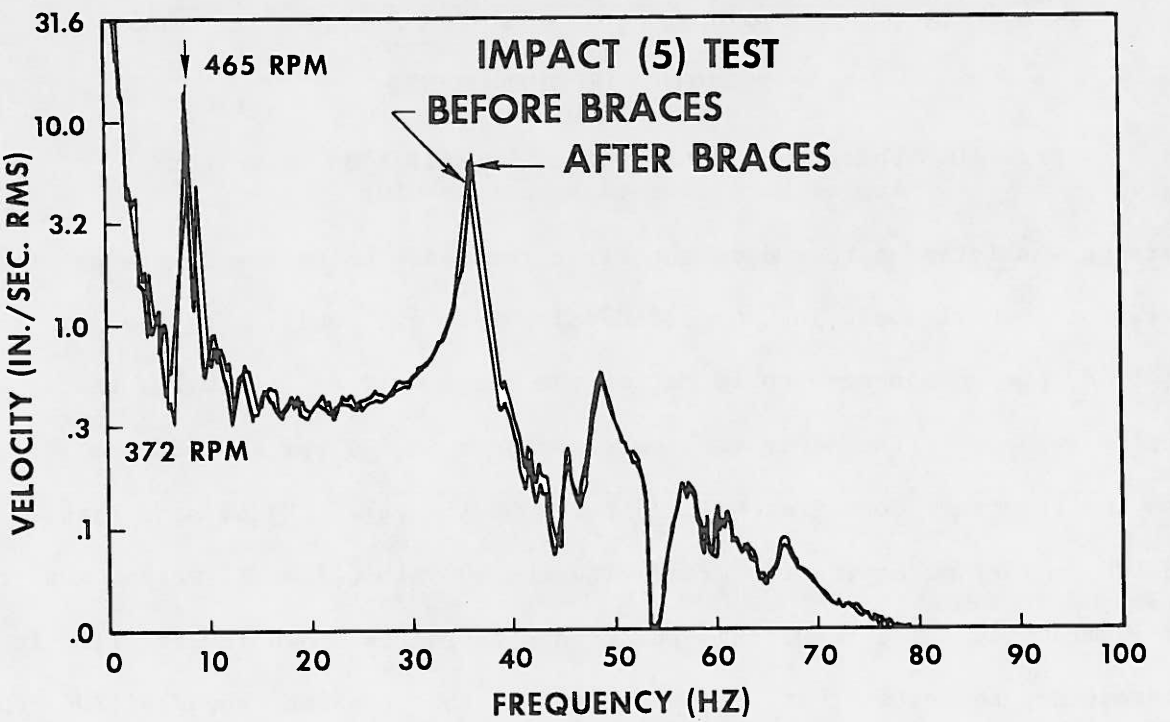


Fig. 9. Velocity Spectra Before and After Installation of Stiffening Braces

sufficient to reduce the problem and therefore, this type of fix was abandoned. The point illustrated here is that it is as important to show that a modification will not work as it is to show that it will make a significant improvement.

A second solution consisted of placing a 4000 lb (17.8 kN) weight on the top of the motor. The results for this case are shown in Fig. 10. This

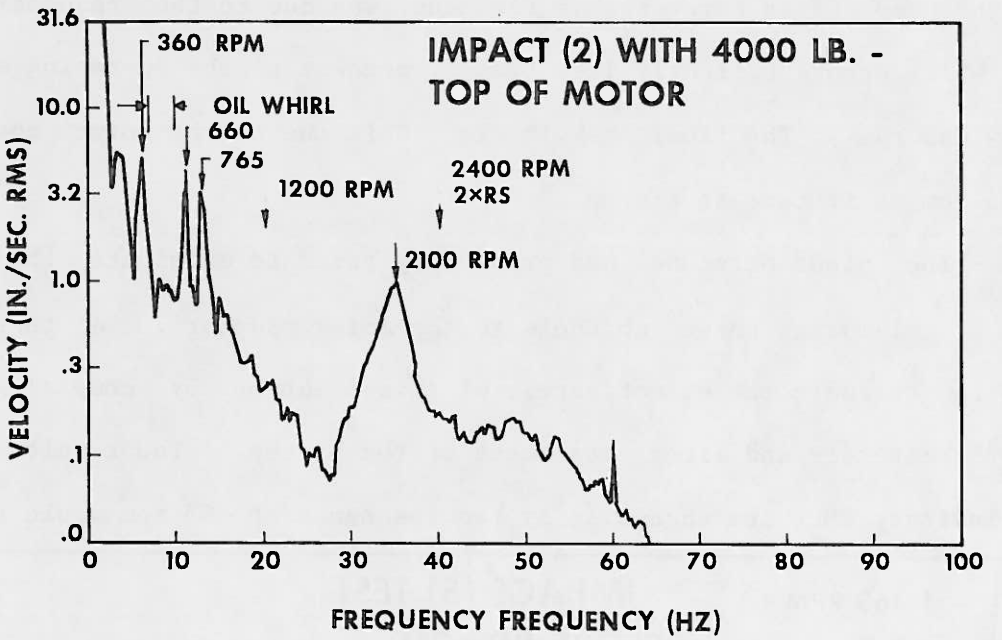


Fig. 10. Velocity Spectrum After Installation of Weight to Top of Motor Due to Impact Loading

approach was intended to reduce the first resonance below the frequency range where oil whirl could lock on and develop into oil whip. Typically, this requires the resonance to be out of the range of 0.35 to 0.50 times the running speed. (The other two new resonances at 660 rpm and 765 rpm result from the temporary container holding the 4000 lbs (17.8 kN) of sand bags).

RESULTS - The motor was restarted with the 4000 lb (17.8 kN) weight and run for 30 minutes. The resulting vibration spectrum is shown in Fig. 11. It is interesting to note that the vibration at the running speed (1200 rpm) remained the same (2.2 mils or 0.05 mm, peak to peak) while the vibration at 465 rpm was completely eliminated. This confirmed the oil whip phenomena as the cause of high vibration at 465 rpm. Subsequently, a permanent weight was attached to the motor to resolve the problem. The pump has run for several years since this modification without recurrence of the high vibration.

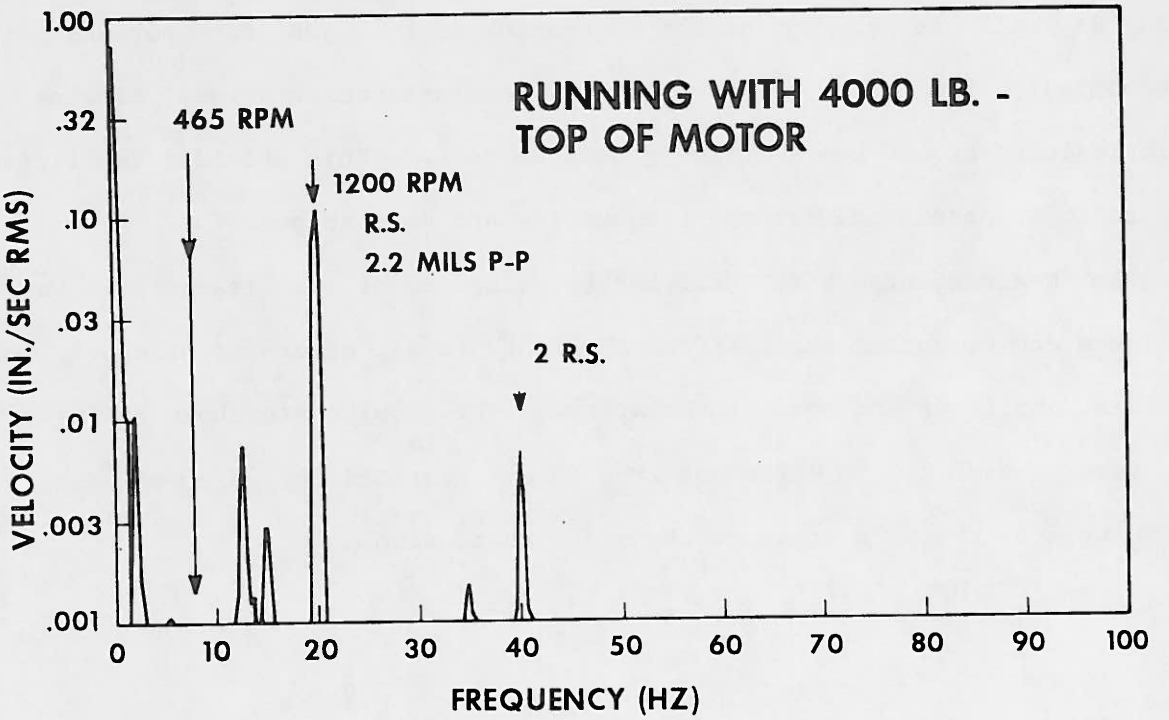


Fig. 11. Velocity Spectrum With Weight on Motor and Motor Running

MEASUREMENT AND ANALYSIS TIME - The above field investigation was performed in one day. The relatively short time required to complete the investigation is attributed to the use of state-of-the-art instrumentation with its capabilities for rapidly analyzing and presenting vibration data in the form of plots identical to those included in this paper.

CASE HISTORY NO. 2 - CHIMNEY STACK NATURAL FREQUENCIES

BACKGROUND - A study was required to determine the wind interaction between a new 500 ft (152 meter) tall stack and a nearby identical existing stack. The greatest uncertainty in the analysis was the influence of the pile foundation of the computed natural frequencies. In order to resolve this uncertainty, it was decided to determine the natural frequencies by analysis of the existing stack vibration from wind forces.

MEASUREMENTS, ANALYSIS, AND RESULTS - The stack was instrumented with vibration transducers at three elevation locations on the liner and outer

shell as well as the top of the foundation (not a job for persons with acrophobia). The wind at the time of the measurements was blowing at approximately at 10 knots at the ground surface. This provided sufficient excitation to obtain the natural frequencies and mode shapes.

The measurements were analyzed by using one of the transducers as a reference and computing the TRANSFER FUNCTION to all other locations. This provides amplitude and phase information. The results are shown in Fig. 12 and were found to be different from those computed by use of assigned stiffness from the pile group to the stack foundation.

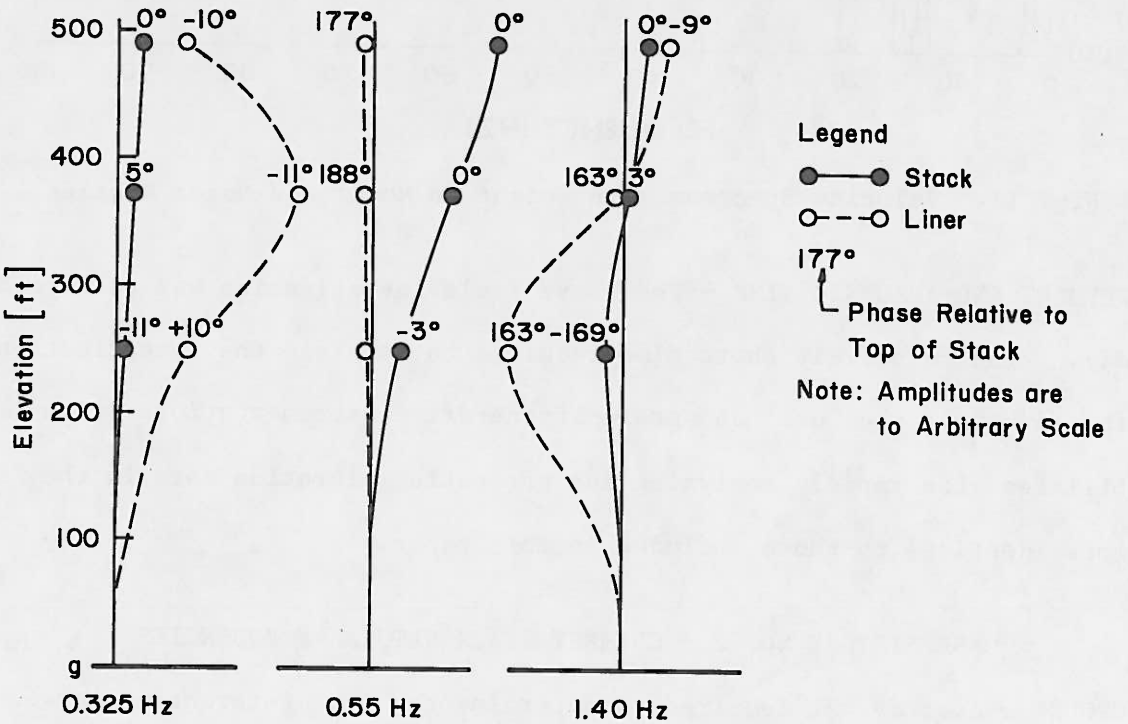


Fig. 12. Mode Shapes of Chimney Stack and Liner

MEASUREMENT AND ANALYSIS TIME - This study was completed in two days. One day was required to install the transducers and the measurements were completed the next day. Again, the power of the spectrum analyzer to perform detailed data analyses is well illustrated.

SUMMARY AND CONCLUSIONS

Spectrum analyzers are very powerful tools which operate on signals from vibration transducers. Vibration data may be displayed, stored, and plotted in either the time domain or frequency domain. Capability for sophisticated operations on the data exist. Two case studies are given which show how spectrum analyzers may be used to solve vibration problems quickly and easily. Use of this equipment is relatively easy and fast but demands that the operator be well versed in the fundamentals of engineering vibrations and their mathematical representation.

ACKNOWLEDGEMENTS

The authors wish to acknowledge the National Science Foundation and the University of Kentucky who provided a spectrum analyzer for the Civil Engineering Department at the University. They also wish to acknowledge the firm of Stone and Webster Engineering Corporation from whose files came the two case studies. Finally, the authors are indebted to Mr. Chiang Lin for proof reading the manuscript.

USE OF SPECTRAL ANALYSIS OF SURFACE WAVES METHOD FOR DETERMINATION OF MODULI AND THICKNESSES OF PAVEMENT SYSTEMS

by

Soheil Nazarian
Research Assistant
The University of Texas at Austin
Austin, Texas

Kenneth H. Stokoe, II
Associate Professor
The University of Texas at Austin
Austin, Texas

W. R. Hudson
The Dewitt C. Greer Centennial Professor
The University of Texas at Austin
Austin, Texas

ABSTRACT

The Spectral-Analysis-of-Surface-Waves (SASW) method is a nondestructive method for determining moduli and thicknesses of pavement systems. By means of a transient impact on the surface of a pavement system (or soil deposit), a group of waves with different frequencies is transmitted to the medium. Seismic wave velocities and eventually elastic moduli and thicknesses of the various layers in the pavement system are determined from analysis of the phase information for each frequency determined between two receivers located on the surface. The method has the advantages of: 1) being non-destructive, 2) having a unique solution, and 3) being capable of full automation.

Three series of tests were performed on State Highway 71 near Columbus, Texas, and the results are presented herein. Testing was performed on an asphaltic concrete pavement (ACP), a continuously reinforced concrete pavement (CRCP) and natural soil occupying the median at the site. Elastic moduli determined from the SASW method are compared with those determined with crosshole seismic tests and Dynaflect measurements. Moduli determined by the SASW method are in agreement with those from crosshole tests, whereas moduli back claculated from dynaflect measurements compare rather unfavorably with the other two methods.

INTRODUCTION

Many different methods have been proposed for evaluating the elastic properties of pavement systems. These methods can be categorized into four groups, namely: (1) static deflection, (2) steady-state dynamic deflections, (3) impact load-response, and (4) wave propagation methods. An in-depth review of these methods has been presented by Lytton et al (1) and Hoar (2). The methods either apply a static or dynamic load to

the system being tested. Methods involving static loading have the drawback of a nonunique solution. In addition, only a summation of the overall stiffness of the pavement system is measured, and separation of this summation into properties of the different layers involves considerable judgement. Dynamic methods such as the dynaflect and falling weight deflectometer are more promising, but the equipment is expensive and again a nonunique solution is obtained. In addition, dynamic tests involve wave propagation testing, but the data obtained from these tests are analyzed assuming static loading. This assumption of static loading for a wave propagation test can result, at a minimum, in significant differences between actual and assumed stress distributions.

In this paper, the spectral-analysis-of-surface-waves (SASW) method for determination of moduli and thicknesses of pavement systems is presented. The SASW method is a wave propagation method which has been under development for some time (Nielsen and Baird (3) and (4) and Heisey et al (5)). Presented herein are new refinements in collecting and analyzing the data along with several case histories which illustrate the value of the method and uniqueness of the solution.

EVALUATION OF ELASTIC PROPERTIES FROM WAVE VELOCITY

Wave motion created by a disturbance on an elastic half-space can be described by two kinds of waves; body and surface waves (Richart et al (6)). Body waves consist of shear (S) and compression (P) waves. Young's modulus, E, shear modulus, G, and Poisson's ratio, ν, of a material are commonly expressed in terms of the wave velocities as:

$$E = \rho(1+\nu)(1-2\nu)V_p^2/(1-\nu) \qquad (1)$$

$$G = \rho V_s^2 \tag{2}$$

and

$$\nu = (0.5(V_p/V_s)^2-1)/((V_p/V_s)^2-1) \tag{3}$$

where V_p, V_s, and ρ are the compression wave velocity, shear wave velocity and mass density, respectively.

The second kind of wave associated with an elastic half-space is a surface wave, also called a Rayleigh wave (R) (Ewing et al (7)). Rayleigh wave velocity, V_R, is constant in a homogeneous half-space and is independent of frequency. Each frequency, f, has a corresponding wave length, L_R, according to:

$$V_R = f\ L_R \tag{4}$$

Rayleigh wave and shear wave velocities are related by Poisson's ratio. Although the ratio of R-wave to S-wave velocity increases as Poisson's ratio increases, the change in this ratio is not significant, and it can be assumed that it is approximately equal to 0.90 without introducing an error larger than five percent.

METHOD OF SPECTRAL-ANALYSIS-OF-SURFACE-WAVES

The spectral-analysis-of-surface-waves method is a powerful and potentially economical method for evaluating elastic properties of pavement systems as well as natural soil deposits. As a result, the method can be used to solve problems in which moduli are used directly, such as overlay designs, or indirectly, such as to control the quality of compaction of pavement materials during construction.

The SASW method is a nondestructive test method in which both the source and receivers are placed on the pavement surface. Rayleigh waves at low-strain levels are then generated and detected. The method has the advantages of repeatability, high accuracy, no boreholes, and a simple set-

up and test procedure. Additionally, the method has the benefits of: 1) determination of a continuous profile of site properties, including modulus values and layer thicknesses, and 2) limited judgement required to reduce the data, with the possibility of full automation. The main disadvantage at this point in the development is that testing is not performed rapidly. For example, each of the three sites presented as case histories took about two hours to test. However, once testing is completely automated, it should be possible to test a site in a matter of minutes.

Investigation of each site with the SASW method consists of the following three phases: 1) field testing, 2) determination of the R-wave dispersion curve, and 3) inversion of the R-wave dispersion curve. Each phase is discussed in the following paragraphs.

Field Testing

An illustration of the test set-up is shown in Fig. 1. The set-up consists of an impulsive source, two vertical geohpones (velocity transducers) and a transient event recorder/analyzer.

Impulsive Source. The source must be capable of transiently generating Rayleigh waves over a wide range in frequencies with adequate amplitude so that they can be detected by the geophones. Simultaneously, the source should generate minimal P- and S-wave energy. For testing presented herein, a 2-lb sledge hammer and chisel were used as the source when the spacing between the source and first receiver was less than about 4 ft. When this spacing became greater than 4 ft, 8-lb and 15-lb sledge hammers were used to a maximum spacing of 16 ft.

Location of Receivers (Geophone Array). Factors that affect appropriate receiver spacing include: 1) velocity of the material, 2) depth of investi-

gation, 3) range of frequencies, 4) attenuation properties of the medium, and 5) sensitivity of the instrumentation. Based upon studies at several soil sites, Heisey et al (5) suggested that the distance between receivers, x, should be less than two wavelengths and greater than one third of a wavelength. This relationship can be expressed as:

$$L_R/3 < x < 2L_R \tag{5}$$

This relationship was used in analyzing all data presented herein.

In addition to the factors cited above, Nazarian and Stokoe (8) have shown that different geometries of the set-up can affect the results. The two most common types of geometrical arrangements for the source and receivers in seismic testing are the common source/receiver (CSR) geometry and the common midpoint (CMP) geometry. In the CSR geometry, either the source or receivers are fixed in one location and the other is moved during the test. In the CMP geometry, both the source and receivers are moved the same distance about an imaginary centerline. For a medium consisting of a stack of horizontal layers with lateral homogeneity, the results of the tests performed with both methods are identical. If the layers are not horizontal or the seismic properties of any layer vary laterally, the CMP geometry is preferred because velocities are averaged over the testing range. However, if only a single CMP experiment is performed, there is no way to determine the dip of the layers.

When using the SASW method, the area between the receivers is important, and the properties of the materials between the source and near receiver have little effect on the results. Thus, the imaginary centerline in the CMP method is located between the receivers. The two receivers are moved away from the imaginary centerline at an equal pace, and the source is

moved such that the distance between the source and near receiver is equal to the distance between the two receivers. This geometry of source and receivers is called common receivers midpoint (CRMP) geometry, hereafter, and is illustrated in Fig. 1.

Nazarian and Stokoe (8) have shown that use of the CRMP geometry in SASW tests significantly reduces scatter in the data at shallow depths. An additional advantage of the CRMP geometry is, that by reversing the location of the source while keeping the receiver location fixed and by averaging the records from these direct and reversed tests, the effect of any internal phase between the two geophones can be eliminated.

Recording Device. A convenient device for spectral analysis of surface waves is a Fourier spectral analyzer. A Fourier analyzer is a digital oscilloscope that by means of a microprocessor attached to it has the ability to perform directly in either the time or frequency domain. Fourier analysis is a powerful tool in decomposition of complicated transient waveforms into a group of simple harmonic waveforms. The benefit of having the ability to view the frequency-domain data in the field cannot be overemphasized.

Determination of R-wave Dispersion Curve

The variation of wave velocity with frequency (or wavelength) is known as dispersion, and a plot of velocity versus wavelength is called a dispersion curve. The dispersion curve is developed from phase information of the cross power spectrum. This information provides the relative phase between two signals (two-channel recorder) at each frequency in the range of frequencies excited in the SASW test. For a travel time equal to the period of the wave, the phase difference is 360 degrees. Thus, for each frequency

the travel time between receivers can be calculated by:

$$t(f) = \phi(f)/(360\ f) \tag{6}$$

where:

f = frequency,

t(f) = travel time of the given frequency, and

$\phi(f)$ = phase difference in degrees of the given frequency.

The distance between the geophones, x, is a known parameter. Therefore, R-wave velocity at a given frequency is simply calculated by:

$$V_R(f) = x/t(f) \tag{7}$$

and the corresponding wavelength of the R-wave is equal to:

$$L_R(f) = V_R(f)/f \tag{8}$$

By repeating the procedure outlined by Eqs. (6) through (8) for every frequency, the R-wave velocity corresponding to each wavelength is evaluated, and the dispersion curve is determined.

Rayleigh wave velocities determined by this method are not actual velocities of the layers but are apparent R-wave velocities. Existance of a layer with a higher or lower velocity at the surface of the medium affects measurement of the velocities of the underlying layers. As such, a method for evaluation of actual R-wave velocities from apparent R-wave velocities is necessary in SASW testing.

Inversion of R-Wave Dispersion Curve

Inversion of the R-wave dispersion curve, or (in short) inversion, is the procedure of determination of the actual propagation velocities at different depths from the dispersion curve. Inversion consists of determina-

tion of the depth of each layer and the shear wave velocity of each layer from the apparent R-wave velocity versus wavelength information.

In a layered medium in which no significant contrast in velocities of the layers exists, the apparent and actual R-wave velocities are approximately equal. But if one or more layers have significantly different properties, the apparent and actual R-wave velocities will be substantially different. This is especially true in a pavement system in which the stiffness of the materials can differ greatly. For example, in case of a CRCP, elastic properties of the concrete are typically many times higher than those of other materials. For this system, the apparent velocities of the underlying layers would be falsely high. Conversely, at a soil site where there may be significant seasonal precipitation, the first few feet of ground are softer in the wet season, and apparent velocities of the underlying layers determined during this season would be too low.

To demonstrate this effect, the dispersion curves for adjacent ACP and CRCP sections are shown in Fig. 2. Although the properties of these two pavement surfaces are different, the subbase and natural soil beneath the pavements are presumably the same since the systems are within a few feet of each other. However, the two dispersion curves for the deposits beneath the pavement surfaces do not agree, with the apparent R-wave velocities associated with the materials beneath the CRCP section consistantly higher than those beneath the ACP section.

In the preliminary investigation of the SASW method, Heisey et al (5) considered that the effective depth of sampling is equal to one third of a wavelength. (Other work suggests that this is a reasonable approximation, especially at soil sites (Gazetas (9)). Heisey et al also assumed that the

apparent and actual R-wave velocities for each wavelength were equal. This crude inversion method is applicable to soil sites with relatively uniform, thick layers, and they successfully applied this method to several soil sites.

A refinement in the inversion process has been developed herein. This refinement is based upon Haskell's (10) matrix for elastic surface waves in a multilayered solid media. To simplify the process of inversion, some assumptions were made. These assumptions include: 1) the layers are horizontal, 2) the velocity of each layer is constant and does not vary with depth, 3) the layers are homogeneous and linearly elastic, 4) the effective sampling depth is equal to one third of the wavelength, and 5) the apparent and actual valocities of the top layer are equal. From item 4, the depth of all layers are known, and from item 5, the actual R-wave velocity of the top layer is available. By assuming that the wavefront passes through the overlying layers with the velocities of those layers, the R-wave velocity profile can be constructed from top to bottom sequentially. Because of the simplifying assumptions used, this refined inversion process does not accurately function under certain conditions. It is not yet possible to handle: 1) relatively thin layers (relative to the thickness of the other layers) with considerable variation in the properties of the overlying layer, and 2) layers with variable velocity with depth. However, the inversion process is under continuous development and improvement.

EXPERIMENT NEAR COLUMBUS, TEXAS

The SASW method was used on three sections with different layerings near Columbus, Texas. These series of tests are particularly important because by means of the SASW method the elastic properties of a concrete pavement system have been evaluated for the first time.

Description of Site

The site was located near Columbus, Texas, on State Highway (SH) 71 about half a mile south of the SH 71 overpass on US 90. This section consists of two south-bound lanes of continuously reinforced concrete pavement, each 12-ft wide, a 4-ft wide asphaltic concrete shoulder, and a natural soil median.

In August, 1981, a preliminary set of SASW tests was conducted on all three sections (CRCP, ACP, and median) by S. Heisey. In March, 1982 a second set of tests was performed at approximately the same location. In conjunction with the second set of tests, a series of crosshole seismic tests was performed under the asphaltic concrete shoulder and median. Unfortunately, due to the lack of appropriate drilling equipment, no crosshole tests could be conducted under the CRCP section. A third set of SASW tests was also performed in May, 1982 on the CRCP section to study further the reproducibility of the results.

Material profiles at the ACP and soil median sections determined from the boreholes drilled for crosshole seismic tests are shown in Fig. 3. It is assumed that the soil profiles under the CRCP and ACP sections are identical below the subbase. The assumed profile for CRCP section is also shown in Fig. 3.

Set-Up and Procedure

The general configuration of the source, receivers, and recording equipment is shown in Fig. 1. Vertical geophones with a natural frequency of about 8 Hz were used as receivers. The CRMP geometry was used for testing in March and May, 1982 as illustrated in Fig. 4. The distance between geophones ranged from one to 16 ft, and reversed tests were performed. The

closer spacings were necessary for determining properties at the shallower depths and the larger spacings for deeper layers.

Common source geometry was used for testing in August, 1981. In this case the location of the source was held fixed, and the receivers were moved. Receivers and receiver spacings were the same as in the 1982 tests. However, reversed testing was not performed in 1981.

PRESENTATION OF RESULTS

The primary objective of the tests performed by the SASW method was to evaluate the elastic properties and thicknesses of the different layers of the ACP and CRCP sections. As this method has been used very little on pavement sections, the reproducibility of the results by different operators and for different attempts was of concern. As such, the first series of tests was conducted by S. Heisey in August, 1981, and the next two series were performed by the authors in March and May, 1982. In addition, the SASW method was used for the first time on a CRCP section.

Soil Median

Average dispersion curves from these two sets of tests performed in August, 1981 and March, 1982 are shown in Fig. 5. Upon comparing these curves, it can be seen that there is no major difference in the results for wavelengths longer than 10 ft, with a maximum difference of 8 percent at a wavelength of about 36 ft. Determination of the average dispersion curve for the data from August, 1981 was somewhat difficult because of scatter in the data. Also, extensive precipitation occurred on the day before testing in March, 1982, which caused the first few feet of the median to be very soft and resulted in a significant drop in the elastic properties of the near-surface material.

ACP Section

Average dispersion curves for the experiments conducted on this section in 1981 and 1982 are shown in Fig. 6. The thicknesses and apparent R-wave velocities for different layers from the 1981 and 1982 tests are in good agreement, and no significant differences can be detected in the average dispersion curves from these attempts. The relative difference between the two curves does not exceed 6 percent. Adequate high frequencies were not generated in the tests performed in 1981. Therefore, no sampling was done in the ACP in this series.

CRCP Section

The most critical section studied was the CRCP section. Fine layering in the pavement system and a large contrast in velocities of the layers in a depth of less than 3 ft required special considerations. Use of a source capable of generating high-frequency waves was essential. For spacings of one and 2 ft, a 2-lb sledge hammer and chosel worked well, generating frequencies as high as 3900 Hz. Good coupling between the concrete and geophones was also necessary to monitor correctly the high frequencies. This was accomplished by epoxying the geophones to the pavement.

The dispersion curve for the third attempt on the CRCP section in May, 1982 is shown in Fig. 7, as an example. Average dispersion curves from all three attempts on this section are shown in Fig. 8. High frequencies were not excited in August, 1981. Therefore, no information on the properties of the concrete and base layers could be obtained. The number of tests performed in March, 1982 was less than those of August, 1981, due to time limitations. The shortest wavelength obtained in the second attempt was approximately 1 ft (equivalent to a sampling depth of 4 in.). The primary concerns in the May 1982 tests were to sample even shallower depths and to check the

reproducibility of the results. Several tests with close spacings (spacing between the geophones equal to one and 2 ft) were performed which resulted in the depth of sampling being decreased to 3 inches. It should be mentioned that the highest frequency excited in these tests was 3900 Hz, whereas in the first attempt it was 3100 Hz. The 800-Hz increase in the upper bound of the frequency content only decreased the depth of sampling by about one inch.

Except for the range of wavelengths from 5 to 8 ft in which there is some scatter, the dispersion curves in Fig. 8 agree with less than a 9 percent difference which demonstrates the high degree of reproducibility of the tests. The deviation for 5-ft to 8-ft long wavelengths corresponds to the few inches above and below the boundary between the subbase and compacted fill and could possibly be due to variations in the level of the subbase-fill interface along the distance covered by the geophones. However, as emphasis was placed on measurement of the pavement system in May, 1982, the results of this series of tests seem more reliable.

Comparison of Elastic Properties

Crosshole Seismic Tests. To evaluate independently wave velocities and moduli at each site, crosshole seismic tests were performed at the ACP and soil median sections. (Details of the testing procedure are presented in Nazarian and Stokoe (8)). Both compression and shear wave velocites were measured. Shear wave velocities determined from the crosshole tests were then compared with S-wave velocities based on the average dispersion curves for the soil median and ACP sections from March, 1982 (Figs. 5 and 6) and the average dispersion curve for the CRCP section from May, 1982 (Fig. 8). This comparison is presented in Figs. 9a, 9b and 9c for the median, ACP and CRCP sections, respectively.

Shear wave velocities determined by the SASW and crosshole methods are in good agreement, especially at the median section. Deviation of the shear wave velocities under the median from these two methods is less than seven percent, except at a depth of about 5 ft where the difference is about 14 percent. At the ACP section, there are some differences between shear wave velocities determined by the two methods as shown in Fig. 9b. The major difference occurs in the subbase, and results from use of the preliminary inversion method presented herein which is not able to handle sudden changes in velocity of a thin layer. If this difference in S-wave velocities from the two methods is ignored, the remainder of the profile differs by less than nine percent for the ACP section. Because the crosshole method is well established as an accurate method of determining in situ shear wave velocities (Stokoe and Hoar (11) and Woods (12)), these close comparisons show the effectiveness of the SASW method.

As no crosshole tests could be perfomred at the CRCP section, it was assumed that the S-wave velocity profile below the CRCP section (i.e. below the depth of 2.5 ft) from crosshole tests performed under the ACP section also represented the material below the CRCP section. Comparison of these two S-wave velocity profiles shows that they agree within 10 percent, and hence the SASW method can also be used effectively on concrete pavements.

Profiles of Young's moduli from the SASW and crosshole tests at the three sections are shown in Fig. 10 and in Tables 1, 2, and 3. In the crosshole tests, Young's moduli were calculated from the P-wave velocities measured in situ. In the case of the SASW tests, shear moduli were determined from the shear wave velocities, and then, with values of Poisson's ratio evaluated from the crosshole tests, Young's moduli were calculated. In

general, Young's moduli from the two test methods are within about 10, 12 and 20 percent at the soil, ACP and CRCP sections, respectively. These close comparisons demonstrate the value of the SASW method.

Dynaflect Testing. Young's moduli were also backcalculated from deflection basins measured by Dynaflect testing on the CRCP section. These moduli are summarized in Table 4 along with those determined by the SASW tests at the same location. The closest comparison between moduli from the two methods occurs in the asphaltic concrete base layer where the values are within about 13 percent. However, in the other layers the moduli differ, on the average, by about 40 percent. Based on the close comparisons of moduli measured independently by the SASW and crosshole tests, it is felt that moduli determined by the SASW tests more accurately reflect the in situ conditions than do the Dynaflect results.

SUMMARY AND CONCLUSIONS

The spectral-analysis-of-surface-waves method for determination of moduli and thicknesses of pavement systems as well as soil sites is described herein. This method can be employed to solve problems in which moduli are used directly, such as overlay designs, or indirectly, such as to control the quality of compaction of pavement materials during construction. The method has the advantages of being nondestructive, having a unique solution and being capable of full automation.

Preliminary studies of the feasibility and testing procedure were conducted by Heisey et al (5). This initial work has been expanded and improved in the following areas:

1. The test set-up has been modified. Instead of the common source geometry which was used, the tests are now performed using a

common reciever midpoint geometry which significantly reduces scatter in the data. Also, the direction of testing is reversed to eliminate the effect of possible internal phase between the receivers and to average the effect of dipping layers.

2. A simple inversion method for elimination of the effect of high- or low-velocity shallow layers has been developed so that moduli at depth can be accurately measured.

The inversion process was employed to determine the elastic properties of three sites with considerably different layerings, namely, an asphaltic concrete pavement, a continuously reinforced concrete pavement and a natural soil. Elastic moduli determined from the SASW method compare favorably with those determined with crosshole siesmic tests. Deviations between moduli determined by the two methods are on the average less than 10, 12 and 20 percent in the median, ACP and CRCP sections, respectively. Elastic moduli determined from the SASW method are also compared with those determined from Dynaflect measurements on the CRCP. The comparison is rather unfavorable, with moduli varying from 13 to 45 percent.

ACKNOWLEDGEMENTS

This work was supported by the Texas State Department of Highways and Public Transportation (TSDHPT) under the Research Project 3-8-79-256. The writers wish to thank Messrs. Gerald Peck and Richard Rogers of that organization for their interest, encouragement and support. Appreciation is also extended to Mr. Waheed Uddin for reducing the dynaflect data. The technical assistance and funding provided by the TSDHPT are sincerely appreciated.

REFERENCES

1. Lytton, R.L., W.M. Moore, and J.P. Mahoney, "Pavement Evaluation: Phase I, Pavement Evaluation Equipment," Report No. FHWA-RD-75-78, Federal Highway Administration, Washington, D.C., 1975.

2. Hoar, R.J., "Field Measurement of Seismic Wave Velocity and Attenuation for Dynamic Analysis," Ph.D. Thesis, The University of Texas at Austin, 1982.

3. Nielsen, John P., and Glenn T. Baird, "Air Force System for Non-destructive Testing of Pavements," Presented at the Symposium on Nondestructive Test and Evaluation of Airport Pavements, Nov. 18-20, 1975, Vicksburg, MS.

4. Nielsen, John P., and Glenn T. Baird, "Evaluation of an Impulse Testing Technique for Nondestructive Testing of Pavements and Recommended Follow-On Research," Published by U.S. Air Force Civil and Environmental Engineering Office, CEEDO-TR-77-46, Tyndall Air Force Base, Florida, September 1977.

5. Heisey, J.S., K.H. Stokoe, II, and A.H. Meyer, "Moduli of Pavement Systems from Spectral Analysis of Surface Waves," Transportation Research Report, No. 852, Transportation Research Board, Washington, D.C., pp. 22-31, 1982.

6. Richart, R.F., Jr., J.R. Hall, Jr., and R.D. Woods, Vibration of Soils and Foundations, Prentice-Hall, Englewood Cliffs, New Jersey, 1970.

7. Ewing, W.M., W.S. Jordetsky, and F. Press, Elastic Waves in Layered Media, McGraw Hill Book Co., Inc., 1957.

8. Nazarian, S., and K.H. Stokoe, II, "Evaluation of Moduli and Thicknesses of Pavement Systems by SASW Method," Report No. 256-4, The Texas State Department of Highways and Public Transportation, Austin, TX, 1982.

9. Gazetas, A., "Vibrational Characteristics of Soil Deposits with Variable Wave Velocity," International Journal for Numerical and Analytical Methods in Geomechanics, Vol. 6, pp. 1-20, 1982.

10. Haskell, N.A., "The Dispersion of Surface Waves in Multilayered Media," Bulletin of Seismological Society of America, Vol. 43, No. 1, pp. 17-34, 1953.

11. Stokoe, K.H., II, and Hoar, R.J.," Variables Affecting In Situ Seismic Measurements," Proceedings of the Conference on Earthquake Engineering and Soil Dynamics, ASCE, Pasadena, CA, Vol. II, pp. 919-939, 1978.

12. Woods, R.D., "Measurement of Dynamic Soil Properties," Proceedings of the Conference on Earthquake Engineering and Soil Dynamics, ASCE, Pasadena, CA, Vol. I, pp. 91-178, 1978.

LIST OF TABLES

Table

1 Comparison of Young's Moduli from Crosshole Seismic and SASW at Soil Median

2 Comparison of Young's Moduli from Crosshole Seismic and SASW at ACP Section

3 Comparison of Young's Moduli from Crosshole Seismic and SASW at CRCP Section

4 Comparison of Young's Moduli Calculated from Wave Velocities and Deflection Measurement at CRCP Section

Table 1 - Comparison of Young's Moduli from Crosshole Seismic and SASW Tests at Soil Median

Depth (ft)	Young's Modulus (psi)		Difference (3)-(2) / (3) (percent)
	Crosshole	SASW	
(1)	(2)	(3)	(4)
2.5	10180	11230	+9.3
5.0	33150	25540	-29.8
7.5	34810*	31480	-10.5
10.0	30230	31880	+5.2
12.5	35050	-	-
15.0	35510	-	-

* Evaluated from shear wave velocity.

Table 2 - Comparison of Young's Moduli from Crosshole Seismic and SASW Tests at ACP Section

Layer	Depth (ft)	Young's Modulus (psi)		Difference (4)-(3) / (4) (percent)
		Crosshole	SASW	
(1)	(2)	(3)	(4)	(5)
Asphalt	0.58	467500	453200	-3.2
Subbase	1.38	110000	198310	+44.5
Compacted Fill	1.67	49500	45610	-8.5
	2.50	32850	37430	+12.2
	3.33	32350	36900	+11.5
Sandy Clay	5.0	42050	38820	-8.3
	7.5	40250	39340	-2.3

Table 3 - Comparison of Young's Moduli from Crosshole Seismic and SASW Tests at CRCP Section

Layer	Depth (ft)	Young's Modulus (psi)		Difference (4)-(3) / (4) (percent)
		Crosshole	SASW	
(1)	(2)	(3)	(4)	(5)
CRCP	0.83	4675000**	3928000	19.0
Asphalt-Treated Base	1.17	-	462380	-
Lime-Stabilized Subbase	1.67	-	223380	-
Compacted Fill	2.50	32850	41450	-20.8
Sandy Clay	5.00	42050	34740	-21.0
	7.50	40250	37960	-6.0

* Beneath asphalt shoulder.

** From surface refraction tests.

Table 4 - Comparison of Elastic Moduli Calculated from Wave Velocities and Deflection Measurements at CRCP Section

Profile	Young's Modulus, E (psi)	
	SASW Method	Deflection Method*
(1)	(2)	(3)
CRC Surface Layer	3928000	5500000
AC Base Layer	462380	600000
Lime Stabilized Subgrade Layer	223380	125000
Natural Subgrade (soil layers)	37960-41450 (up to 7.5 ft)	28000

* Moduli were backcalculated from fitted deflection basins using elastic theory (ELSYM5).

LIST OF FIGURES

Figure

1 Schematic of Experimental Arrangement for SASW Tests

2 Comparison of Dispersion Curves under Adjacent Asphaltic Concrete and Continuously Reinforced Concrete Sections

3 Material Profile at Each Test Section

4 Pattern of SASW Tests used in March, 1982 and May, 1982

5 Average Dispersion Curves Determined in August, 1981 and March, 1982 for Natural Soil (Median)

6 Average Dispersion Curves Determined in August, 1981 and March, 1982 for Asphaltic Concrete Shoulder

7 Dispersion Curve Determined on May 1982 for Continuously Reinforced Concrete Section

8 Average Dispersion Curves Determined in August, 1981, March and May, 1982 for Continuously Reinforced Concrete Pavement

9 Comparison of Shear Wave Velocities from Crosshole and SASW Methods

10 Comparison of Young's Moduli from Crosshole and SASW Methods

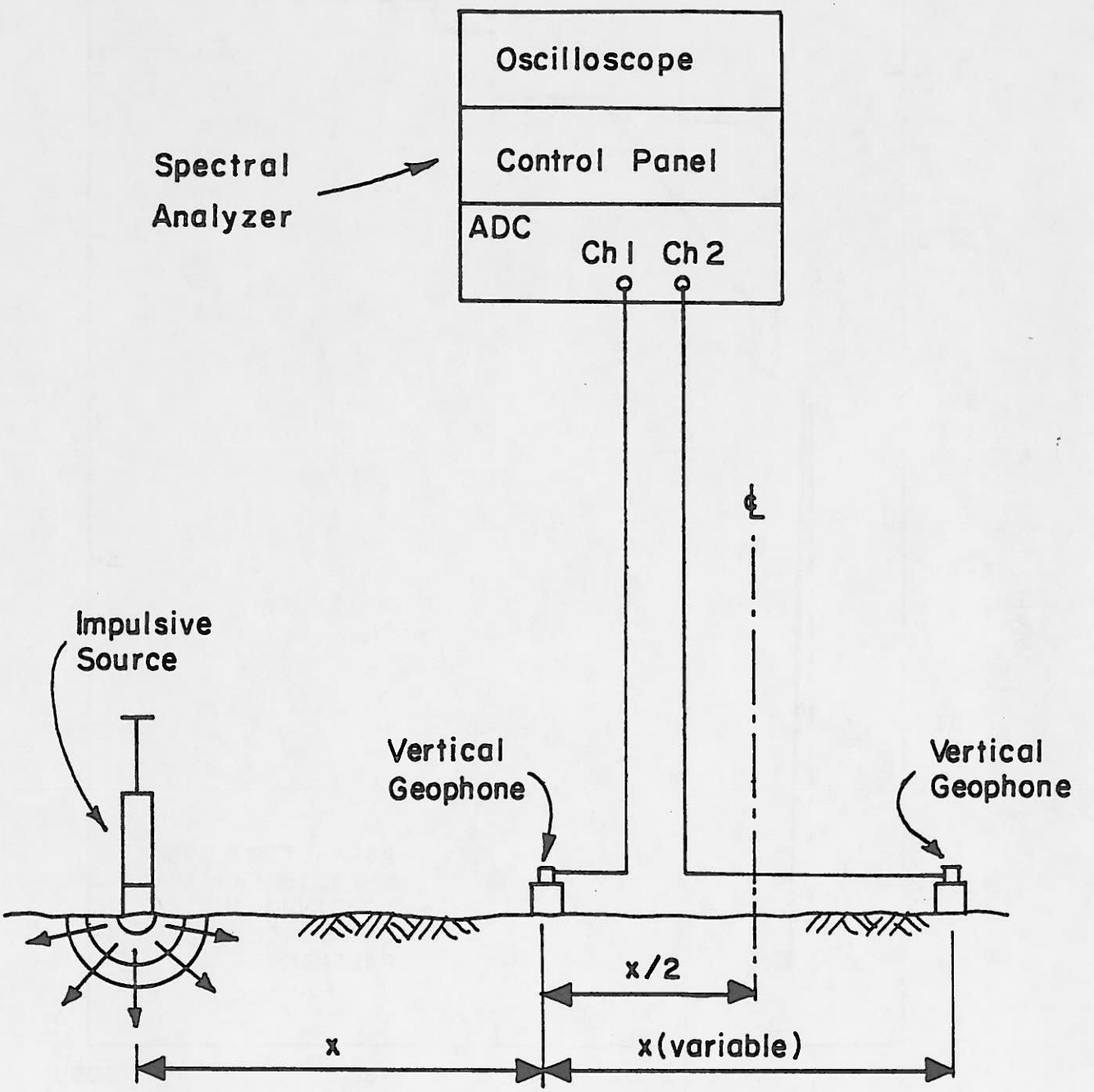


Fig. 1 - Schematic of Experimental Arrangement for SASW Tests

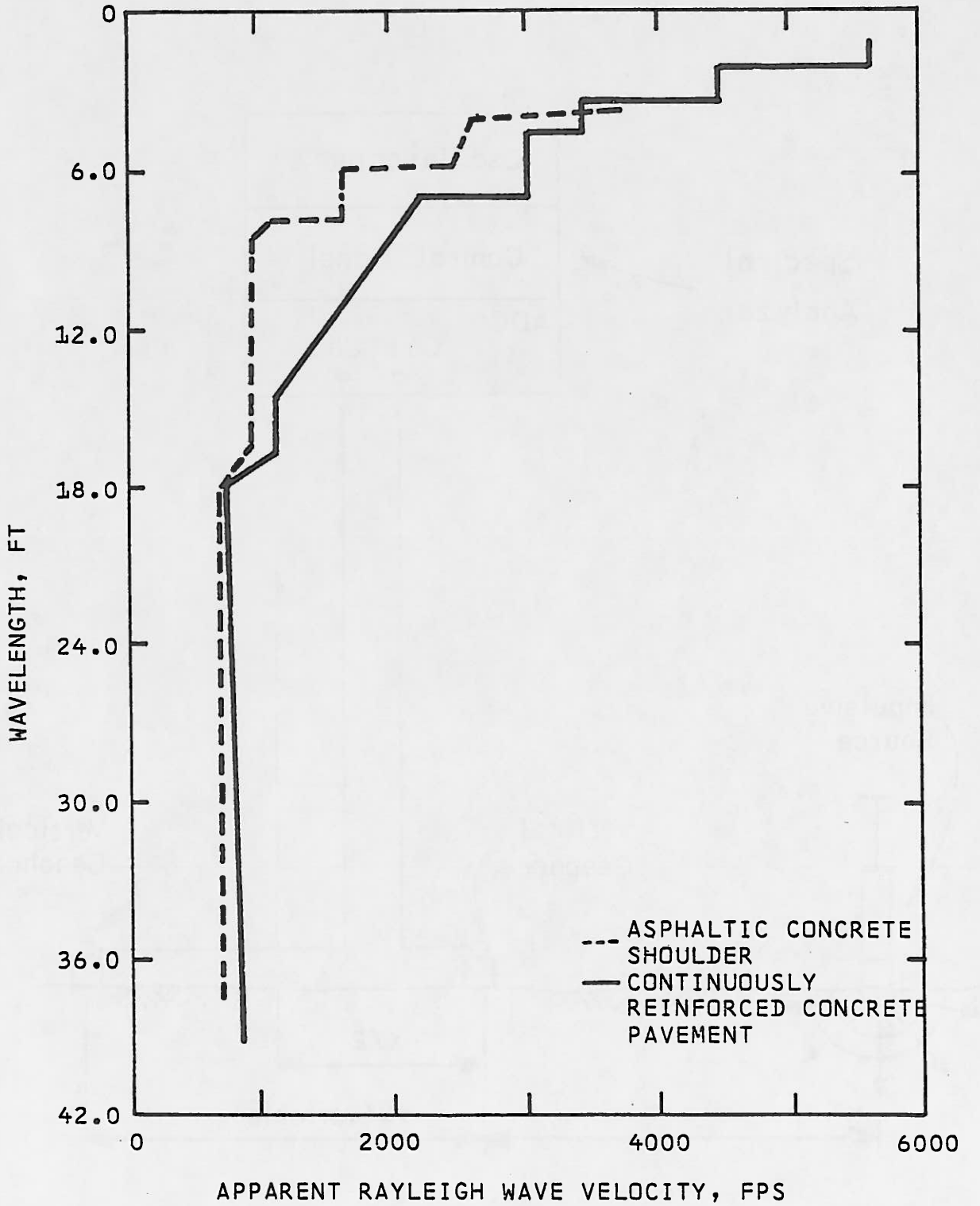


Fig. 2 - Comparison of Dispersion Curves Under Adjacent Asphaltic Concrete and Continuously Reinforced Concrete Sections

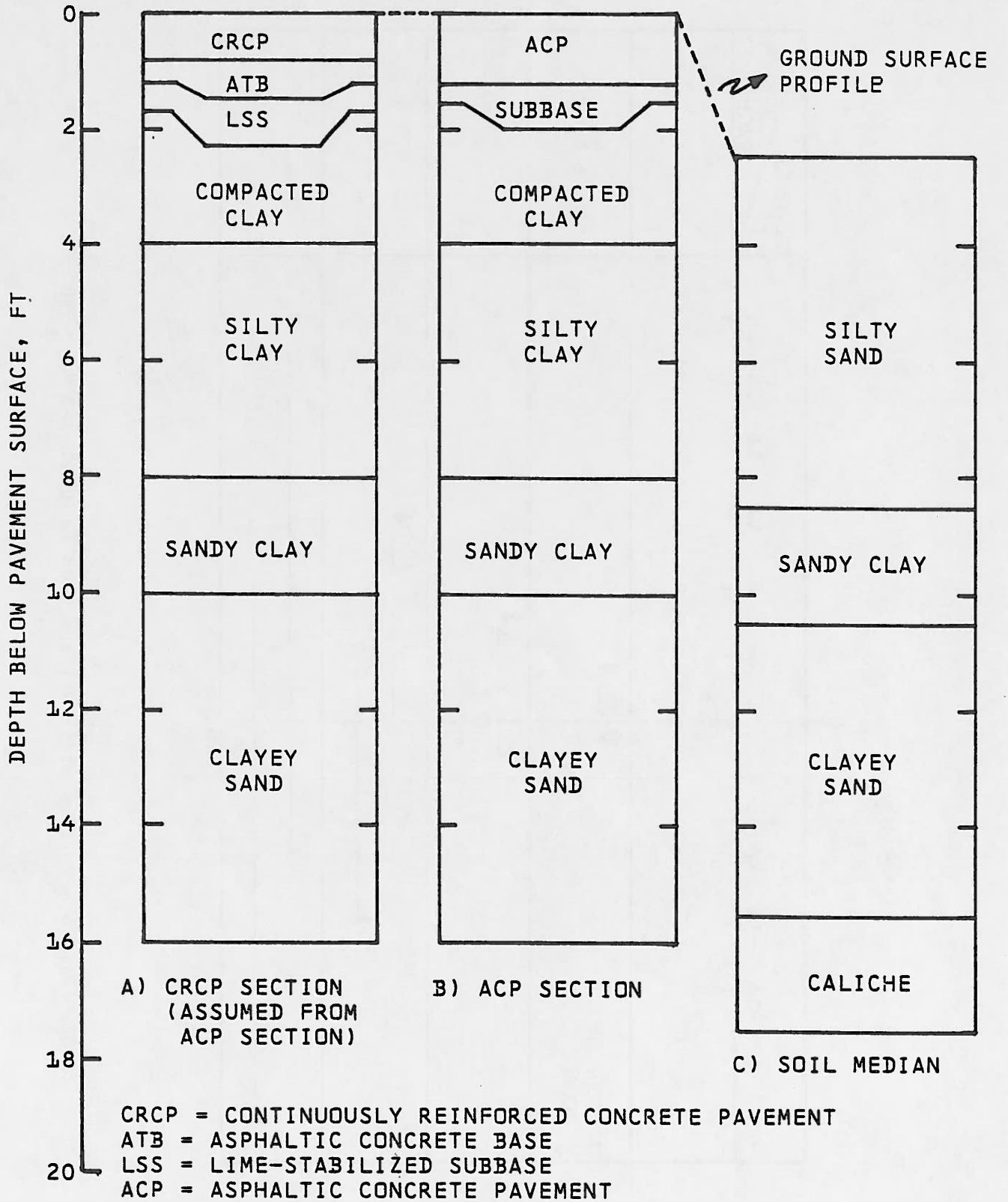


Fig. 3 - Material Profile at Each Test Section

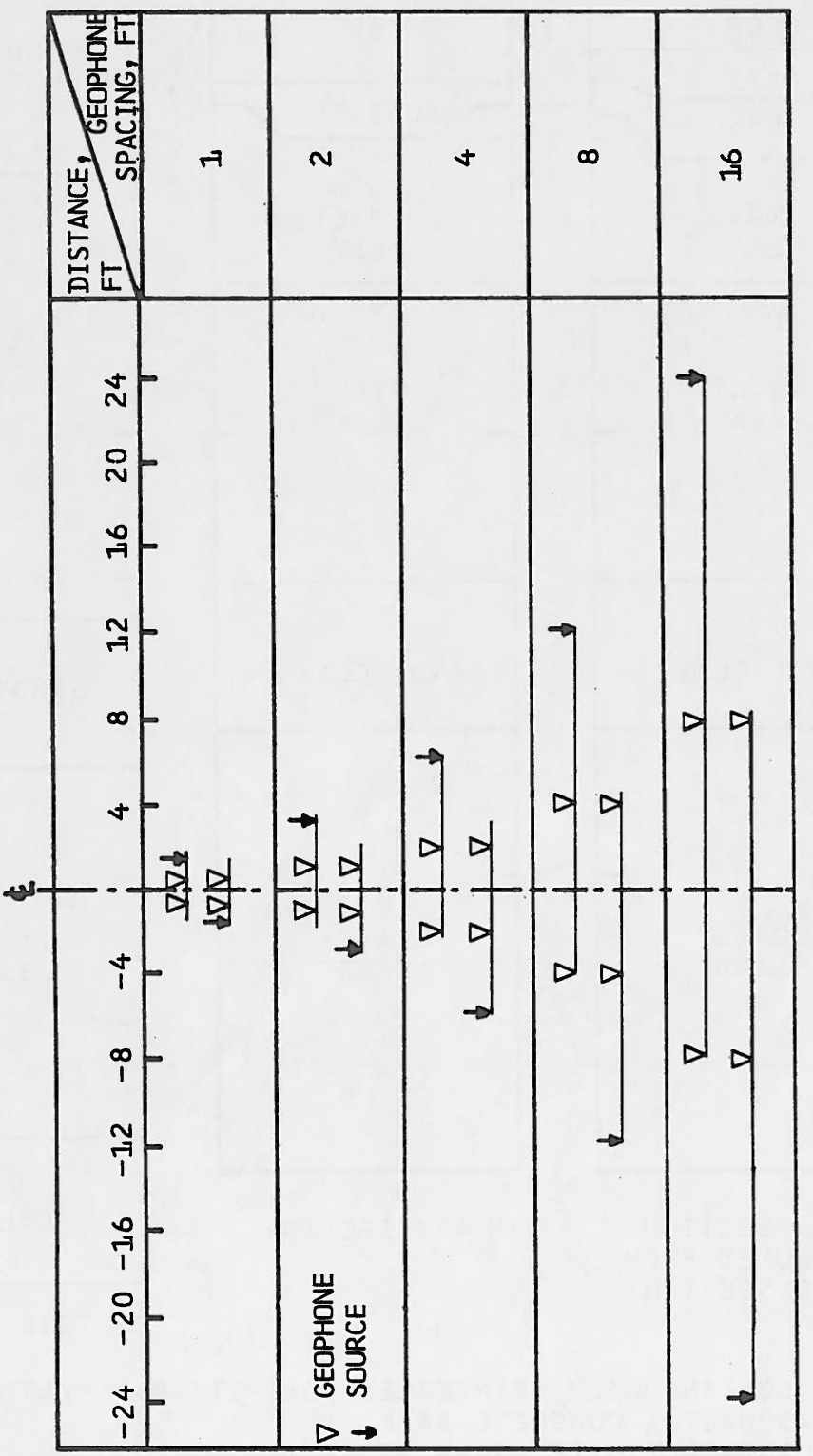


Fig. 4 - Pattern of SASW Tests Used in March and May, 1982

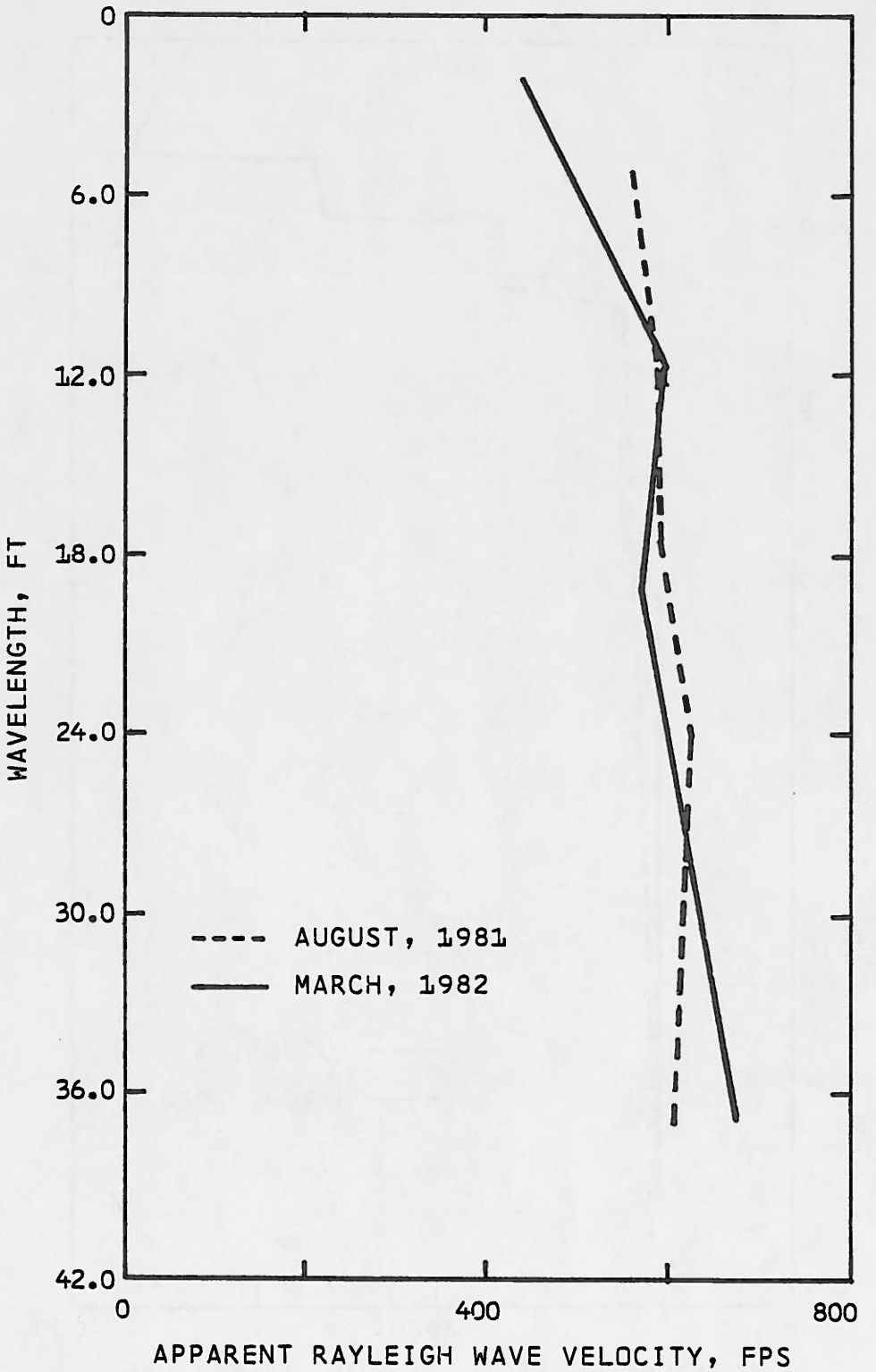


Fig. 5 - Average Dispersion Curves Determined in August, 1981 and March, 1982 for Soil Median

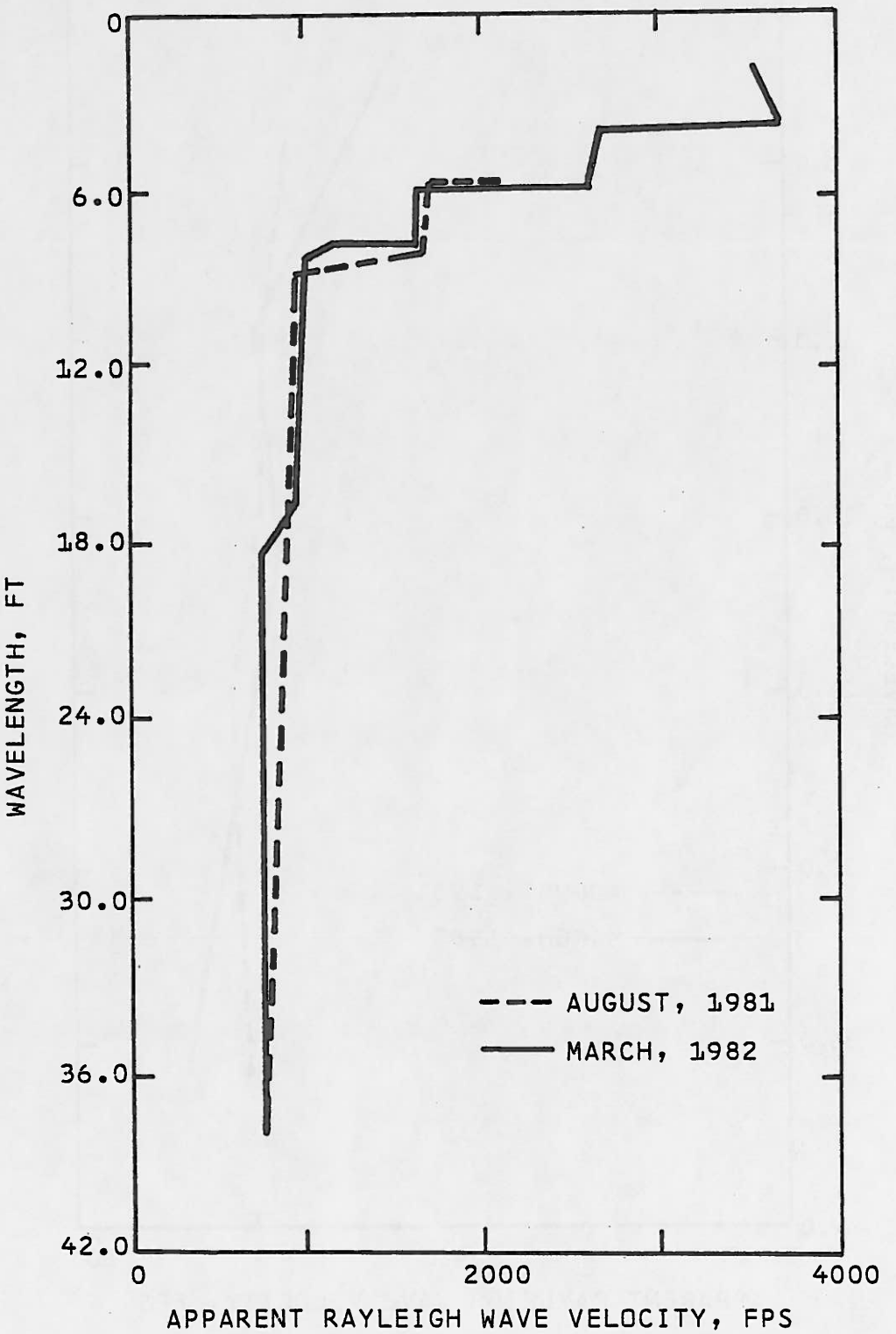


Fig. 6 - Average Dispersion Curves Determined in August, 1981 and March, 1982 for Asphaltic Concrete Shoulder

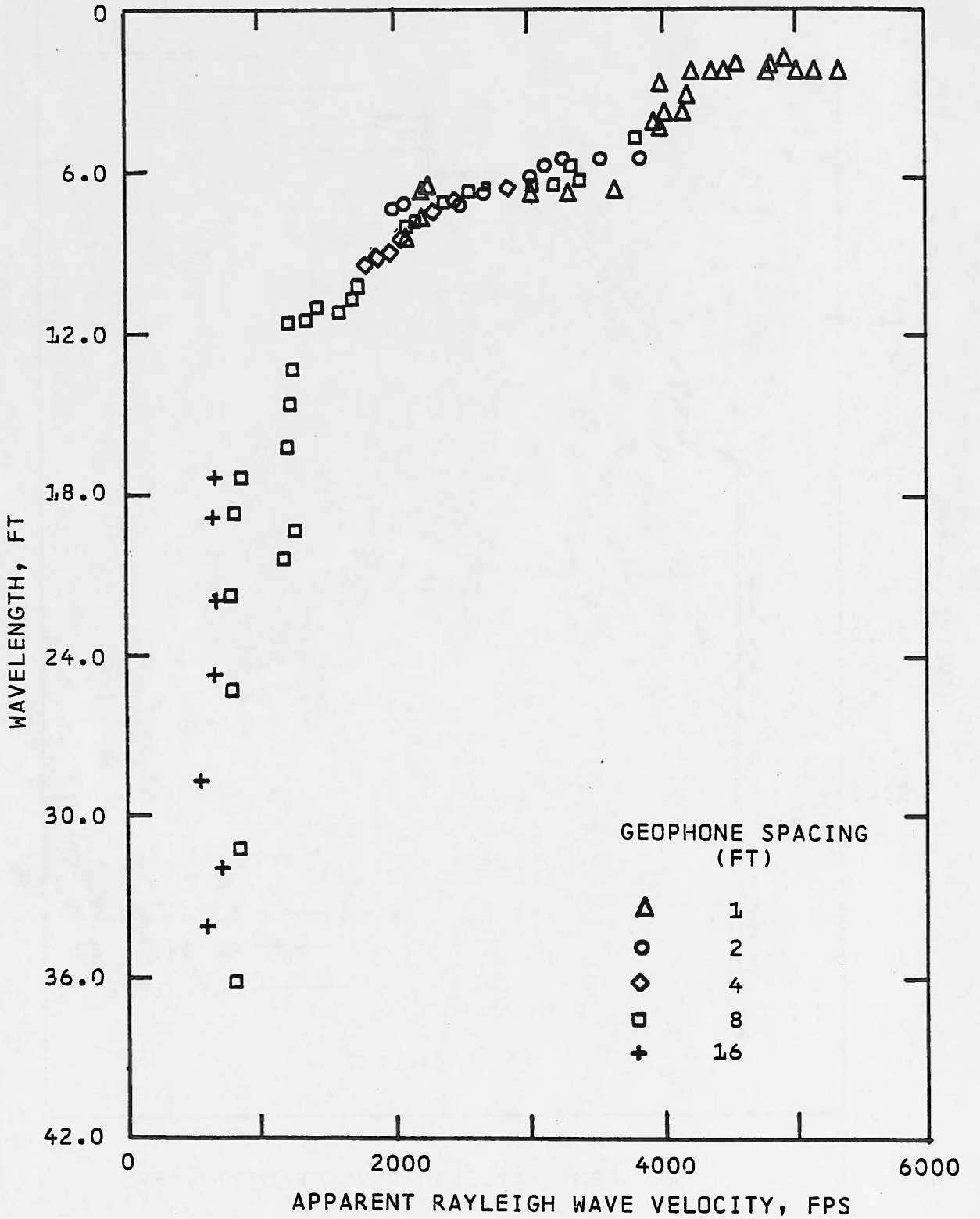


Fig. 7 - Dispersion Curve Determined in May, 1982
for Continuously Reinforced Concrete Section

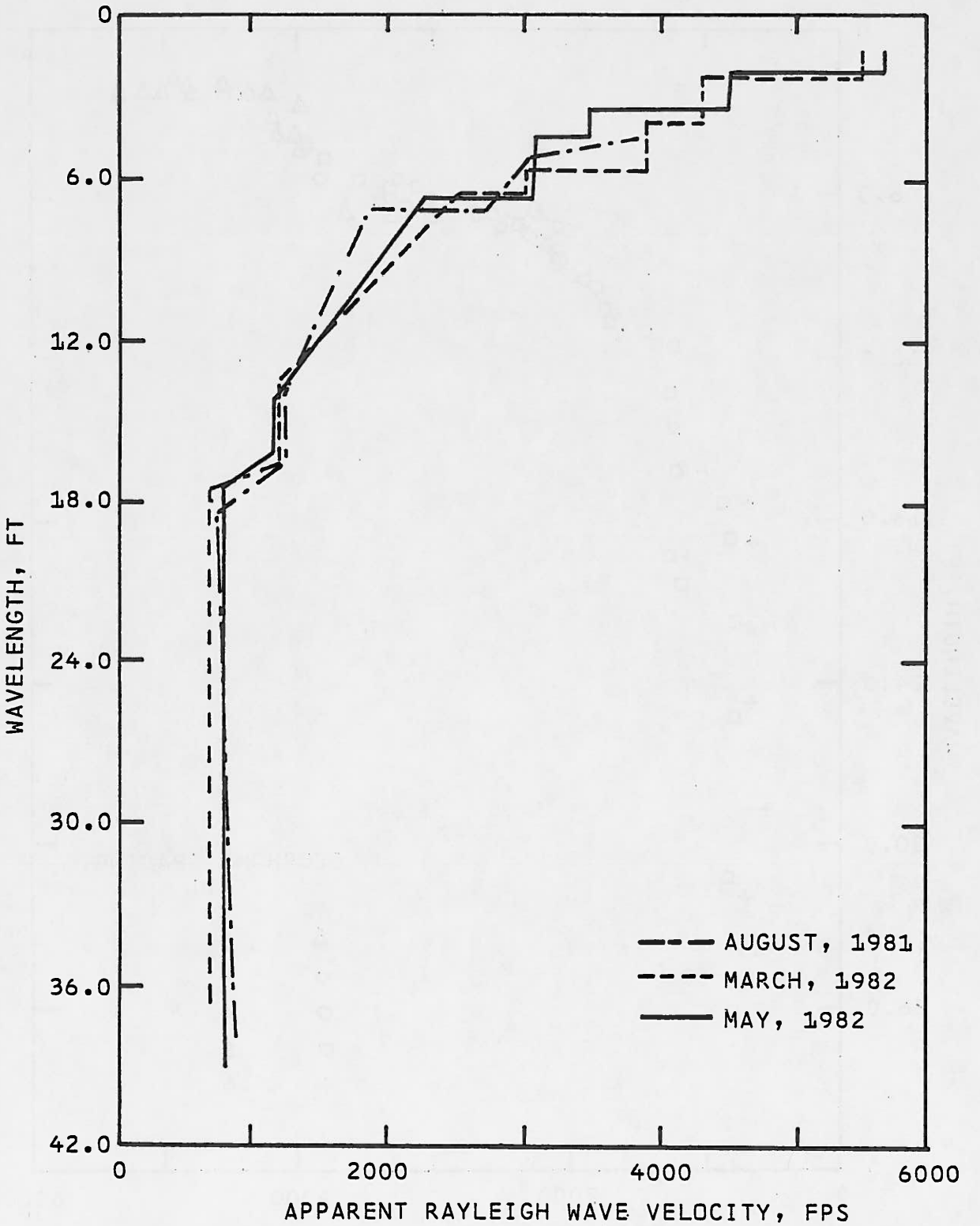


Fig. 8 - Average Dispersion Curves Determined in August, 1981, March and May, 1982 for Continuously Reinforced Concrete Pavement

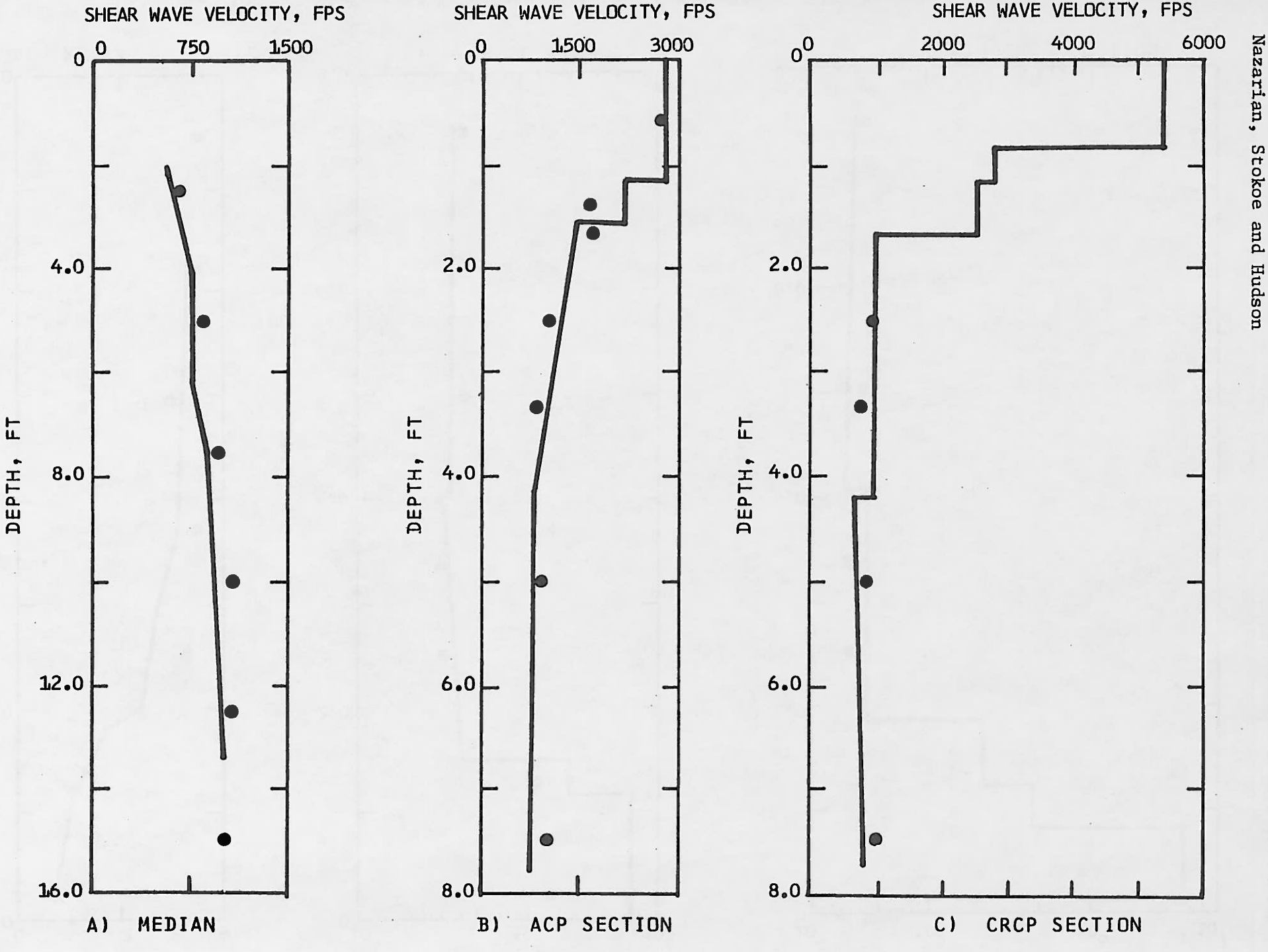


Fig. 9 - Comparison of Shear Wave Velocities from Crosshole and SASW Methods

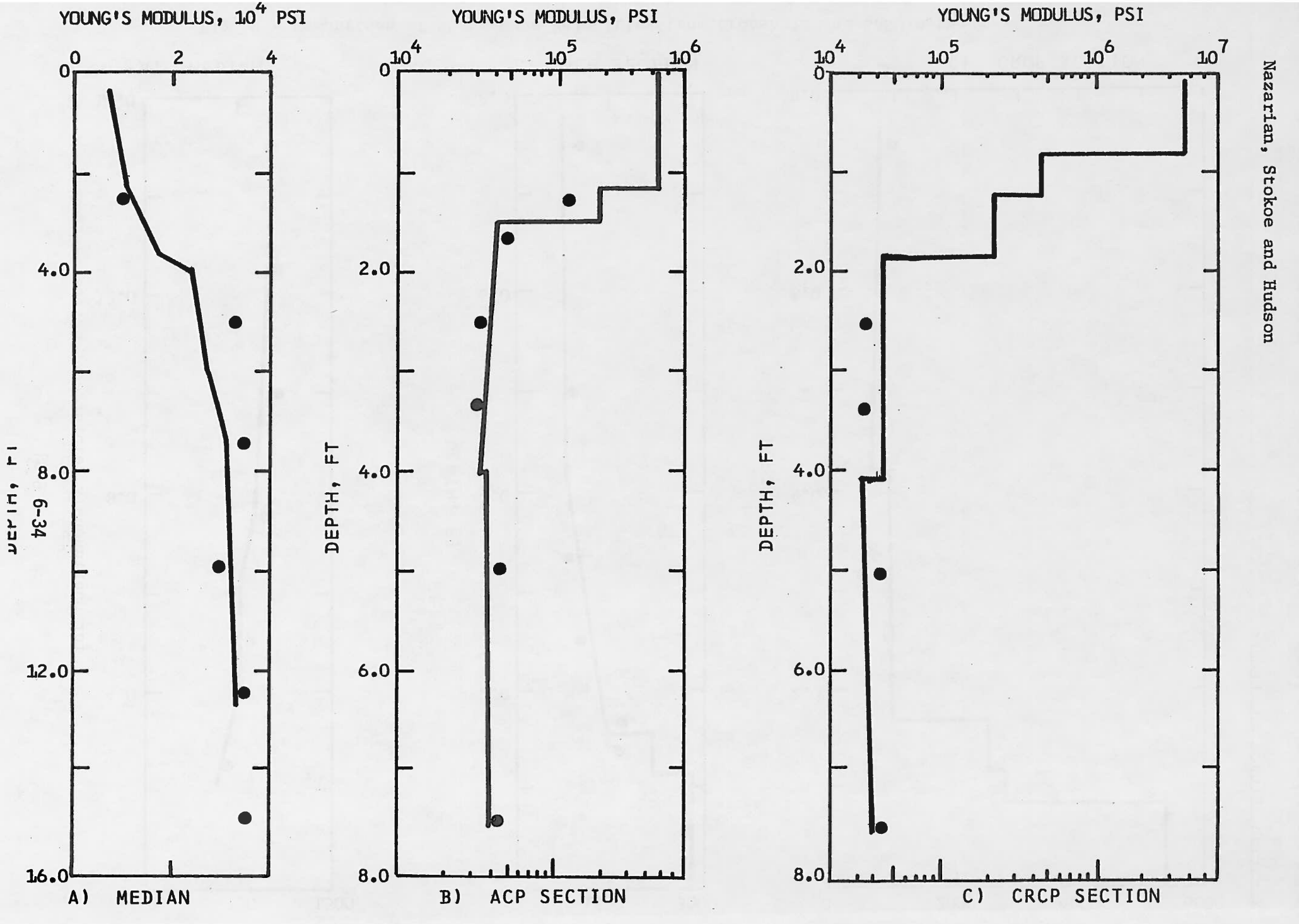


Fig. 10 - Comparison of Young's Moduli from Crosshole and SASW Methods

GROUND PENETRATING RADAR

A NEW TOOL FOR GEOTECHNICAL ENGINEERING

James C. Fowler, Ph.D.

ABSTRACT

The use of ground-probing radar as a reflection mapping tool has expanded greatly in the last few years. This tool has been used to obtain near surface information which is very useful to geotechnical engineers. Using the lightweight field equipment now available, it is possible to obtain data in the field quickly and efficiently.

INTRODUCTION

The use of ground-probing radar to detect geologic features has received a lot of attention in the last few years. Early tests in coal mines by John Cook (5) indicate that radar could be used to locate features which were of interest in a mining activity. Later tests by others (Moffat and Puskar (8); Dolphin, Beatty, and Tanzi (6)) expanded upon this early work and showed that ground-probing radar can be used to penetrate many different types of rocks. Much of this early work was done with heavy laboratory equipment. Therefore, the field techniques were relatively static. That is, the transmit and receive antennas were placed at only a few locations and the data was interpreted using techniques similar to those used in interpretation airborne radar. The ability to get unique interpretations of the data was very difficult.

During the last few years, work has been done (Annan and Davis (1); Morey (9); Coon, Fowler and Schafers (4)) using some of the technology developed by the seismic exploration industry. This includes sophisticated data acquisition techniques, and computer data processing. This paper will show results obtained with these new techniques.

Radar Theory

Ground penetrating radar systems utilize electromagnetic energy to map the presence of shallow reflection within the earth. The principles are similar to those used by seismic reflection systems, except that seismic systems utilize sound energy instead of electromagnetic waves.

The earth is not totally transparent to electromagnetic energy and the ability of this energy to propagate through the earth is dependent upon many factors. The mose important are the conductivity and dielectric constant of the earth material, and the frequency of the radiation.

The conductivity of the earth is a measure of its ability to conduct electrical currents. Conductivity is the inverse of resistivity. Resistivity surveys are relatively common for enegineering problems. If the ground has low resistivity then the electric field will be shorted and the radar energy will not penetrate the ground.

The dielectric constant determines the velocity of the radar energy through the ground. For most earth materials the relative dielectric constant ranges from 3 to 80. Table I shows the range of dielectric constants and corresponding velocities for typical earth materials. Note that the material with the highest dielectric constant is water. The large difference between the radar velocity in water and that in other materials means that water saturated zones will produce strong reflections.

TABLE 1

DIELECTRIC PROPERTIES

OF

COMMON GEOLOGIC MATERIALS

	DIELECTRIC CONSTANT (ε_r)	VELOCITY
AIR	1	0.30 m/ns 1.00ft/ns
SNOW	3	0.17 m/ns 0.58ft/ns
ICE	3.2	0.17 m/ns 0.56ft/ns
DRY SAND	3	0.17 m/ns 0.58ft/ns
SANDSTONE	4	0.15 m/ns 0.5 ft/ns
LIMESTONE	6	0.12 m/ns 0.41ft/ns
GRANITE	9	0.10 m/ns 0.33ft/ns
WET SOIL	16	0.08 m/ns 0.25ft/ns
WATER	80	0.03 m/ns 0.11ft/ns

The frequency of the radar energy is important in two ways. First, at low frequencies the earth acts primarily as a conductor thus the electromagnetic energy does not propagate well. At higher frequencies the earth starts to act more like a dielectric. The frequency at which this conversion occurs is dependent upon the material but for most of earth materials the changes occur between 1MHz and 10MHz.

As the frequency becomes higher the wavelength of the energy becomes smaller. When this occurs the earth tends to scatter the energy more. Therefore, for maximum penetration the wavelength must be kept as long as possible. For most earth materials the useful frequency range in between 50MHz and 500MHz. This corresponds to wavelengths on the order of a few feet.

Figure 1 shows radar operating ranges for typical earth materials. The maximum range varies from a few feet in clay materials to hundreds of feet in hard rock materials. It can also be seen that as the frequency gets higher the penetration range becomes shorter.

Radar Hardware

The principle ground-probing radar in use today is a short pulse radar. This system consists of four major subsystems. These are shown in diagram form in Figure 2.

The transmitter emits a short-pulse of electromagnetic energy which is coupled into the ground through the antenna. Electrical discontinuities in the earth cause portions of this energy to be reflected back to the

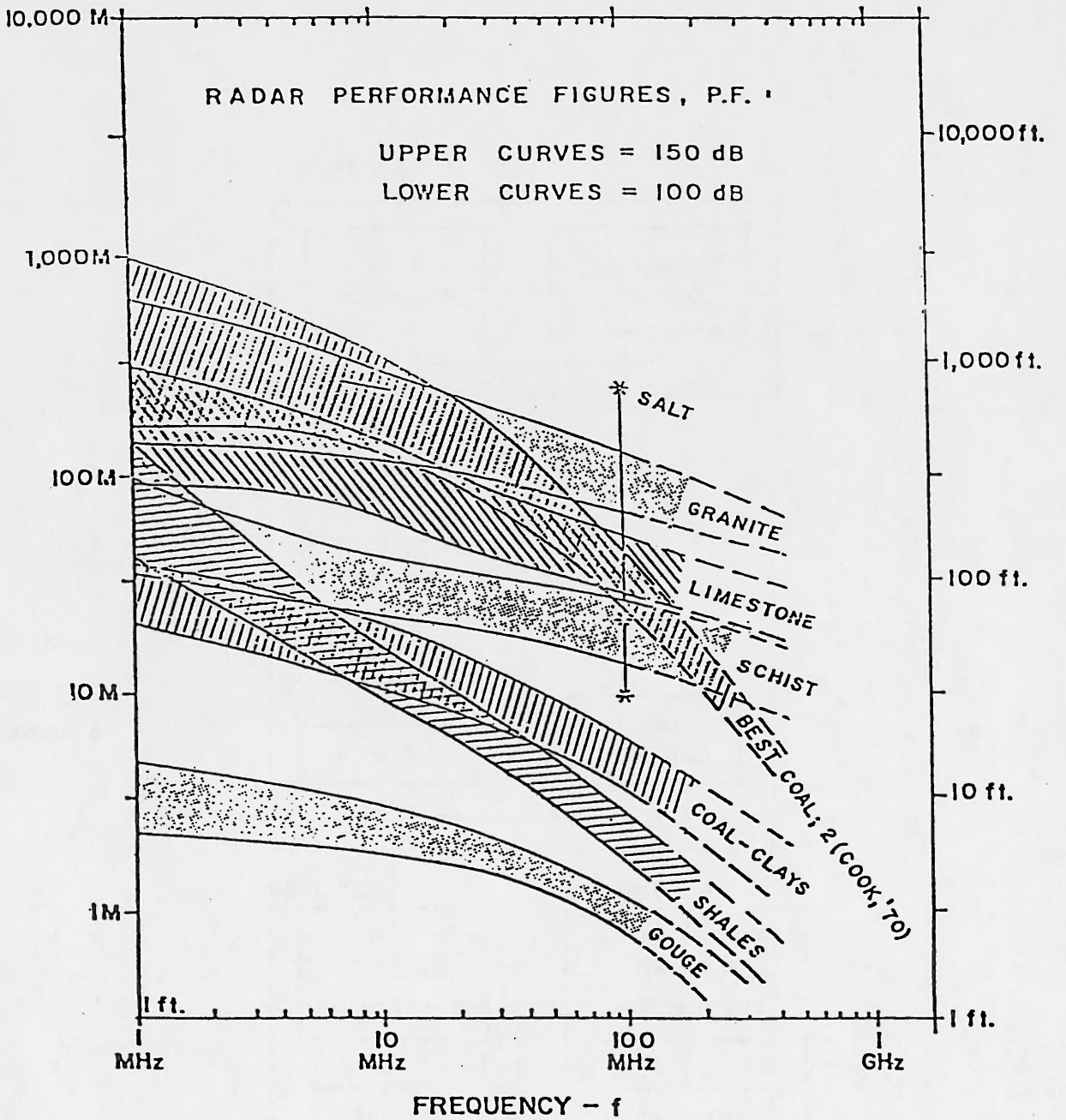


Figure 1. Radar Probing Distances through Some Typical "Rocks"

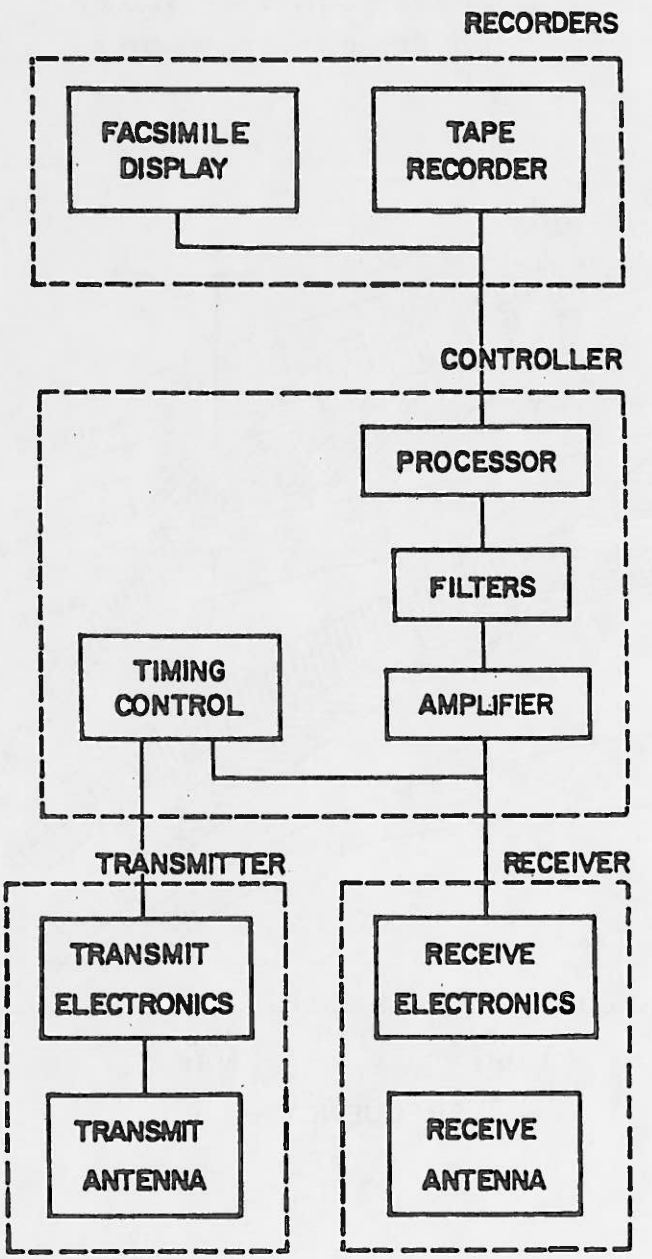


Figure 2. Ground-probing radar block diagram

receiver. The receiver converts the high frequency electromagnetic energy into a low frequency signal by use of a sampling technique. This low frequency signal is then sent to the controller. The transmitter and receiver are contained in separate enclosures so that each unit can be moved along the survey line independently. The controller provides the timing signal to both the transmitter and receiver. The preliminary signal processing functions are also accomplished in the controller. These are the time gain amplifier, which boosts the end of the received trace with respect to the early arrivals, and the switch selectable bandpass filter. Also located in the controller is the microprocessor which controls all of the recording functions.

The final subsystem is the recording system. Normally, two different types of recorders are used. The first recorder is the analog tape recorder which is used to provide a permanent record of the data to act as input for later processing. The second recorder is a facsimile recorder which produces a display of the data which can be interpreted in the field. This display serves both as a data quality control and a preliminary interpretation tool. The final interpretation is usually performed on reprocessed data.

As stated above, the short-pulse radar transmits a short pulse of electromagnetic energy. The desired signal would look like a single cycle of a sine wave. Figure 3 shows a typical transmitted waveform. Note that the actual pulse is not a single cycle but several cycles. This is due to the limited bandwidth of the transmit antenna which is usually only two or three octaves. The basic width of this pulse is

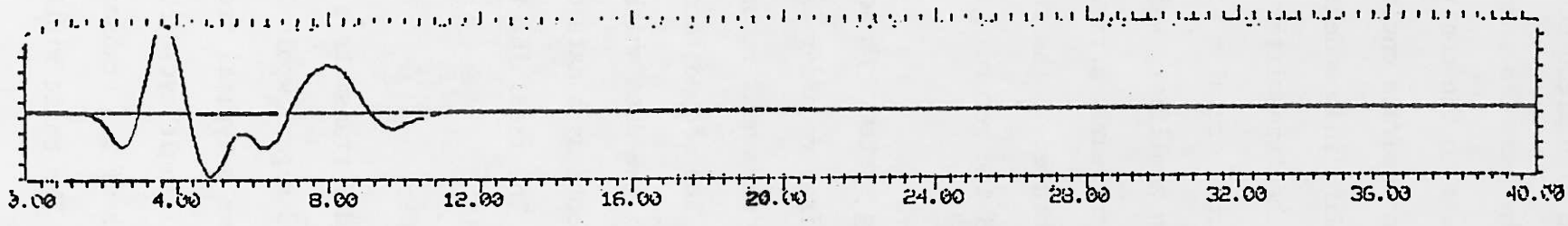


Figure 3. Transmitted waveform

determined by the size of the transmit antenna. The antennas are generally characterized by the center frequency of the transmitted pulse. In the case of the pulse shown in Figure 3, the antenna is a 350MHz antenna.

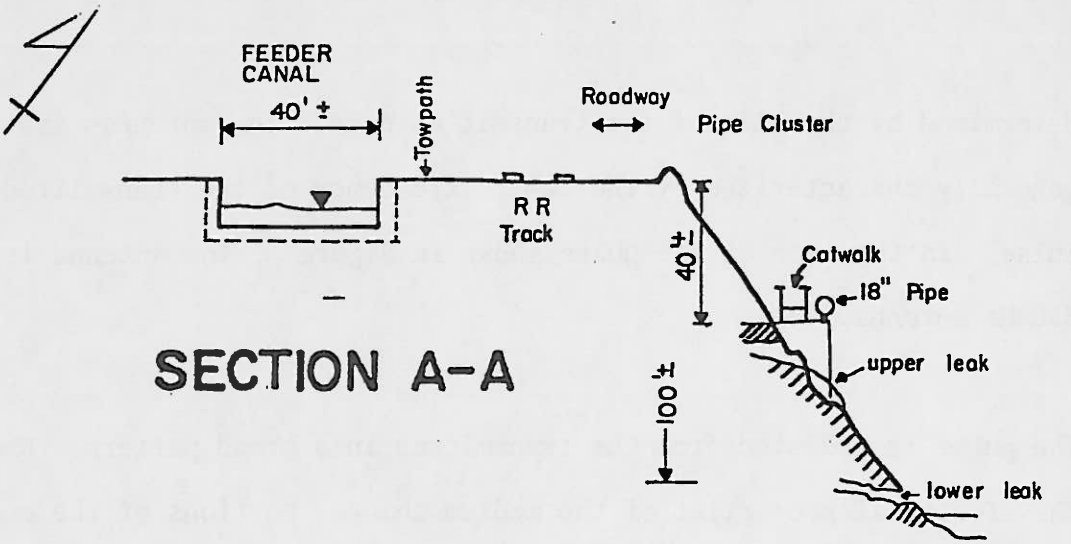
The pulse is radiated from the transmitter in a broad pattern. Whenever the electrical properties of the medium change, portions of the energy are reflected back to the receiver. By measuring the amount of time it takes for this reflected energy to get back to the antenna and by knowing the velocity, it is possible to get an estimate of the distance to the target.

Field Experiments

The first example of a ground-probing radar survey is from upstate New York. Figure 4 shows a diagram of the survey area. A section of a feeder canal was leaking water. The water from the canal was flowing from the side of the mountain. The objective of the survey was to try to identify the path taken by the water so that grout could be injected to seal the canal.

The surface in this area consisted of a layer of about ten feet thick of grained soils. Then, another ten foot thick layer of fractured rock and finally, solid rock. The survey was conducted along the tow path next to the canal.

Figure 5 shows the radar data from this survey. The intensity of the display is proportional to the amplitude of the radar return. Thus



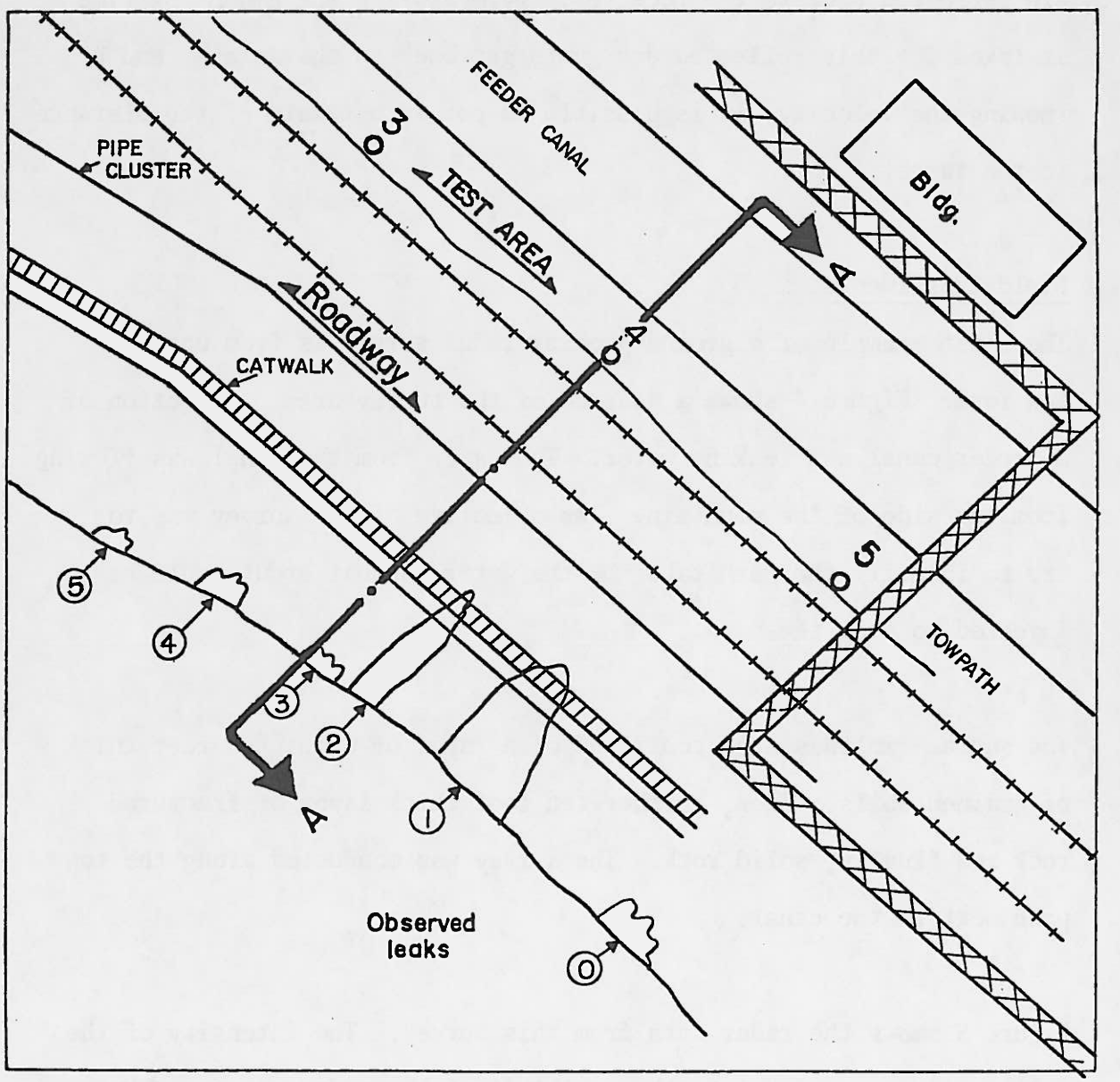


Figure 4. Test site #1

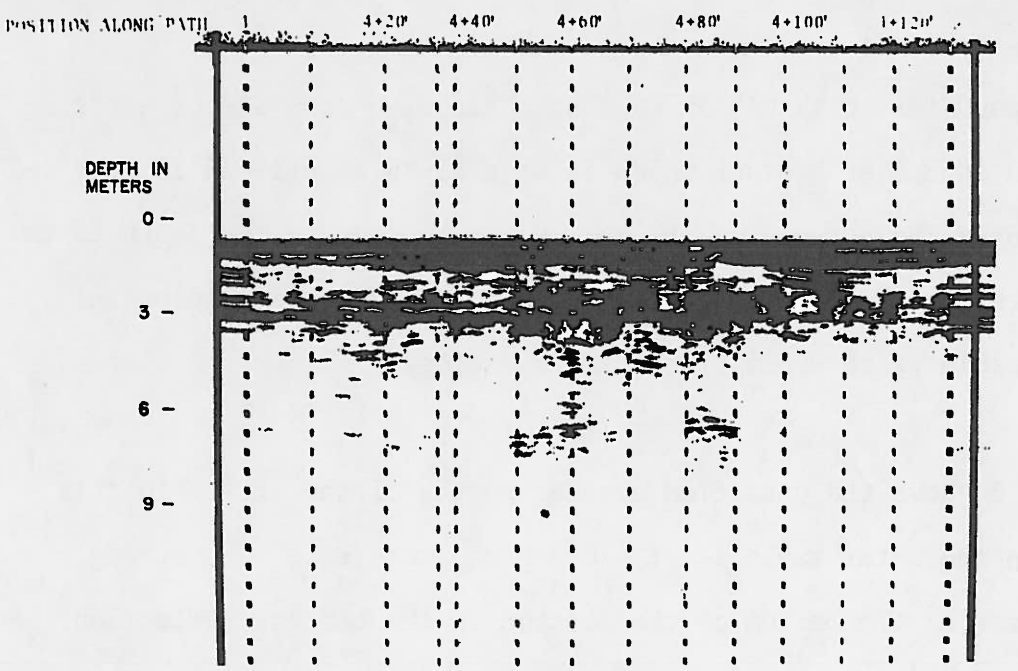


Figure 5. Reflection profile over saturated rock

the dark areas represent regions of high return signal. The boundary between the coarse grained soil and the fractured rock is visible at a depth of about ten feet. Three areas stand out in this section. They occur at a depth of about 20 feet at position 4 + 60 and 4 + 8, and at 12 feet at position 4 + 70. These dark returns represent areas of high water concentration.

Subsequent drilling indicated that significant amounts of water were flowing through the fractured rock at these positions.

The second test site was in Canada. This site consists of a coarse grained sand over bedrock which is at a depth of between 20 feet and 100 feet. The purpose of the survey was to measure the depth to the water table and then measure changes in the subsurface below the water table which would effect the hydrology.

Figure 6 shows the data from a radar survey of the area. In this section the water table is at a depth of four feet. The strong reflector at the bottom of the section is the bedrock reflection. The intermediate reflectors represent clay lenses and other changes in porosity. Figure 7 shows an interpreted section for this data.

In order to provide more information on the hydrology of the area, a series of velocity tests were conducted. Using the velocity information it was possible to calculate dielectric constants and thicknesses for each layer. Using the dielectric constant data for each layer and assuming complete water saturation in the layers it was possible to

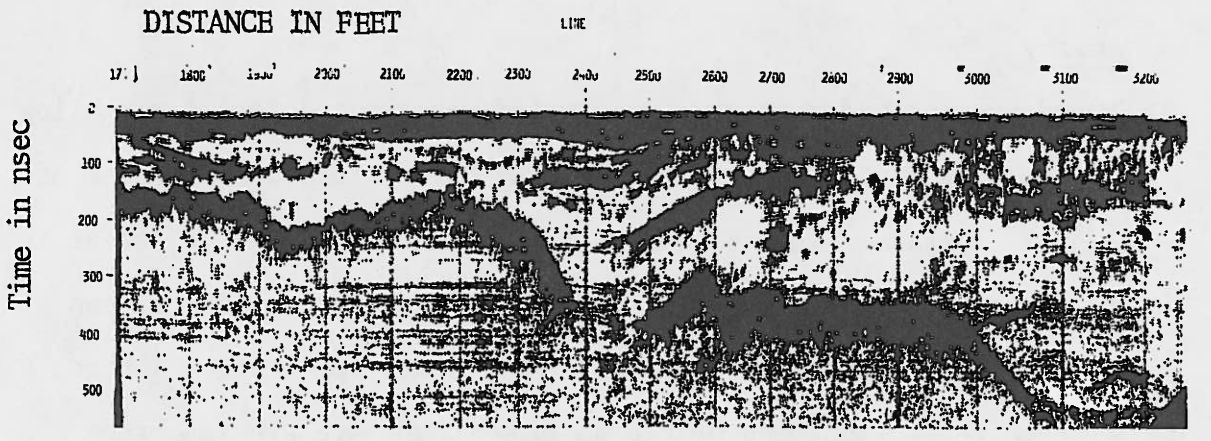


Figure 6. Radar profile over saturated sand

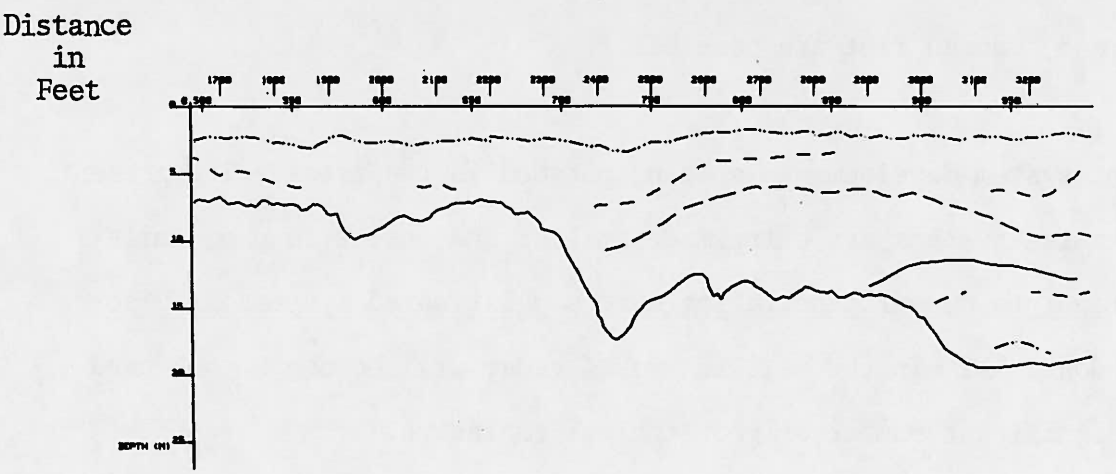


Figure 7. Interpreted data section

calculate porosity values for each layer. This information is shown in Table II.

Summary

Ground-probing radar is now an accepted geophysical tool for shallow surface investigations. It can provide high resolution pictures of the near surface. In addition to the work described above, radar is currently being used to detect buried toxic waste containers, map cavities in limestone areas, and in many other applications where accurate reflection maps of the shallow subsurface are important.

The major limitations on the use of radar involve the conductivity of the near surface. In areas where resistivity is low the penetration range will be limited to a few feet. In other areas penetrations of up to one hundred feet are possible.

Current system development is being pursued in two areas. The present short pulse systems are being made smaller and easier to use, while research into deeper penetrating more sophisticated systems is also being done. Within the next few years radar will become a tool used by a significant number of geotechnical engineers.

TABLE II

LAYER	DEPTH IN METERS	DIELECTRIC CONSTANT	MOISTURE CONTENT %
1	3.84	6.4	13.2
2	6.79	21.8	35.4
3	13.36	20.3	33.8
4	15.58	23.1	35.8

REFERENCES

1. Annan, A.P., and J.L. Davis (1976). Impulse radar sounding in permafrost. Radio Science, 11, No. 4.
2. Annan, A.P., J.L. Davis, and D. Gendzwill (1978). Radar sounding in potash mines Saskatchewan, Canada. Presented at the 48th Annual International Meeting of the Society of Exploration Geophysicists, San Francisco, California.
3. Chan, L.C., D.L. Moffatt, and L. Peters (1979). A characterization of subsurface radar targets. Proceedings of the IEEE, 67, No. 7, 991-1000.
4. Coon, J.B., J.C. Fowler, and C.J. Schafers (1981). Experimental uses of short pulse radar in coal seams. Geophysics, 46, No. 8, 1163-1168.
5. Cook, J.C. (1975). Radar transparencies of mine and tunnel rocks. Geophysics, 40, No. 5, 865-885.
6. Dolphin, L.T., W.B. Beatty, and J.D. Tanzi (1978). Radar probing of Victoria Peak, New Mexico. Geophysics, 43, No.7, 1141-1448.
7. Fowler, J.D., L.A. Rubin, W.L. Still (1977). Detection, delineation and location of hazards using ground-probing radar in coal mines. 18th U.S. Symposium on Rock Mechanics.
8. Moffatt, D.L., and R.J. Puskar (1976). A subsurface electromagnetic pulse radar Geophysics, 41, No. 3, 506-518.
9. Morey, R.M. (1974). Continuous subsurface profiling by impulse radar. Proceedings of Engineering Foundation Conference on Subsurface Exploration for Underground Excavation and Heavy Construction, 213-232. American Society of Civil Engineers, New York.

BOREHOLE GEOPHYSICS AS APPLIED TO A FOUNDATION INVESTIGATION IN LIMESTONE: A CASE HISTORY

White, Robert M., Law Engineering Testing Company, Marietta, Ga. 30067, Brusey, Walter G., Burns and Roe, Inc., Oradell, New Jersey 07649

ABSTRACT

The decision to rely primarily on borehole geophysics has enhanced the technical quality and economic feasibility of the foundation investigation of a coalfired steam plant in the South Carolina Coastal Plain. The Cross Generating Plant's foundation consists of tremmied (poured in the wet) caissons socketed into a limestone of highly variable strength and porosity.

The strength of the upper limestone for caisson socket location was investigated primarily by use of acoustic velocity, compensated density and caliper logs. A trial program utilized geophysically logged geotechnical borings, laboratory tests, Menard pressure meter, and full scale caisson load tests. Preliminary surface refraction work proved useful to anticipate horizontal changes in the upper limestone strength.

Voids where location and extent threatened the caisson integrity were located by the above mentioned geophysical logging program and were grouted. The effectiveness of the grouting program was assessed by cross-hole seismic surveys which indicated the direction of grout flow and the general effectiveness of the grouting.

The tremmied caissons were inspected for necking and low quality concrete by geophysically logging tubes attached to the reinforcing cages and cored holes in selected caissons. Acoustic velocity and density logs were primarily used.

INTRODUCTION

The use of geophysics to improve foundation investigations both from the point of view of information gained and of cost has been discussed in geotechnical literature for several years but its application is still relatively rare. Geotechnical engineers have in general not developed sufficient comfort with geophysics to utilize it routinely. This paper is a case history of the application of borehole and surface geophysics to a large foundation investigation. It is hoped that it will provide encouragement toward regular use of geophysics in foundation investigations.

Santee Cooper's Cross Generating Plant is located north of Charleston in the South Carolina Coastal Plain. The near-surface geology consists of approximately 50 feet of Quaternary sands, silts and clays overlying a 50 foot thickness of the Santee Limestone. The Santee Limestone is highly variable in terms of strength and porosity. Voids are common and range up to 13 feet in vertical dimension. The Santee overlies the Black Mingo Formation, a dense silt.

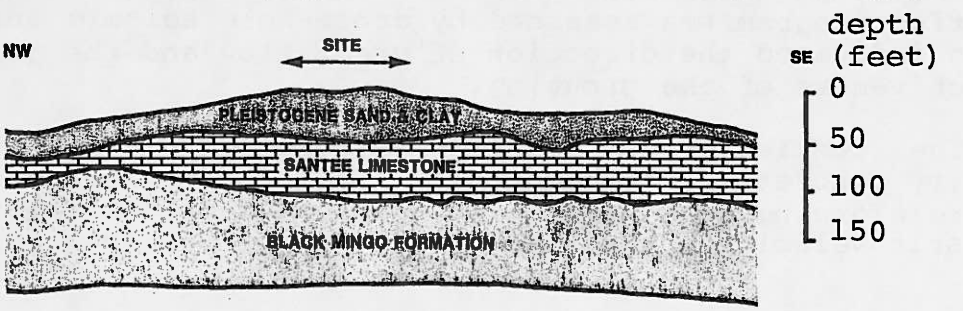


Figure 1 SITE NEAR SURFACE GEOLOGY

The selected foundation consisted of tremmied (poured in the wet) caissons socketed into a hard layer in the upper third of the Santee Limestone. As tremmied caissons cannot be inspected as directly as dry caissons and as the limestone properties were highly variable, the geotechnical investigation needed to be very extensive - sufficient in fact to allow predesign of each caisson. Voids were common in the upper and lower zones of the limestone and characterization of them was also required. The high potential cost of closely spaced geotechnical borings coring the limestone and the difficulty in satisfactorily coring and conventially describing and testing the Santee Limestone created the impetus for considering alternative foundation investigation techniques.

TRIAL GEOPHYSICAL INVESTIGATION

It was decided to investigate the use of geophysically logged unsampled borings to replace conventional geotechnical borings with associated hand classification, and laboratory testing. A trial program consisted of geophysically logging available conventional geotechnical borings. Logging functions were:

Compression Wave Velocity

Compensated Density

Neutron

Gamma Ray

Single Point Resistance, and

Caliper

Borehole pressure meter tests were also utilized in the trial program.

All of the geophysical logging functions used were originally developed in the petroleum industry where they are the primary method of data gathering from exploration borings. Alger (1) is an excellent state of the art review of borehole geophysics applied to petroleum exploration. Keys and MacCary (2) contains a good description of the physics of the most common geophysical logging functions.

The application of geophysical logging to foundation investigations was advanced among others by Birdwell Corporation. Myung and Helander (3) and Lawrence and Baltosser (4), papers by Birdwell employees, contain a basis for using velocity and density logs to measure formation strength.

Geophysical logs provide continuous measurements of in situ formation physical properties. Often the calculation of a desired formation property such as porosity is best accomplished by the use of multiple log functions.

Figure 2 shows a suite of geophysical logs used during the trial program and the interpreted soil and rock description. The gamma ray, neutron and single point resistivity (not shown) logs were used to lithologically describe the subsurface. The relative percentage of clay, silt and sand within the overburden soils was noted but little emphasis was placed on this. Within the limestone, the relative amounts of clay and silt and the location of phosphatic stratgraphic marker horizious were interpreted from these logs.

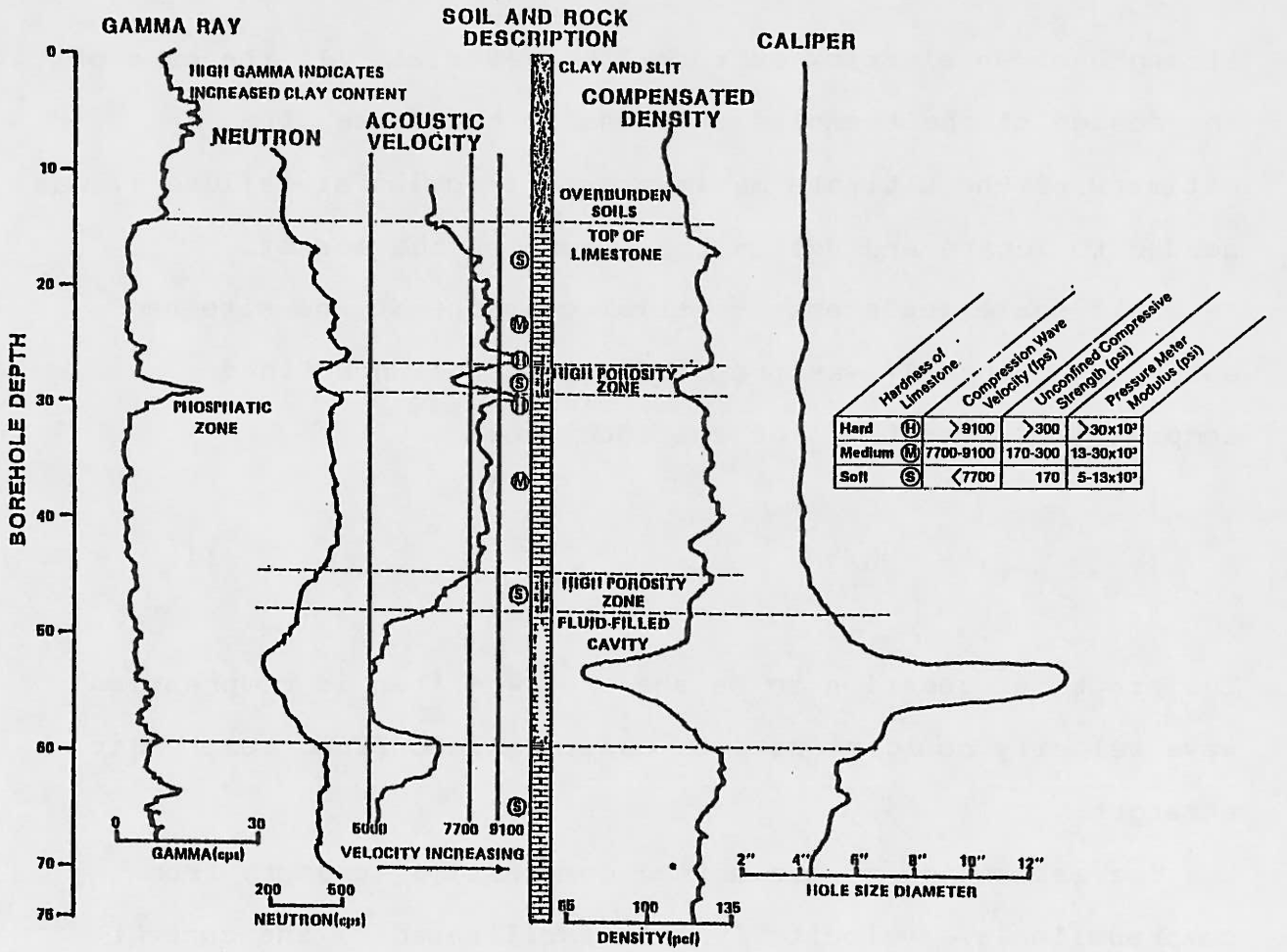


Figure 2 GEOPHYSICAL LOGS USED IN THE CROSS TRIAL LOGGING PROGRAM

The existence of cavities and zones of high porosity was accurately determined by using the density, velocity, neutron and caliper logs in conjunction with drilling penetration rates.

The strength of the limestone for caisson socket location was the primary goal of the geotechnical investigation. There is strong theoretical and experimental basis for expecting compression wave velocity to correlate well with the in situ

strength of an elastic, or rock-like material. In the case of the design of the tremmied caissons at the Cross site, an estimate of the ultimate maximum skin friction at failure τ_f was needed to locate and design the length of the socket.

Full scale load tests of trial caissons at the site had established that τ_f was proportional to the unconfined compression strength q_u of the rock, ie:

$$\tau_f \propto q_u/2 \qquad (1)$$

The practical question to be answered was then if compression wave velocity could be used to estimate unconfined compressive strength.

The estimation of unconfined compressive strength from compression wave velocity (V_p) is facilitated by the concept of the Modulus Ratio, proposed by Deere and Miller (5), who demonstrated empirically that for a given rock (elastic material) a constant ratio (MR) exists and that

$$MR = \frac{E_T}{q_u} \qquad (MR = \text{Modulus Ratio}), \qquad (2)$$

and that therefore q_u could be estimated from E_T.

In elastic theory, compression wave velocity is related to Young's Modulus (E_d) in the following way:

$$E_d = \frac{V_p^2 \cdot \gamma_T (1-2\mu)(1+\mu)}{g\,(1-\mu)\,.\,144} \qquad (3)$$

E_d = Young's Modulus (dynamic) in pounds per square inch

V_p = Compression Wave Velocity in feet per second

μ = Poisson's Ratio (dynamic)

g = Acceleration due to gravity in feet per second^2

γ_T = Unit Weight in pounds per cubic foot

The dynamic Young's Modulus (E_d) is greater than the static Young's Modulus (E_T) by a factor typically between 1 and 10 with higher reductions in weaker rock. The end result of this is that:

$$\tau_f \propto V_p^2 \qquad (4)$$

and that V_p^2 could be used to estimate the desired τ_f. The trial program in fact showed that V_p^2 did in fact predict laboratory q_u and E_T and even more consistently pressure-meter modulus.

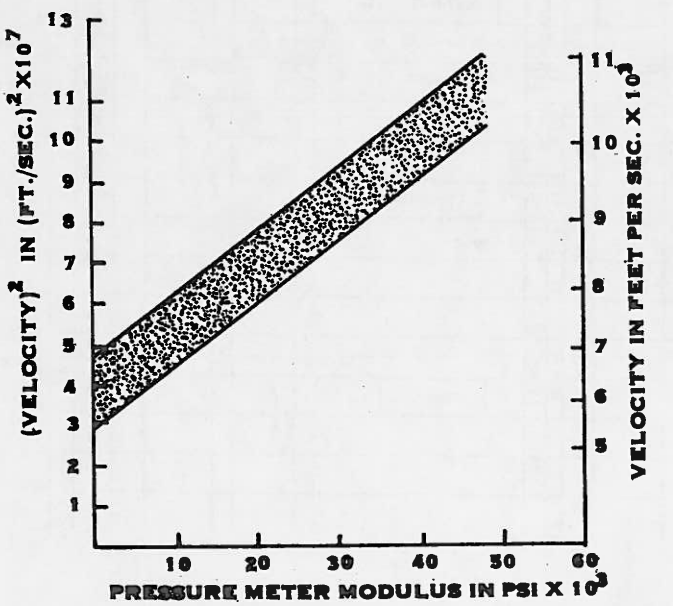


Figure 3 PRESSURE METER MODULUS VS VELOCITY FOR THE CROSS TRIAL LOGGING PROGRAM

Density logging was used as a backup or confirming log to the velocity log. Although the strength of an elastic material is not directly related to the material density, it is indirectly related as E_T increases inversely with porosity in most rocks.

GEOTECHNICAL INVESTIGATION

Production geophysical logging began with an average of six drill rigs and one geophysical logging van working approximately half time. The product of the geotechnical data gathering were plots of velocity and density versus depth and interpreted limestone sections indicating strength, porosity and cavities.

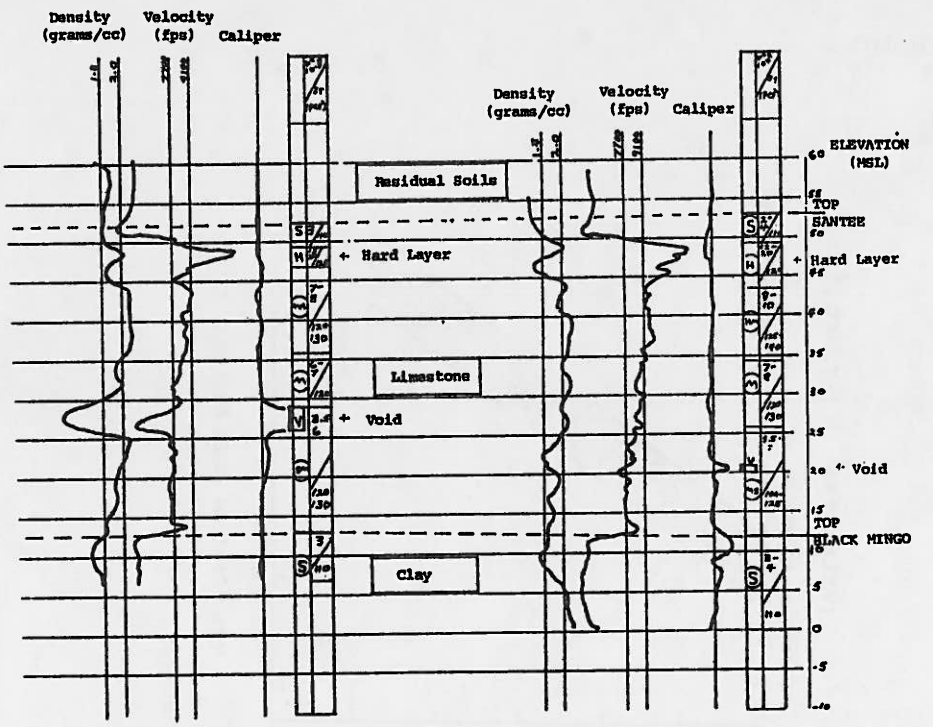


Figure 4 GRAPHIC GEOPHYSICAL LOG

The interpreted cross sections were available to the designers within 24 hours of drilling. A single site geophysicist was able to produce the product, the interpreted cross section of limestone characteristics with depth, as well as manage the geophysical logging operation on a real time basis. This represented a considerable savings in time and money over the procedures attendant to conventional geotechnical borings and rock coring.

A preliminary seismic refraction survey interpreted in conjunction with the velocity logged borings allowed extrapolation of the borehole geophysical data and proved useful to anticipate horizonal changes in the upper limestone strength. The refraction survey encountered both of the subsurface conditions that traditionally limit the usefulness of the technique, the blind zone and hidden layer conditions. In the blind zone condition, a layer intermediate in velocity can be not detected. In the hidden layer condition, a low velocity layer underlies a high velocity layer resulting in the low velocity layer being not detected. Interpretation of the refraction survey was accomplished by combining the data set from the surface refraction survey with the downhole velocity data allowing a correct solution despite blind and hidden layer conditions.

The third or final high velocity layer in the refraction

survey solution represented the hard limestone layer in the upper Santee Limestone which was utilized for socketing the caissons. Comparing the refraction results with the borings allowed the conclusion that when the final velocity was greater than 9000 feet per second, sufficient socketing material existed but when the final velocity was below 9000 feet per second, the hard layer was either very thin or missing. The refraction survey then provided a fast first look at this condition over the site. It should be noted that this use of the refraction data could not have been made without velocity logged borings.

GROUTING INVESTIGATION

Voids where location and extent threatened the foundation integrity or performance were located by the previously mentioned geophysical logging program and were grouted. The effectiveness of the grouting program was assessed by cross-hole seismic surveys which indicated the direction of grout flow and the degree of success achieved in filling the cavities.

The cross-hole survey in this case consisted of recording the waveform generated by small explosives set off in boreholes with geophones in other boreholes for the purpose of measuring acoustic properties of the rock between the boreholes. The

survey was executed as part of the tertiary grouting program with energy and receiver holes on an average of 25 feet apart. Compression and shear wave velocities were measured and in this case the compression wave velocity information was most useful.

Initially, cross-hole measurements were made prior to and after grouting to gauge the direction of grout flow and its effectiveness in filling voids. As the program continued, measurements were made only after grouting. Meaningful interpretation of the cross-hole data was facilitated by borehole velocity logging of the energy and receiver holes. Without this the variability of the limestone velocity and the instance of refracted first arrivals would have strongly reduced the interpretability of the survey.

CAISSON INSPECTION

The tremmied caissons were inspected for necking and low quality concrete by geophysically logging tubes attached to the reinforcing cages and cored holes in selected caissons.

Previous logging of test caissons provided by Dr. Ken Stokoe at the University of Texas aided in the design of the program. The following figure shows the results of logging two of the University of Texas test shafts. Neutron logging was used with these caissons because it responds to porosity and

clay. Honeycombing (high porosity) and clay inclusions were the types of defects installed in these caissons.

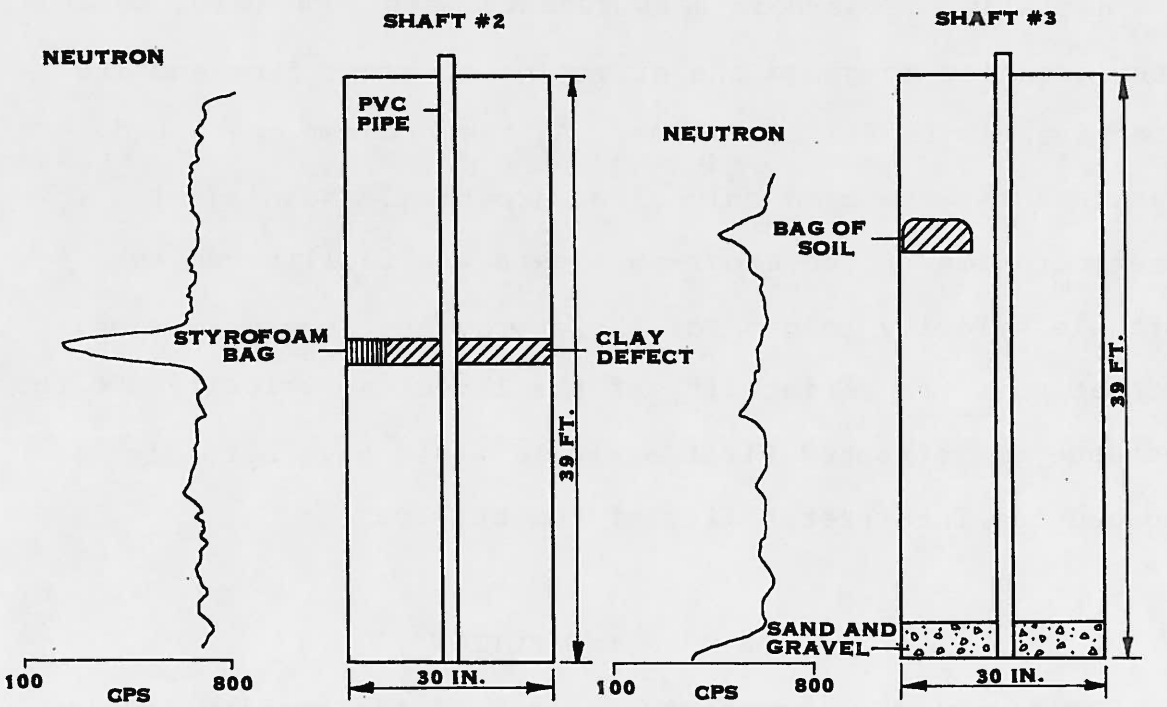


Figure 5 UNIVERSITY OF TEXAS CAISSONS

Accoustic velocity and density were the logs primarily used to inspect the caissons at the Cross site. Compression wave velocity correlates well with concrete strength for the reasons

developed earlier in the paper. High strength concrete commonly has compression wave velocities in the 14,000 to 15,000 feet per second range. As mix density was carefully controlled in the caisson concrete, the density log proved valuable in noting areas of segregation or honeycombing. Density logging tools designed for quantitative use are required for this purpose. The gamma ray log is useful for indicating contamination of the tremmied concrete with clayey soil as the clay has more natural gamma radiation than the concrete. The following figure illustrates the use of these logs in caisson logging.

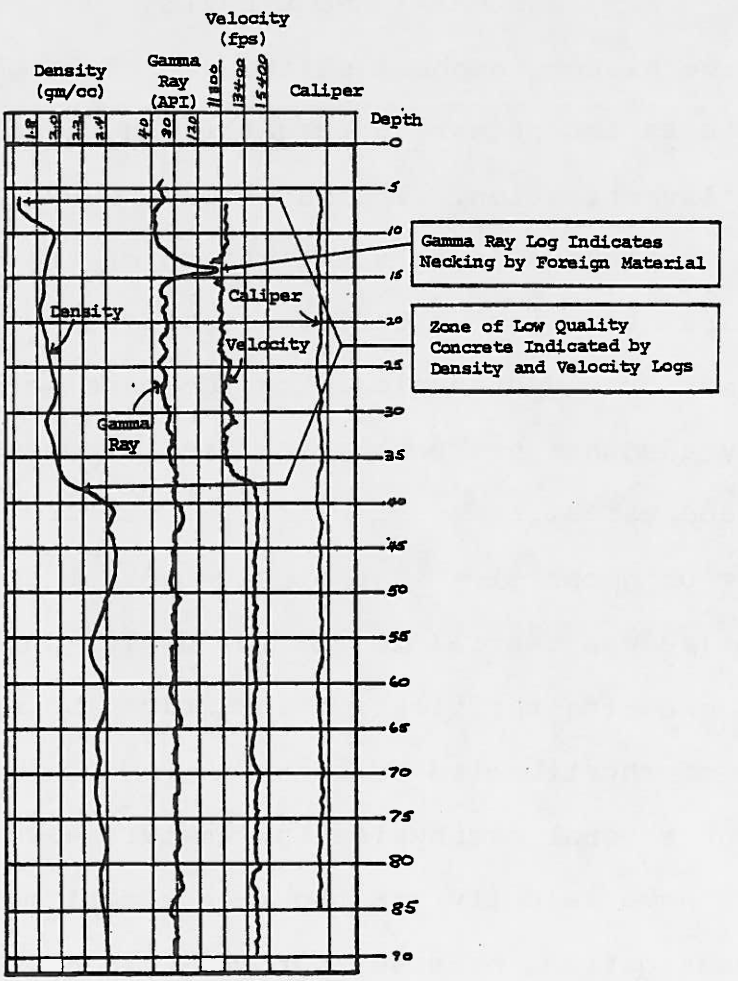


Figure 6 GRAPHIC GEOPHYSICAL CAISSON LOG

Two practical considerations regarding caisson logging involve reinforcing steel and hole condition. Reinforcing steel is a high velocity, high density material. As the purpose of the logging is to measure concrete properties, the tubes installed for logging should be offset from the reinforcing cage by at least 4 inches, as the radius of investigation of the geophysical tools are between 2 and 6 inches. For useful logs to be made, the PVC or light steel tubes installed need to be straight and round in cross section.

SUMMARY AND OVERVIEW

This case history emphasizes the use of geophysical measurements as the primary data gathering technique on a large foundation investigation. The borehole geophysical data provided a continuous in situ estimation of the desired strength parameters in a material (relatively weak limestone) where conventional geotechnical borings were neither technically adequate nor cost effective in comparison with borehole geophysics.

The use of geophysics in the geotechnical investigation at the Cross site was central to the foundation investigation, an associated grouting verification investigation and the inspection of the tremmied caissons.

Although several geophysical parameters were utilized, compression wave velocity was the measurement most significant to the investigation, because in rock it is a good estimator of desired engineering strength parameters. Compression wave

velocity was measured in boreholes via a velocity logging tool, between boreholes by cross-hole surveys and from the surface with a refraction survey. These three data sets were not interpreted separately but instead where they overlapped were treated as one data set. Without this approach, the refraction and cross-hole surveys would have produced misleading results.

REFERENCES

1. Alger, Robert P.(1982), Geological Use of Wire Line Logs, Chapter 6 of Developments in Petroleum Geology - 2, edited by G.D. Hobson, Applied Science Publishers Ltd., Barking, England.

2. Keys, W. Scott and MacCary, L.M. (1976), Application of Borehole Geophysics to Water-Resources Investigations, Book 2 of Collection of Environmental Data, U.S. Department of the Interior, Geological Survey.

3. Myung, John I. and Helander, Donald P. (1972), Correlation of Elastic Moduli Dynamically Measured by In-Situ and Laboratory Techniques, SPWLA Thirteenth Annual Logging Symposium. Reprinted in SPWLA Reprint Volume titled Acoustic Logging, 1978.

4. Lawrence, H.W. and Baltosser, R.W. (1968), Engineering Problems and Downhole Geophysical Solutions, Fourth Annual Idea Conference, New Mexico Tech. Available through Birdwell, a division of Seismograph Service Corporation.

5. Deere, D.U., and Miller, R.P. (1966), Engineering Classification and Index Properties for Intact Rocks, Technical Report No. AFWL-TR-65-116, Air Force Weapon Lab, Kirtland Air Force Base, New Mexico.

THE SPT - A SUMMARY OF SOME RECENT STUDIES

AUTHOR'S NOTE

The paper which follows was presented at the 1982 ORVSS as a substitute presentation. It was impossible to prepare the transcript and figures in time for publication.

The paper has not been changed to include recent findings of the author and others. There have been several "discoveries" during the past year concerning energy measurement during performance of the SPT. The procedures and the applicability of SPT energy measurement are still being evaluated by several geotechnical researchers and practicioners. Those who are interested in SPT energy measurement are encouraged to audit the activities of ASTM Subcommittee D18.02.

THE SPT - A SUMMARY OF SOME RECENT STUDIES

Charles O. Riggs

Abstract

Test data are presented which show that the driving energy of the Standard Penetration Test (SPT) when performed with a large fraction of the drill rigs operating in North America is significantly higher than previously reported by some investigators. The test data suggest that there is no significant difference in N-values obtained with some true free fall penetration test systems and by operators using some cathead and rope systems. It is shown that investigators who use stress wave integration devices to measure SPT energy should first "calibrate" the device to a physical reference base such as a series of 30 in. (0.76 m) free fall drops of an SPT hammer.

Introduction. The field test most used by geotechnical engineers and geologists during exploration for structural foundations and earthworks, the Standard Penetration Test (SPT), has been extensively studied and analyzed during the last decade (1 thru 9). Some of the experiments have provided some valuable information; whereas, some experiments have only proven what field wise engineers and geologists have known about the SPT for several years. Unfortunately, some of the experiments which have been performed under controlled laboratory or field conditions have been presented to describe the general performance characteristics of the SPT without considering the possible effects of the field environment. Also, some studies that have been performed to evaluate a specific situation have been presented or included in presentations to represent the general situation.

What is probably needed at this point is an unbiased study and summary of the available data by a field wise geotechnical engineer with a lot of "free" time who generally understands drilling equipment, drilling personnel, SPT

hardware and the nature of the SPT and who is not prejudiced by commercial involvement or from extensive involvement with local practices. This presentation is an attempt to review and summarize some recent studies. The reader is forwarned that the author is in the employ of a manufacturer of drill rigs and SPT equipment.

The Test. The SPT can be described as a soil penetration test wherein a 2.0 in. (51 mm) outside diameter, open-ended, split-barreled sampler is driven 18 in. (0.46 m) below the bottom of a soil boring using a 140 lb (63.5 kg) drive weight falling approximately 30 in. (0.76 m). The driving resistance or N-value is the number of hammer blows required to drive the sampler the final 12 in. (0.31 m) of penetration.

Many of the early tests were performed in North America with "drill rigs" similar to the one shown on Figure 1 using the "cathead and rope method." The configuration of the equipment probably provided an efficient SPT system. For these early systems, the single rope sheave and the relatively short rope probably provided a relatively low resistance to a free-fall of the 140 lb (63.5 kg) drive weight when two or less rope wraps were used on the cathead.

Recent Evaluations of the SPT. The report of one recent study by Kovacs et al (3) suggests:

1. that the N-value of the SPT is related to the manufacturer's design of the drill rig and the geometry of the hammer and anvil used to perform the test, and

2. that there is a "national average energy" for the SPT which is in the range of 39 to 76 percent of 4200 in.-lb (475 J) (140 lb falling 30 in. = 4200 in.-lb).

As will be shown later, there is substantial data which show that the cathead and rope SPT energy of a large percentage of the drill rigs operating in North America which are the product of a single manufacturer is higher than



Figure 1. The type of "drill rig" that was used for many years to perform the Standard Penetration Test.

the upper bound of 76 percent suggested by Kovacs et al. Because ownership of these particular drill rigs predominate within well defined, large geographic regions, the concept of a "national average energy" or a "national energy range" is questionable.

Even though an SPT split spoon sampler is not energized into the soil being tested, the efficiency of an SPT hammer drop has been presented by researchers in terms of energy with an "energy ratio" or an "operation efficiency." Generally, energy ratio has been defined or used by several investigators as the SPT hammer impact energy divided by 4200 in.-lb (475 J). Some investigators suggest that the measured energy ratio should be based on the actual hammer fall height. Goble and Ruchti (1) suggest for the purpose of communication and comparison of N-value energy from drill rig to drill rig that energy ratio should be based on a constant 4200 in.-lb (475 J) (the kinetic energy at impact of 30 in. (0.76 m) free fall drop of a 140 lb (63.5 kg) hammer) and that operation efficiency is a better term to use when corrections are made according to the measured hammer fall height.

Impact energy can be determined at least approximately from impact velocity measurements with basic mass-velocity-energy relationships or by integrating a force-time trace (stress wave) obtained with a load cell placed within the sampling rod column. Energy losses at impact would not be detected from a hammer velocity measurement. A currently available device which records and integrates the force-time trace to obtain SPT energy within the sampling rods is shown on Figure 2.

The 39 to 76 percent national average energy range proposed by Kovacs et al is largely based on information provided to Kovacs by other investigators. Much of the information consists of energy measurements made with electronic stress wave integration devices. Many of the measurements reported to Kovacs

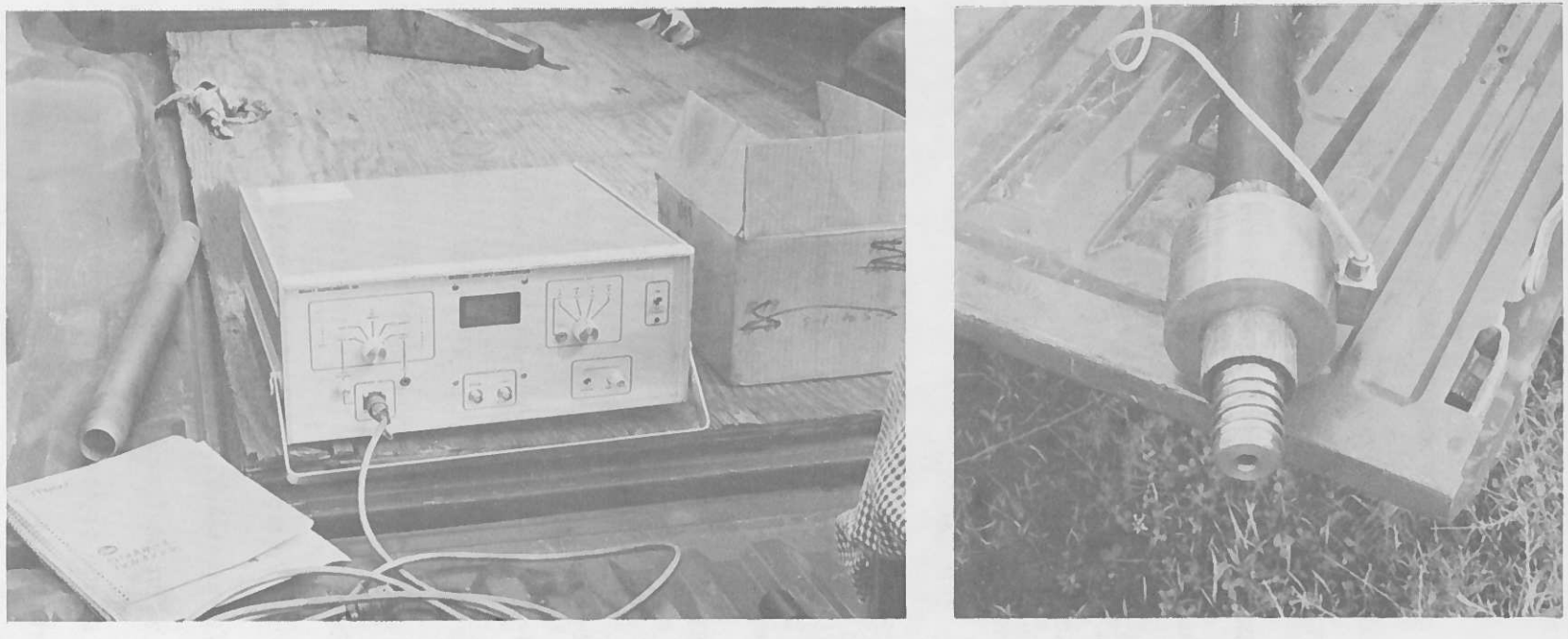


Figure 2. The Binary Instruments Model 102 SPT Calibrator.

were made without "calibrating the calibrator" to a physical reference base such as a series of 30.0 in. (762 mm) free fall hammer drops. Test data reported by Riggs, Schmidt and Rassieur (6) strongly suggest that the output of a calibration device which integrates the force-time trace from the impact of an SPT hammer should be compared with a series of 30.0 in. (762 mm) free fall drops of a 140 lb (63.5 kg) SPT hammer. Representative test data from this study show that calibrator readings can vary significantly when different calibrator-load cell combinations are used to measure the energy of the same hammer-anvil-drill rod system. Some of the SPT energy measurements reported by Kovacs et al were obtained during the performance of tests where 3 or 4 cathead rope wraps were used on the cathead and the operators' typical rhythmic procedures were altered to control hammer fall height.

As part of their study, Kovacs et al (3) used a Binary Instruments SPT Calibrator (Refer to Figure 2), a digitizing oscilloscope which records the force-time trace for integration and a hammer velocity measuring device to determine and compare energy ratio measurements for a few cathead and rope SPT systems. With a relatively small data sample they determined that energy ratio computed from impact velocity measurements is approximately equal to energy ratio obtained by integrating the force-time trace (Refer to Figure 3) when the SPT hammer is the enclosed, safety type (Refer to Figure 4). Most cathead and rope penetration tests are now performed with this type of hammer.

Goble and Ruchti (1) made impact velocity measurements and computed energy ratios based on impact velocity for 15 different cathead and rope operators using several different CME drill rigs. They concluded that "The Standard Penetration Test, when performed by a conscientious operator with the cathead and rope method, should provide a hammer impact energy of about 86 percent of a 30 inch free fall drop of a 140 lb hammer." Fourteen of the operators tested

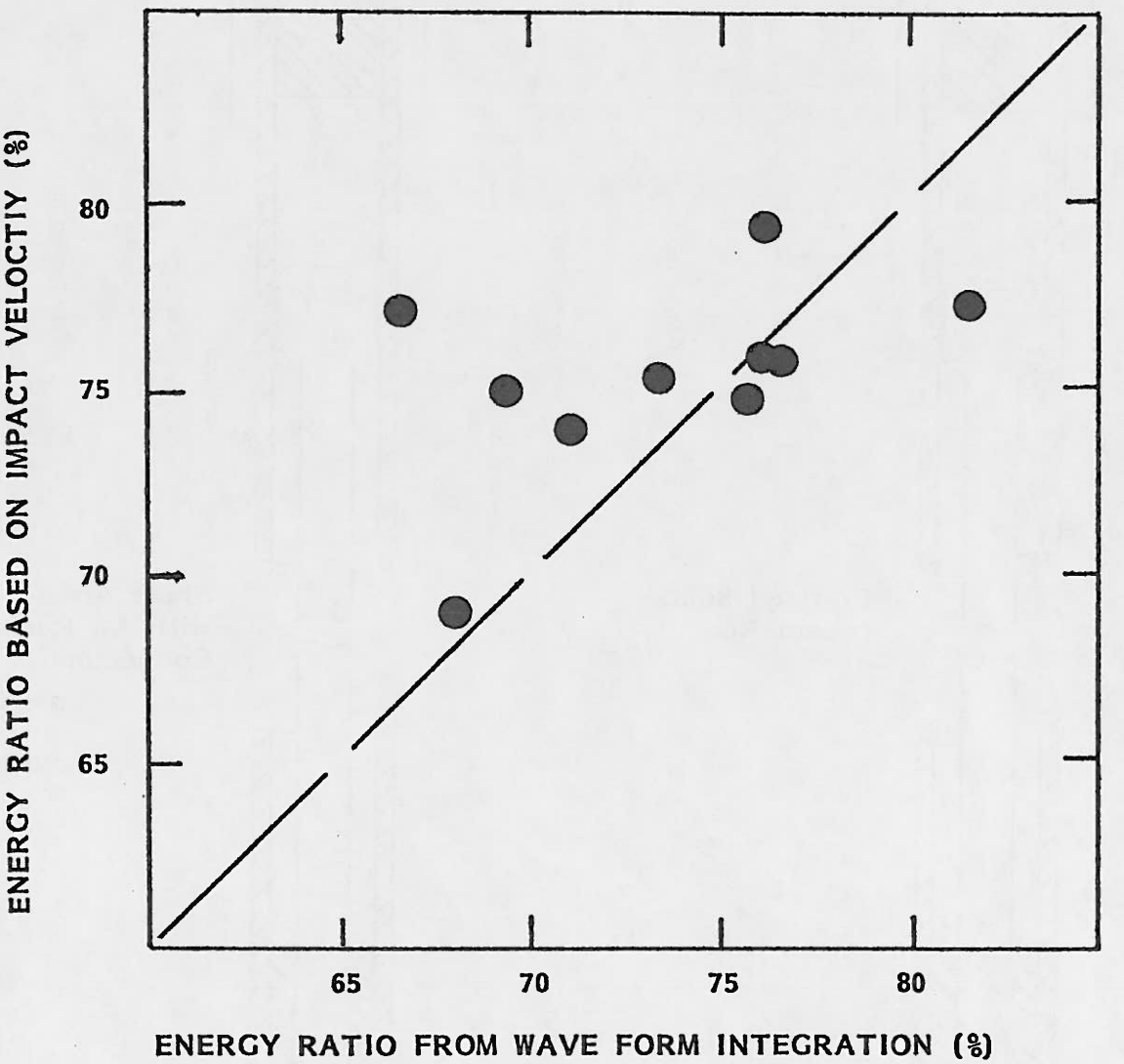


Figure 3. Values of SPT hammer impact energy obtained simultaneously with a velocity measuring device and a stress wave integration device. Each data point represents the mean of a series of hammer drops with safety type hammers. (From Kovacs et al, Reference 3)

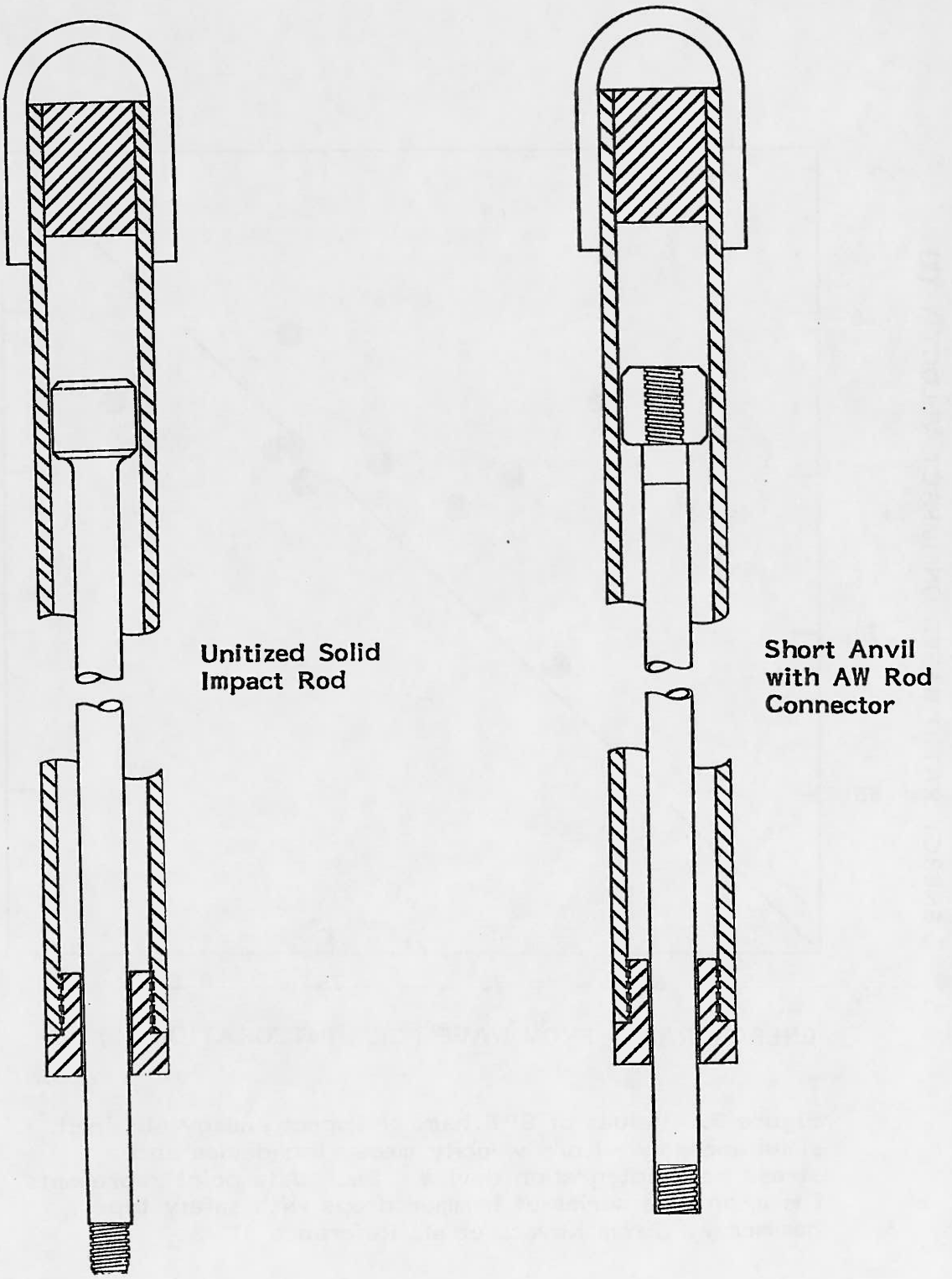


Figure 4. Two types of 140 lb (63.5 kg) safety type hammers that are used to perform the SPT.

by Goble and Ruchti used 2 rope wraps on the cathead. One operator used one wrap. Extensive personal inquiries have since indicated that using two or less cathead rope wraps is the accepted North American practice.

Combined energy computations from velocity measurements by Kovacs et al and Goble and Ruchti are summarized on Figures 5 and 6. Figure 5 shows mean energy ratio (measured energy/4200 in.-lb (475 J)) based on impact velocity and mean hammer lift for 14 operators. (Goble and Ruchti did not measure hammer lift for some operators.) Figure 6 shows the range of mean energy ratio and the total number of hammer blows recorded within each increment of the range. The combined data of Figure 6 represent about 20 different operators working on about 10 different drill rigs, all of which were manufactured by one manufacturer (CME). The data reported in Figures 5 and 6 only include the tests observed by these investigators with the operator using two rope wraps on the cathead.

Riggs, Mathes and Rassieur (4) reported the results of a field study wherein penetration tests were performed in several borings advanced on 15 ft (4.5 m) centers into a weathered, moist loess (eolian clayey silt) deposit using both an automatic free fall hammer, i. e. the CME 140 lb Automatic SPT System, and the cathead and rope method (Refer to Figure 7). The cathead and rope tests were performed by 5 operators working on 4 different CME drill rigs.

The free-fall characteristics of the CME 140 lb Automatic SPT System drive weight and CME safety hammers were investigated by Riggs, Schmidt and Rassieur (5). Data obtained with the Binary Instruments SPT Calibrator indicate that the free fall impact energy transfer of the automatic system drive weight is in the range of 90 to 100 percent of the free fall energy of CME safety hammers (Refer to Table 1).

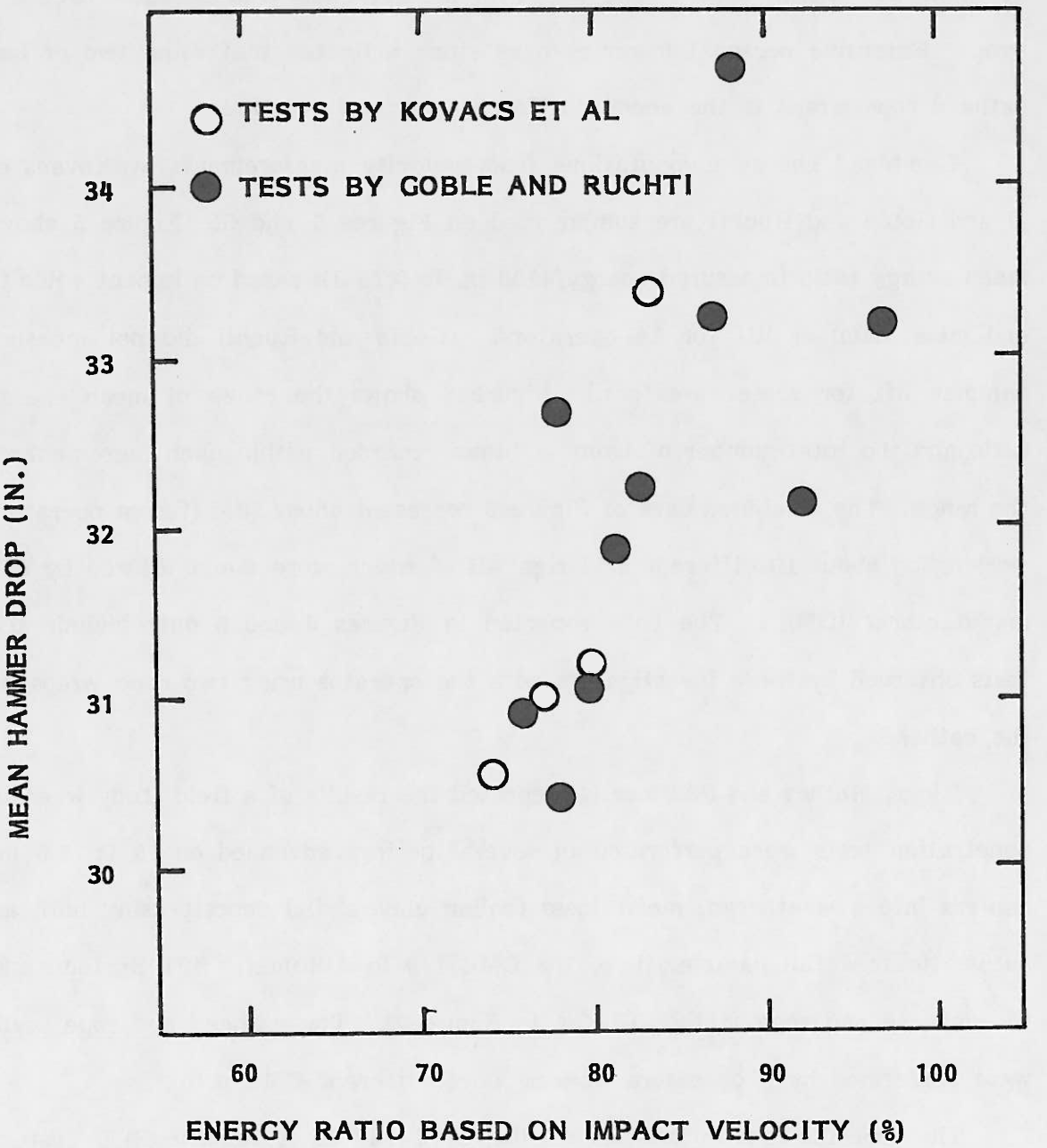


Figure 5. Hammer lift and energy ratio based on impact velocity. Each data point is the mean of several hammer drops by fourteen different operators. (From Goble and Ruchti, Reference 1 and Kovacs et al, Reference 3)

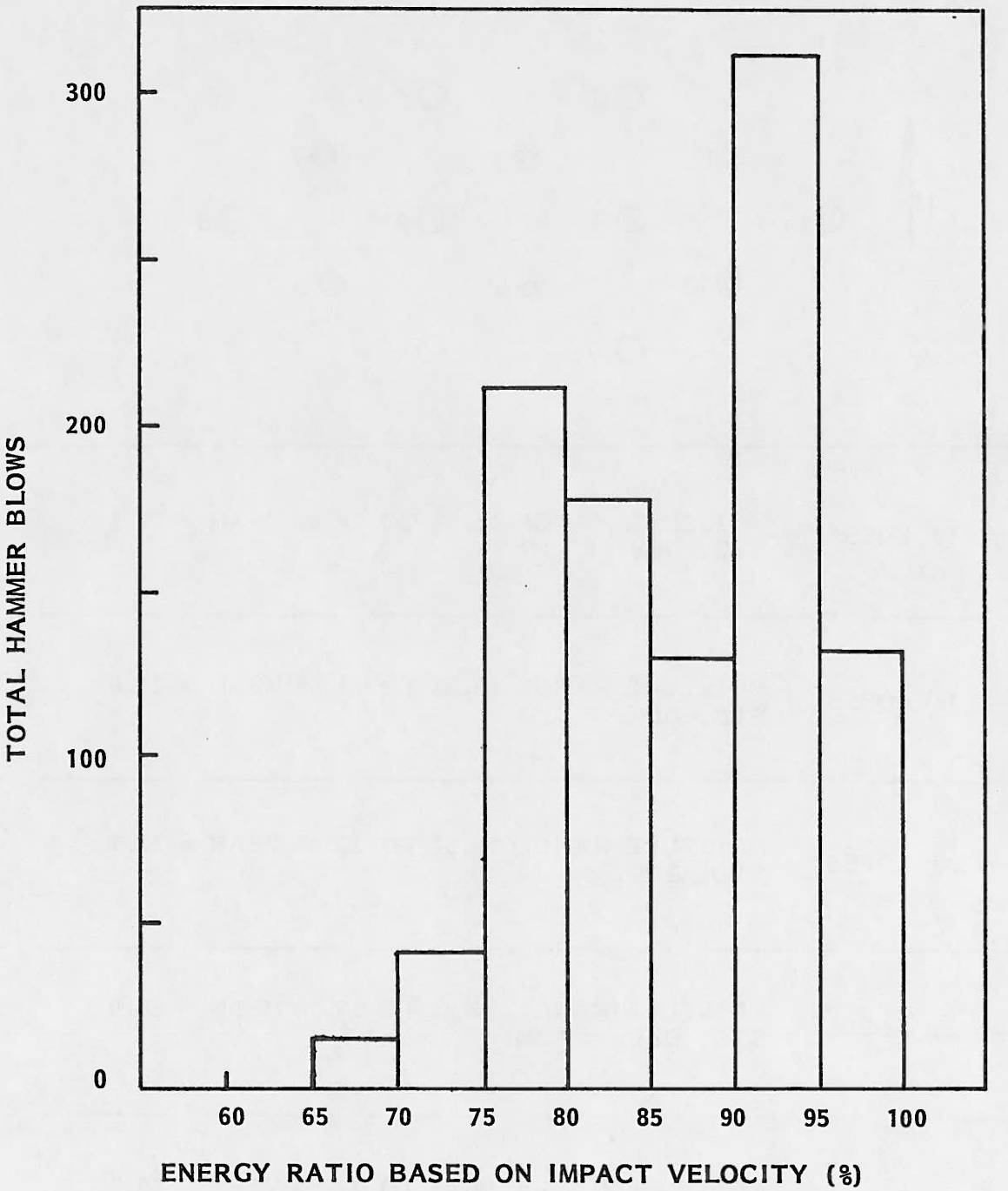
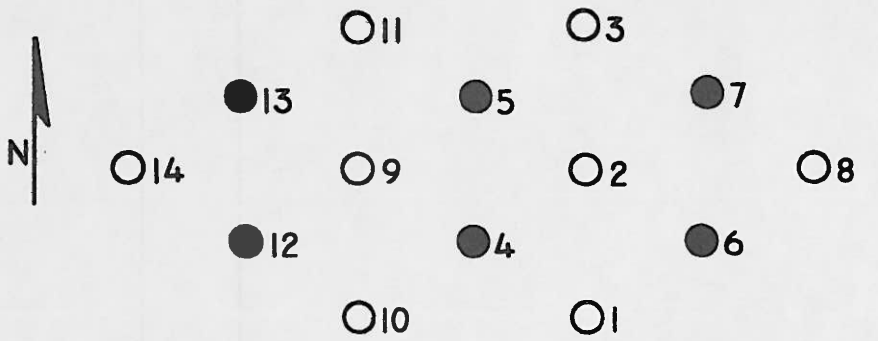


Figure 6. Distribution of energy ratio based on impact velocity from several operators using two rope wraps on a cathead. (From Goble and Ruchti, Reference 1 and Kovacs et al, Reference 3).



10' LOESS — MOISTURE RANGE 21.8% TO 24.4% MEAN = 22.8
STD. DEV. = 0.74

15' LOESS — MOISTURE RANGE 19.8% TO 21.6% MEAN = 20.6
STD. DEV. = 0.57

20' LOESS — MOISTURE RANGE 19.5% TO 23.4% MEAN = 22.1
STD. DEV. = 1.02

25' LOESS — MOISTURE RANGE 15.9% TO 23.5% MEAN = 20.9
STD. DEV. = 1.94

30' LOESS — MOISTURE RANGE 24.0% TO 27.4% MEAN = 25.7
STD. DEV. = 1.12

○ Cathead and Rope Tests ● Automatic Hammer Tests

Figure 7. Boring layout and soil profile at the site of the field study by Riggs, Mathes and Rassieur (Reference 4).

TABLE I

ENERGY MEASUREMENTS

DATE	*SYSTEM	LOAD CELL	CALIBRATOR	NO. OF DROPS	MEAN ENERGY	COEF. OF VAR.
10-7-81	A-1	52119	206	20	96.9	1.85
10-8-81	B-1	52119	206	21	96.1	2.19
10-21-81	A-2	52119	206	15	98.2	0.96
10-25-81	A-2	52122	206	23	108.1	1.04
11-6-81	B-2	52125	203	5	57.0	1.75
11-6-81	A-2	52125	203	42	55.6	1.49
11-12-81	B-1	52125	203	5	55.0	1.82
12-5-81	A-1	52119	206	17	109.6	1.16
12-5-81	A-1	52119	206	19	108.3	1.19
12-5-81	A-1	52119	206	20	111.9	1.06
12-5-81	A-1	52119	206	17	113.6	1.36
12-5-81	A-1	52119	206	22	115.0	1.86
12-5-81	A-1	52119	206	26	114.0	2.05
12-5-81	B-1	52119	206	10	114.1	5.18
12-5-81	A-1	52119	206	24	116.7	2.45
12-30-81	B-1	52119	206	9	114.7	2.13
12-30-81	A-2	52119	206	9	118.2	0.92
8-6-82	C-5	52125	206	5	103.8	1.85
8-6-82	S-4	52125	206	5	104.0	3.04
8-6-82	B-10	52125	206	6	116.0	3.32
9-2-82	C-7	52125	206	8	101.2	2.97
9-2-82	C-4	52125	206	6	101.0	3.38
9-2-82	B-15	52125	206	9	109.3	4.35
9-2-82	D-12	52125	206	9	109.9	3.76

*A = CME 140 lb Automatic SPT Hammers: Operational Series

B = CME Safety Hammer with Unitized Impact Rod and Anvil: Each Blow Obtained by Tying the Hammer on a String 30.0 in. (762 mm) and Cutting the String to Obtain Free Fall.

C = CME 140 lb Automatic SPT Hammer Drive Weight: Dropped Using a Tripping Device, 30.0 in. (762 mm) Fall Height.

D = CME Safety Hammer with Old Style, Short Impact Block: Each Blow Obtained by Tying the Hammer on a String 30.0 in. (762 mm) and Cutting the String to Obtain Free Fall.

S = Solid Steel Cylinder with Same Diameter as the CME 140 lb SPT Hammer: Dropped with Tripping Device, 30.0 in. (762 mm) Fall Height.

% 4200 in.-lb or 475J

The results of the field penetration tests are summarized on Tables 2 and 3. The field test data indicate that N-values obtained with the CME 140 SPT Automatic System are practically equal to N-values obtained by cathead and rope operators on CME drill rigs using CME safety type hammers.

Summary. The results of the studies by Goble and Ruchti (1) and Riggs et al (4, 5) and the tests performed by Kovacs et al (3) suggest that the conclusion of Goble and Ruchti that "The Standard Penetration Test, ..., should provide a hammer impact energy of about 86 percent of a 30 inch free fall drop ...." cannot be strongly disputed and that the N-values obtained with a free fall SPT system are within the range of N-values that would be obtained by cathead and rope operators on CME drill rigs using CME safety type hammers. This summary cannot be generalized further because there is not sufficient published data available at this time concerning the cathead and rope SPT energy characteristics of drill rigs and hammers built by other manufacturers. Available test data indicate that the 39 to 76 percent SPT energy range suggested by Kovacs et al is too wide and too low to be representative of SPT energies of the drill rigs with cathead and rope systems that predominate within some well defined large geographic regions of North America.

References

(1) Goble, G. G., and Ruchti, P., "Measurements of Impact Velocity on Penetration Testing Systems," Report, Department of Civil, Environmental and Architectural Engineering, University of Colorado, Boulder, Colorado, October 1981.

(2) Kovacs, W. D., Evans, J. C., and Griffith, A. H., "A Comparative Investigation of the Mobile Drilling Company's Safe-T-Driver with the Standard Cathead and Manila Rope for the Performance of the Standard Penetration Test," Report, School of Civil Engineering, Purdue Engineering, 1975.

(3) Kovacs, W. D., Salomone, L. A., and Yokel, F. Y., "Energy Measurement in the Standard Penetration Test," NBS Building Science Series 135, National Bureau of Standards, Washington, D C, August 1982.

TABLE 2

SUMMARY OF N-VALUES FROM CATHEAD AND ROPE TESTS

Depth (ft)	Boring No. **								Mean N-Value	Standard Deviation
	8*	3	2	1	11	9	10	14*		
10	20	14	14	12	6	8	8	11	10.3	3.44
15	16	11	14	10	11	14	11	12	11.9	1.72
20	14	10	11	9	10	11	9	12	10.0	0.89
25	10	10	10	10	9	10	11	10	10.0	0.63
30	7	5	4	6	7	5	5	5	5.3	1.03

* N-values from these two "outer" borings (Refer to Figure 7) are not included in the computation of the means and standard deviations so that an equal number of N-values from each method would be used for comparisons.

** Boring 1 - Operator A with CME-450

Borings 2, 10, 11 - Operator B with CME-55

Boring 3 - Operator C with CME-450

Borings 8, 9 - Operator D with CME-45B

Boring 14 - Operator E with CME-75

(5 ft = 1.5 m)

TABLE 3

SUMMARY OF N-VALUES PERFORMED WITH

THREE CME 140 LB AUTOMATIC SPT HAMMERS

Depth (ft)	Boring No.						Mean N-Value	Standard Deviation
	7	6	5	4	13	12		
10	7	9	12	9	9	6	8.7	2.07
15	11	10	11	10	11	11	10.7	0.52
20	9	8	11	10	11	5	9.0	2.28
25	9	8	10	8	7	9	8.5	1.05
30	4	4	5	4	7	6	5.0	1.26

(5 ft = 1.5 m)

(4) Riggs, C. O., Mathes, G. M., and Rassieur, C. L., "Field Testing of an Automatic SPT Hammer System," Paper Submitted for Publication to the Geotechnical Testing Journal.

(5) Riggs, C. O., Schmidt, N. O., and Rassieur, C. L., "Reproducible SPT Hammer Impact Force with an Automatic Free Fall SPT Hammer System," Paper Submitted for Publication to the Geotechnical Testing Journal.

(6) Schmertmann, J. H., and Palacios, A., "Energy Dynamics of SPT," Journal of the Geotechnical Engineering Division, ASCE, Volume 105, No. GT8, 1979.

(7) Schmertmann, J H., and Smith, T. V., "A Summary of SPT Energy Calibration Services Performed for the Florida DOT Under Service Contract 99700-7150-010," Final Research Report 245*D73, College of Engineering, University of Florida, Gainesville, Florida, September 1977.

(8) Serota, S. and Lowther, G., "SPT Practice Meets Critical Review," Ground Engineering, Volume 6, No. 1, 1973.

(9) Shioi, Y., Uto, K., Fuyuki, M., and Iwasaki, T., Chapter III of "Present State and Future Trend of Penetration Testing in Japan," prepared for Xth International Conference on Soil Mechanics and Foundation Engineering, Stockholm, June, 1981.

APPENDIX

PAST PROCEEDINGS
OF THE
OHIO RIVER VALLEY SOILS SEMINARS

ORVSS I
BUILDING FOUNDATION DESIGN AND CONSTRUCTION

October 16, 1970
Lexington, Kentucky

AND WHY DO WE DO IT THIS WAY? by R. C. Deen, Assistant Director of Research, Kentucky Bureau of Highways.

A CASE STUDY - PIPE PILING FOR A DEEP FOUNDATION PROBLEM by Don Fuller, P.E., L.S., Fuller, Mossbarger and Scott Civil Engineers, Inc.

DESIGN, CONSTRUCTION AND PERFORMANCE OF SPREAD FOOTINGS ON A NON-UNIFORM FOUNDATION by Robert Lennertz, M. ASCE, The H. C. Nutting Company.

DESIGN, CONSTRUCTION AND TESTING OF DRILLED PIERS ON SHALE AND THINLY BEDDED LIMESTONE by George J. Thelen, P.E.

BUILDING FOUNDATION FAILURE RELATED TO SOIL SHRINKAGE by Aubrey D. May, Chief Engineer, Stokley and Associates.

INNOVATIONS IN FOUNDATION DESIGN AND CONSTRUCTION by D. J. Hagerty, Assistant Professor, Civil and Environmental Engineering Department, University of Louisville.

ORVSS II
EARTHWORK ENGINEERING, START TO FINISH

October 15, 1971
Louisville, Kentucky

PRELIMINARY SITE SELECTION STUDIES WITH REMOTE SENSING TECHNIQUES by David J. Barr, Department of Civil Engineering, University of Cincinnati.

SITE EVALUATION WITH REMOTE SENSING TECHNIQUES APPLIED TO SUSPECT KARST TOPOGRAPHY by Melville D. Hensey, Engineering Division, The Proctor and Gamble Company.

EXPLORATION METHODS by Dr. Vincent P. Drnevich, P.E., Assistant Professor of Civil Engineering, University of Kentucky.

THE SELECTION OF STRENGTH PARAMETERS AND THEIR USE IN THE STABILITY ANALYSIS OF EARTH ROCK EMBANKMENTS by Woody McGraw and Don Tupman, Louisville District, U.S. Army Corps of Engineers.

CONTRACTOR'S PROBLEMS by Richard Geottle.

ENVIRONMENTAL CONSIDERATIONS IN SOILS ENGINEERING by D. Joseph Hagerty, Asst. Professor of Civil Engineering, University of Louisville and Joseph L. Pavoni, Asst. Professor of Civil and Environmental Engineering, University of Louisville.

ORVSS III
LATERAL EARTH PRESSURES

October 27, 1972
Fort Mitchell, Kentucky

INSTRUMENTATION FOR STRESS AND STRAIN MEASUREMENTS IN SOILS by Stanley D. Wilson, Executive Vice-President, Shannon and Wilson, Inc.

DEEP EXCAVATION AND BUILDINGS SUPPORTED BY TIE-BACK SYSTEM by Richard Geottle, P.E., Richard Geottle, Inc., James J. Flaig, P.E., H. C. Nutting Company, Arthur J. Miller, P.E., Miller, Tallarico, McNinch, and Hoeffel Consulting Engineers, and Steven E. Schaefer, EIT, Miller, Tallarico, McNinch, and Hoeffel Consulting Engineers.

LATERAL PRESSURES AND MOVEMENTS CAUSED BY PILE DRIVING by D. Joseph Hagerty, A.M. ASCE, Assistant Professor of Civil Engineering, University of Louisville.

FACTORS TO BE CONSIDERED IN THE DESIGN OF BACKFILL FOR LARGE DIAMETER FLEXIBLE METAL CONDUITS by David C. Cowherd, M.S., P.E.

GENERALIZED SLIDING WEDGE METHOD FOR SLOPE STABILITY AND EARTH PRESSURES ANALYSIS by Dr. Vincent P. Drnevich, Assistant Professor of Civil Engineering, University of Kentucky.

LATERAL PRESSURES AND PRESTRESSED TIE-BACK WALLS by P. C. Rizzo and R. D. Ellison, E. D'Appolonia Consulting Engineers, Inc., and R. J. Shafer, Herbert F. Darling, Inc.

DESIGN AND CONSTRUCTION OF SUPPORTED TEMPORARY EXCAVATIONS IN URBAN ENVIRONMENT by Yves Lacroix and Walter T. Jackson, Woodward-Moorhouse and Associates, Inc.

ORVSS IV
GEOTECHNICS IN TRANSPORTATION ENGINEERING

October 5, 1973
Lexington, Kentucky

RETRIEVAL AND USE OF GEOTECHNICAL INFORMATION by D. Joseph Hagerty, Assistant Professor of Civil Engineering, University of Louisville, Nicholas G. Schmitt, Soils Engineer, Law Engineering Testing, William J. Pfalzer, Research Engineer Assistant, Kentucky Bureau of Highways.

IN SITU SHEAR STRENGTH PARAMETERS BY DUTCH CONE PENETRATION TESTS by C. T. Gorman, Research Engineer Assistant, Kentucky Bureau of Highways, T. C. Hopkins, Research Engineer Principal, Kentucky Bureau of Highways, and V. P. Drnevich, Associate Professor of Civil Engineering, University of Kentucky.

REINFORCED EARTH - DESIGN AND CONSTRUCTION by David S. Gedney, Regional Engineer, Region 15, Federal Highway Administration and John L. Walkinshaw, Highway Engineer, Federal Highway Administration.

APPLICATIONS OF THE FINITE ELEMENT METHOD TO GEOTECHNICS AND TRANSPORTATION ENGINEERING by Yang H. Huang, Associate Professor of Civil Engineering, University of Kentucky.

RELIABILITY ANALYSIS AND COST OPTIMIZATION OF EMBANKMENTS by Warren J. Baker, Chrysler Professor and Dean, College of Engineering, University of Detroit.

STABILITY ANALYSIS - ITS POTENTIAL AND ITS LIMITATIONS by T. H. Wu, Professor of Civil Engineering, The Ohio State University.

ORVSS V
ROCK ENGINEERING

October 18, 1974
Clarksville, Indiana

EXPLORATION AND TESTING IN ROCK by Joseph Hagerty, Civil Engineering Department, University of Louisville, and James Coulson, Tennessee Valley Authority.

A ROCK CLASSIFICATION SCHEMA by R. C. Deen, Assistant Director, Kentucky Bureau of Highways, Division of Research, C. D. Tockstein, Research Engineer Assistant, Division of Research, and M. W. Palmer, Research Engineer Assistant, Division of Research.

FOUNDATION ON OR IN ROCK by E. D'Appolonia, E. D'Appolonia Consulting Engineers, Inc.

ROCK FOUNDATIONS (A Panel Discussion) Comments by: C. R. Lennertz, H. C. Nutting Company, Harry Thomas, US Army Corps of Engineers, and Milton M. Greenbaum, Greenbaum and Associates.

DESIGN OF OPEN EXCAVATIONS IN ROCK by D. Ross-Brown Dames & Moore.

ROCK EXCAVATION (A Panel Discussion) The Producer's Viewpoint by J. A. Waddell, Martin Marietta Aggregates, Consideration of Effects on Surroundings by D. J. Hagerty, University of Louisville, and Geologic and Support Considerations for Rock Excavations by J. Mahar, University of Illinois.

ROCK ENGINEERING ON SOME RECENT PROJECTS by Don U. Deere, Consultant in Engineering Geology and Rock Mechanics, University of Florida.

ORVSS VI
SLOPE STABILITY & LANDSLIDES

October 17, 1975
Fort Mitchell, Kentucky

GEOLOGIC PERSPECTIVES--THE CINCINNATI EXAMPLE by Robert W. Fleming, U.S. Geological Survey.

IMPORTANCE OF GEOLOGIC STRUCTURE IN STABILITY OF ROCK SLOPES by Robert L. Schuster, William K. Smith, and Fitzhugh T. Lee, U.S. Geological Survey.

CUT AND FILL ORDINANCE AS ADOPTED BY THE CITY OF CINCINNATI by James R. Krusling, P.E.

DRILLED PIER RETAINING WALLS by Merle F. Nethero, Geotechnical Engineer - Vice President, H. C. Nutting Company.

REGARDING FAILED SLOPES by H. A. Mathis, Kentucky Department of Transportation.

EFFECTS OF WATER ON SLOPE STABILITY by Tom C. Hopkins, Research Engineer Chief, David L. Allen, Research Engineer Principal, and Robert C. Deen, Assistant Director, Kentucky Department of Transportation, Division of Research.

ORVSS VII
SHALES AND MINE WASTES:
GEOTECHNICAL
PROPERTIES, DESIGN, AND CONSTRUCTION

October 8, 1977
Lexington, Kentucky

GEOTECHNICAL PROPERTIES OF SOME EASTERN KENTUCKY SURFACE MINE SPOILS by V. P. Drnevich and R. J. Ebelhar, University of Kentucky, and G. P. Williams, U.S. Department of Agriculture, Forest Service

GUIDELINES FOR COMPACTED SHALE EMBANKMENTS by L. E. Wood and C. W. Lovell, Purdue University, and W. W. Sisiliano, Indiana State Highway Commission

ENGINEERING EVALUATION OF A CLEVELAND SHALE by V. K. Khosla, Heron Testing Laboratories, Inc. and R. L. Murdoch, Barbar and Hoffman, Inc.

PHYSICAL AND ENGINEERING CHARACTERISTICS OF COAL PREPARATION PLATE REFUSE by C. S. Bishop and J. G. Rose, University of Kentucky

REBOUND PROPERTIES OF REMOLDED CLAY SHALES by C. R. Ullrich, University of Louisville

GENERAL REPORT ON DESIGN AND CONSTRUCTION by G. A. Leonard, Purdue University

USE OF MINE WASTE IN TAILINGS DAMS by W. F. Brummund, Golder Associates

COAL REFUSE: ITS BEHAVIOR RELATED TO THE DESIGN AND OPERATION OF COAL REFUSE DISPOSAL FACILITIES by R. G. Almes and A. Butail, E. D'Appolonia Consulting Engineers, Inc.

USE OF COMPACTED SHALE AS DAM EMBANKMENTS by C. A. Fetzer, U.S. Army Corps of Engineers

AIRPORT EMBANKMENT UTILIZES COAL STRIP MINE WASTE by J. M. Sheahan and T. F. Hunkele, Richardson, Gordon and Associates

OBSERVATION EVALUATIONS OF COAL REFUSE EMBANKMENT STABILITY by W. W. Parker and R. E. Gray, GAI Consultants, Inc.

CONVENTIONAL AND UNCONVENTIONAL APPROACHES USED TO LOCATE AND ELIMINATE HAZARDOUS MINE WASTE DAMS IN OHIO by V. V. Rajadhyaksha, Ohio Department of Natural Resources

GEOTECHNICAL OVERSIGHT NULLIFIES PROPER PROCEDURES by B. Rosen, Marks-Rosen, Inc.

WEST VIRGINIA EXPERIENCES WITH REVIEW OF COAL REFUSE DISPOSAL FACILITIES by G. Hall and M. K. Robinson, West Virginia Coal Refuse and Dam Control Section, and R. E. Smith, Woodward-Clyde Consultants

CLOSED CIRCUIT COAL REFUSE AS A STRUCTURAL FILL by D. C. Cowherd, Bowser-Morner Testing Laboratories, Inc.

DYNAMIC DESIGN CONSIDERATIONS OF LOOSE FINE COAL REFUSE by R. D. Ellison and Y. Y. Cho, E. D'Appolonia Consulting Engineers, Inc.

PROPERTIES OF COAL MINE FLOOR SHALE by R. W. Stephenson and J. D. Rockaway, University of Missouri-Rolla

ORVSS VIII
EARTH DAMS AND EMBANKMENTS
DESIGN, CONSTRUCTION, PERFORMANCE

October 14, 1977
Louisville, Kentucky

SIGNIFICANT ENGINEERING-GEOLOGY FEATURES AT DAMSITES IN FLAT-LYING SEDIMENTARY ROCKS by Alberto S. Nieto, Department of Geology, University of Illinois at Urbana-Champaign, Urbana, Illinois

SMALL DAMS - PARTICULAR PROBLEMS AND CONSIDERATIONS by Walter E. Hanson and David E. Daniels, Hanson Engineers, Inc., Springfield, Illinois

FOUNDATION SEEPAGE PROBLEMS AT WOLF CREEK DAM by Frank B. Couch, Jr., Nashville District, U.S. Army Corps of Engineers, Nashville, Tennessee

DESIGN AND CONSTRUCTION OF HIGHWAY EMBANKMENTS IN NEW YORK STATE by Lyndon H. Moore, Soil Mechanics Bureau, New York State Department of Transportation, Albany, New York

MOVEMENTS OF A NATURAL SLOPE AND AN EMBANKMENT - TWO CASE HISTORIES by E. C. Palmer, W. L. Nuzzo, Richard G. Almes, Richard Brissette, and E. D'Appolonia, E. D'Appolonia Consulting Engineers, Inc., Pittsburgh, Pennsylvania

COMMENTS ON SEISMIC STABILITY EVALUATION OF EMBANKMENT DAMS by Gonzalo Castro, Geotechnical Engineers, Inc., Winchester, Massachusetts

ORVSS IX
DEEP FOUNDATIONS

October 27, 1978
Fort Mitchell, Kentucky

INTERPRETATION AND ANALYSIS OF PILE LOAD TESTS by Bengt H. Fellenius, BHF Consultants, Inc.

AXIAL COMPRESSION AND UPLIFT RESISTANCE OF STEEL H-PILES by David R. Friels, Test Inc., Memphis, Tennessee

LOAD TRANSFER MEASUREMENTS IN CONCRETE PILES by William L. Durbin, P. Denny Retter, and Pauletta France, Woodward Clyde Consultants, Kansas City, Missouri

FRICTION PILES IN SAND - A REVIEW OF STATIC DESIGN PROCEDURES by William A. Cutter and David L. Warder, ATEC Associates, Inc., Indianapolis, Indiana

A PILE DESIGN AND INSTALLATION SPECIFICATIONS BASED ON THE LOAD FACTOR CONCEPT by G. G. Goble, Department of Civil and Architectural Engineering, University of Colorado, Boulder, Colorado

TESTS TO OBTAIN BEHAVIOR OF DRILLED SHAFTS UNDER AXIAL LOAD by Lymon C. Reese, College of Engineering, University of Texas at Austin, Texas

CONTRACTING FOR DEEP FOUNDATIONS - LEGAL ASPECTS by C. Robert Lennertz, H. C. Nutting Company, Cincinnati, Ohio

ORVSS X
GEOTECHNICS OF MINING

October 5, 1979
Lexington, Kentucky

A CRITICAL EVALUATION OF COAL MINING SUBSIDENCE PATTERNS by T. D. O'Rourke and Susan M. Turner, School of Civil and Environmental Engineering, Cornell University, Ithaca, New York

EVALUATION OF DAMAGE POTENTIAL TO EARTH DAMS BY SUBSURFACE COAL MINING AT REND LAKE, ILLINOIS by Alberto S. Nieto, Department of Geology, University of Illinois at Urbana-Champaign, Urbana, Illinois

GEOTECHNICAL CONSIDERATIONS FOR DEADHEADING A MARION 5761 SHOVEL by Kenneth E. Darnell, Geologic Consultants, Inc., J. Richard Cheeks, Stokely-Cheeks and Associates, and Dennis Albers, Amax Coal Company

DISPOSAL OF COAL PROCESSING WASTES AT SITES OF LIMITED SIZE by Barry K. Thacker and David D. Cowherd, Bowser-Morner Testing Laboratories, Inc., Dayton, Ohio

SEEPAGE AND STABILITY ANALYSIS FOR AN INUNDATED MILL TAILING IMPOUNDMENT, A CASE STUDY by W. A. Charlie and T. V. Edgar, Department of Civil Engineering, Colorado State University, and R. A. Kilborn, Climax Molybdenum Company, Climax, Colorado

CHEMICAL ADDITIVES TO CHANGE THE DURABILITY OF SHALES by M. Surendra and C. W. Lovell, School of Civil Engineering, Purdue University, West Lafayette, Indiana

POINT LOAD STRENGTH TESTING OF COAL SPOIL by Barney Hale and C. W. Lovell, School of Civil Engineering, Purdue University, West Lafayette, Indiana

THE REVIEW AND REGULATION OF SLOPE STABILITY - A TECHNICAL PERSPECTIVE by Bruce C. Vandre, U.S. Department of Agriculture Forest Service, Intermountain Region, Ogden, Utah

THE NECESSITY FOR SCRUTINIZING GOVERNMENT MINING REGULATIONS BY David C. Cowherd, Bowser-Morner Testing Laboratories, Inc., Dayton, Ohio

ORVSS XI
EARTH PRESSURES & RETAINING STRUCTURES

October 10, 1980
Clarksville, Indiana

GROUND MOVEMENTS ASSOCIATED WITH DEEP BRACED CUT EXCAVATIONS by Thomas D. O'Rourke, Cornell University, Ithaca, New York.

TIE-BACK MEMBRANE WALLS IN VENEZUELA by Charles O. Riggs, Central Mine Equipment Company, St. Louis, Missouri.

DESIGN, CONSTRUCTION, AND PERFORMANCE OF ANCHORED BULKHEADS by Yves Lacroix, Woodward-Clyde Consultants, Chicago, Illinois, and Dimitrios K. Atmatzidis, University of Patras, Greece.

LARGE BURIED METAL CULVERT DESIGN AND CONSTRUCTION by Ernest T. Selig, University of Massachusetts, Amherst, Massachusetts.

DESIGN, CONSTRUCTION AND PERFORMANCE OF A CELLULAR COFFERDAM IN DEEP WATER by Edward B. Kinner, Haley & Aldrich, Inc., Cambridge, Massachusetts, Max D. Sorota, Fay, Spofford & Thorndike, Inc., Boston, Masschusetts, and Mark X. Haley, Haley & Aldrich, Inc., Cambridge, Massachusetts.

PRACTICAL UNDERPINNING OPERATIONS by James J. Kerr, Spencer, White & Prentis, Inc., Rochelle Park, New Jersey.

ORVSS XII
GROUNDWATER: MONITORING, EVALUATION & CONTROL

October 9, 1981
Fort Mitchell, Kentucky

FUNDAMENTAL ASPECTS OF GROUNDWATER FLOW by D. Joseph Hagerty, Civil Engineering Department, University of Louisville, Louisville, Kentucky.

INSTALLATION OF ADEQUATELY SEALED PIEZOMETERS by Claude A. Fetzer, Cincinnati, Ohio, and Paul M. Plummer, Miami Conservancy District, Dayton, Ohio.

APPLICATION OF COMPUTER MODEL TO GROUNDWATER FLOW AND CONTAMINANT TRANSPORT INVESTIGATION by P. S. Huyakorn and D. E. Dougherty, GeoTrans, Inc., Reston, Virginia.

HYDROGEOLOGIC AND WATER QUALITY ASSESSMENT FOR AN EXISTING CLASS I (HAZARDOUS) WASTE DISPOSAL SITE by Theodore A. Gleason and Robert F. Kaufmann, Converse Ward Davis Dixon, Inc., Cincinnati, Ohio.

DEWATERING SURFACE MINES IN THE INTERIOR COAL PROVINCE by John E. O'Rourke and Kevin O'Connor, Woodward-Clyde Consultants, San Francisco, California.

DEWATERING OF A CONSTRUCTION SITE AND AN EXISTING STRUCTURE UTILIZING DEEP WELLS by Grover C. Cox, III, Bowser-Morner Testing Laboratories, Inc., Dayton, Ohio.

MULTI-USE WELL SYSTEM FOR HIGH-RISE OFFICE BUILDING IN INDIANAPOLIS by Bruce Bailey and William A Cutter, ATEC Associates, Indianapolis, Indiana.

DESIGN, INSTALLATION, AND OPERATION OF DEWATERING SYSTEM FOR PUMPING STATION APPROACH CHANNEL by M. Mike Alizadeh, Shannon & Wilson, Inc., St. Louis, Missouri.

HORIZONTAL DRAINS: PREDICTING EFFECTIVENESS IN ADVANCE OF INSTALLATION by Charles S. Bishop, Engineering-Science, Lexington, Kentucky, and William E. Munson, Kentucky Department of Transportation, Lexington, Kentucky.

DEWATERING FOR SOIL IMPROVEMENT by Robert D. Anderson and Daniel B. Kleiman, Griffin International Corp. Inc., Irvington, New York, and Wojciech Wolski, Warsaw Agricultural University, Warsaw, Poland.

SYNTHETIC FABRICS (GEOTEXTILES) IN DRAINAGE APPLICATIONS by Phil J. Sullivan, E. I. DuPont Co., Pittsburgh, Pennsylvania.

ORVSS XIII
RECENT ADVANCES IN
GEOTECHNICAL ENGINEERING PRACTICE

October 8, 1982
Lexington, Kentucky

RELIABILITY IN GEOTECHNICAL ENGINEERING by Milton E. Harr, Purdue University, West Lafayette, Indiana.

INSTRUMENTATION OF SHEET PILE COFFERDAM AT LOCK AND DAM 26 REPLACEMENT SITE by Christopher B. Groves, Shannon & Wilson, Inc., St. Louis, Missouri, and Brian Kleber, U.S. Army Corps of Engineers, St. Louis District, St. Louis, Missouri.

PROBLEMS ASSOCIATED WITH CONSTRUCTION OF A ROCKFILL EMBANKMENT by James E. Paris, U.S. Army Corps of Engineers, Nashville District, Nashville, Tennessee.

THREE-DIMENSIONAL SLOPE STABILITY by O. W. Lovell, Purdue University, West Lafayette, Indiana.

LOOSE SAND PIPES IN GLACIAL OUTWASH: HOW DID THEY DEVELOP AND ARE THEY SIGNIFICANT? by William A. Cutter and Bruce Bailey, ATEC Associates, Inc., Indianapolis, Indiana.

USE OF CYLINDER PILE RETAINING WALL TO STABILIZE EXCAVATION SIDES AND PROTECT EXISTING STRUCTURES by P. Deo and D. Nona, Neyer, Tiseo & Hindo, Ltd., Farmington Hills, Michigan.

SAMPLING AND TESTING OF THE MAQUOKETA SHALE IN NORTHWESTERN ILLINOIS by Terje Preber, Dames & Moore, Inc., Park Ridge, Illinois.

DESIGN CONSIDERATIONS USING SPT'S by Yo Y. Cho, Binary Instruments, Inc., Pittsburgh, Pennsylvania.

CHEMICAL GROUTING UTILIZED FOR UNDEPINNING AND WATER CONTROL FOR A PIT INSTALLATION by Joseph P. Welsh, Hayward Baker Company, Odenton, Maryland, and Russell Snyder, Martin Marietta Refractories Division, Hunt Valley, Maryland.

Some of the proceedings of the current and previous Ohio River Valley Soils Seminars are still available at nominal cost. Address Inquiries to:

Office of Continuing Education
College of Engineering
University of Kentucky
Lexington, Kentucky 40506